Electronic Thesis and Dissertation Repository

9-12-2023 3:30 PM

Molecular identification and characterization of Heat shock protein 70 family proteins essential for Turnip mosaic virus infection in Arabidopsis thaliana

Ziwei Tang,

Supervisor: Wang, Aiming., *London Research and Development Centre, Agriculture and Agri-Food Canada (AAFC)*
Co-Supervisor: Bernards, Mark A., *The University of Western Ontario*
A thesis submitted in partial fulfillment of the requirements for the Doctor of Philosophy degree in Biology
© Ziwei Tang 2023

Follow this and additional works at: https://ir.lib.uwo.ca/etd

Part of the Plant Pathology Commons

Recommended Citation

ABSTRACT

Turnip mosaic virus (TuMV) belongs to the RNA virus family of *Potyviridae* and genus *Potyvirus*. TuMV incurs agricultural losses by causing diseases in vegetable, oilseed, forage, and biofuel crops globally. Viruses are obligate intracellular parasites depending on the host cellular machinery to proliferate. Thus, molecular identification and functional characterization of host factors essential in the viral infection process may open up a new avenue towards developing genetic virus resistance. Eukaryotic translation initiation factor 4E (eIF4E) or its isoform (eIF(iso)4E) is a critical host factor for many potyviruses including TuMV. Heat shock protein 70 family proteins (HSP70) have been identified in the eIF(iso)4E protein complex isolated from *Arabidopsis thaliana* infected with TuMV. I hypothesized that at least some *A. thaliana* HSP70s are host factors for TuMV infection since they are associated with the most essential and multiple functional TuMV host factor eIF(iso)4E.

To explore the roles of HSP70s in TuMV infection, TuMV infection assay in *A. thaliana* HSP70 mutants were performed. Combining the HSP70s identified from eIF(iso)4E protein complex, five HSP70s: cytoplasmic HSP70-1, HSP70-2, and HSP70-8, as well as endoplasmic reticulum (ER)-located HSP70-11 and HSP70-12 were selected for further analysis of their involvement in TuMV infection using different systems.

I confirmed interaction of all five HSP70s with eIF(iso)4E and discovered their interactions with TuMV viral proteins: replicase NIb and coat protein CP. I found that the HSP70s colocalized with TuMV replication complex in infected plant leaf cells. HSP70-1 and HSP70-2 have mostly inhibitory effect on TuMV infection by accelerating the degradation of NIb via the ubiquitin-proteosome pathway. Consistent to my hypothesis, HSP70-11 and HSP70-12 facilitate TuMV infection, probably by inhibiting the degradation of TuMV protein NIb and CP as well as the host factor eIF(iso)4E. The proviral effect of HSP70-11 and HSP70-12 possibly depends on their ER-localization. Finally, the effect of HSP70-8 on TuMV infection was ambiguous. While HSP70-8 accelerated the degradation of TuMV NIb and CP, TuMV infection was reduced in HSP70-8 knockout *A. thaliana* plants. Together, these data suggest that HSP70s play complex roles in TuMV, possibly associated with their chaperone activities on different viral proteins and host factors.

Keywords: HSP70, plant virus, potyvirus, TuMV, host factor, eIF(iso)4E, replicase, coat protein, viral replication complex, recessive resistance, genetic resistance

SUMMARY

Viruses rely on invading host cells for survival and multiplication because they are too simple to produce their own material and energy. They need to use the proteins from the host cell to survive and reproduce. These host proteins are named host factors. When viruses infect hosts, they may cause diseases or even death. Studying host factors increases knowledge on how viruses infect hosts and how to control diseases caused by viruses. One way to stop virus from infecting a host is to disable one or more host factors, preventing the virus from using them. This is a useful way to fight virus infection especially in plants, as plants usually have more than one version of proteins with the same function. Therefore, disabling one essential host factor does not harm the normal growth of the plant because it still has other versions to use.

In this thesis, I studied *Turnip mosaic virus* (TuMV), which causes problems in many important crops. We looked into a family of host proteins called the Heat shock protein 70s (HSP70) to see if TuMV takes advantage of them as host factors for infection. In plants, HSP70s are responsible for maintaining the protein's proper shape and location and balancing cellular protein production and recycling.

We found that two HSP70s located in the endoplasmic reticulum (ER), or the membrane system within the cell, are host factors for TuMV infection. They are found in the same place where the virus replicates within the host, and they interact with virus protein responsible for virus replication. They may help virus infection by preventing the virus protein from breaking down.

On the other hand, the HSP70s located in the cytoplasm have an opposite effect on TuMV infection compared with two HSP70s located in the ER. Though they also locate in the virus replication compartments and interact with virus protein, the cytoplasm HSP70s have a negative impact on TuMV infection by promoting the degradation of virus protein. Moreover, if the ER-located HSP70s were modified so that they did not target the ER, the modified HSP70s acted like the cytoplasm-located HSP70s and inhibited TuMV infection.

ACKNOWLEDGEMENTS

First and foremost, I am indebted to my supervisor Dr. Aiming Wang who took me as a student in the Department of Biology, the University of Western Ontario, and supported my studies financially. During the five years he walked me through the ragged path of research with his experience as one of the best scientists in plant virology and hearty encouragement. In the process I not only became skilled in experiment techniques in plant virology but also developed valuable tools for a researcher: critical and independent thinking as well as hypothesis oriented scientific method, which will always benefit me in my future career.

I am also grateful to my co-supervisor Dr. Mark Bernards for his instructions on my project ever since its start. He helped me to gain better scientific writing skills with all the feedback from revising my writing. I would like to extend my gratefulness to members of my committee Dr. Yuhai Cui, Dr. Raymond Thomas, and Dr. Richard Gardiner for the wonderful insights on my project they provided me on all the meetings throughout these years. I am equally thankful to the Department of Biology, the University of Western Ontario and the London Research and Development Centre, Agriculture and Agri-Food Canada for the funding support, facility, teaching opportunities and various courses and training activities that expended my experience, knowledge, and connections.

I owe gratitude to current and former members in Dr. Aiming Wang's lab without whom I could not finish the project. I thank Dr. Shanwu Lyv for sharing with me the data from his IP-MS. I thank Shaokang Zhang for his idea in switching HDEL tag in the HSP70s as well as detection of HSP70s' effect on protein level of their interaction partners. I would also thank especially Rongrong He, Dr. Zhaoji Dai, Dr. Guanwei Wu, Dr. Aaron Simkovich for their valuable advice on experiment procedures. I thank Dr. Yinzi Li, Brian Weselowski, and Jamie McNail for their technical support as well as the housekeeping of the lab so that I could access to vectors and orders conveniently. Moreover, I would like to thank Dr. Fangfang Li, Dr. Liping Wang, and Dr. Xiuling Yang for all the inspiring discussions we had and for creating a supportive environment which is a pleasure to work in every day.

Finally, I have to acknowledge my dad and my mom, Da Tang (唐达) and Qiang Ma (马蔷), as well as my child Shihe Wang (王十禾), for their emotional support. It is them who inspired me to pursue a PhD degree, encouraged me to continue in the career of biology, and gave me the meaning of my life.

TABLE OF CONTENTS

LIST OF TABLES

LIST OF FIGURES

LIST OF ADDREVIATIONS

6K1	the first 6 kDa protein
6K2	the second 6 kDa protein (also referred to as 6K)
AAFC	Agriculture and Agri-Food Canada
ABRC	Arabidopsis Biological Resource Center
AbMV	*Abutilon mosaic virus*
ADP	adenosine diphosphate
ATP	adenosine triphosphate
ATF6	activating transcription factor 6
BaMV	*Bamboo mosaic virus*
BBSV	*Beet black scorch virus*
BiFC	bimolecular fluorescence complementation
BiP	binding immunoglobulin protein
bZIP	basic leucine zipper
cDNA	complementary DNA
CDPK	calcium-dependent protein kinases
ChiVMV	*Chilli veinal mottle virus*
CI	the cylindrical inclusion protein
CITE	cap-independent translation elements
ClYVV	*Clover yellow vein virus*
CNV	*Cucumber necrosis virus*
Co-IP	co-immunoprecipitation
Col-0	ecotype Columbia
COPI(II)	coat protein complex I (II)
CP	coat protein or capsid protein
CRISPR/Cas	clustered, regularly interspaced, short palindromic repeat associated protein
C-terminal	carboxyl-terminal
CVD	C-terminal variable domain
CWMV	*Chinese wheat mosaic furovirus*
Cyv-1	*Clover yellow vein virus* resistance in pea
Cyv-2	*Clover yellow vein virus* resistance in pea mapped to eIF4e
DAG	aspartic acid-alanine-glycine motif
DCL4	dicer-like 4
DDO	double dropout
DEAD	aspartic acid-Glutamic acid-Alanine-Aspartic acid motif
DMSO	dimethyl sulfoxide
DNA	deoxyribonuleic acid

DNase	deoxyribonuclease
dpi	days post infiltration
DREB2	dehydration responsive element binding
EDTA	ethylenediaminetetraacetic acid
eEF	eukaryotic translation elongation factor
eIF	eukaryotic translation initiation factor
eIF(iso)4E	eukaryotic translation initiation factor isoform 4E
eIF4E	eukaryotic translation initiation factor 4E
ER	endoplasmic reticulum
ERES	endoplasmic reticulum exit sites
FLAG	sequence motif DYKDDDDK (D, aspartic acid; Y, tyrosine; and K, lysine)
GCN2	general control non-repressible 2
GDD	glycine-asparagine-asparagine (GDD) motif
GFP	green fluorescent protein
GMO	genetically modified organism
HC-Pro	the helper component protease
HDEL	histidine-aspartic acid-glutamic acid-leucine motif
hpi	hours post infiltration
hpt	hours host transformation
HSE	heat shock elements
HSF	heat shock factors
HSP70	the 70 kDa heat shock protein
HSR	heat shock response
IP-MS	immunoprecipitation-mass spectrometry
IRE1	inositol-requiring transmembrane kinase/endonuclease
IRES	internal ribosome entry site
kb	kilobase
kDa	kilodalton
LB	T-DNA left border
LMV	*Lettuce mosaic virus*
LP	left genomic primer
LC-MS/MS	liquid chromatography–tandem mass spectrometry
m^{7}G	methyl-7-guanosine
MAPK	mitogen-activated protein kinases
MNSV	*Melon necrotic spot virus*
Mo1	*Lettuce mosaic virus* resistance in lettuce
mRNA	messenger RNA
NBD	nucleotide binding domain

NBS-LRR	nucleotide binding site-leucine rich repeat
nCBP	the novel cap-binding protein
NEF	nucleotide exchange factors
NIa	the nuclear inclusion a protein
NIa-Pro	the nuclear inclusion a protease
NIb	the nuclear inclusion b protein
N-P-K	nitrogen-phosphorus-potassium fertilizer
nsv	*Melon necrotic spot virus* resistance in melon
N-terminal	amino-terminal
NVD	N-terminal variable domain
ORF	open reading frame
P1	the first protein
P3	the third protein
P3N-PIPO	PIPO as a translational fusion with the N-terminus of P3
PABP	poly(A)-binding protein
PCaP1	plasma membrane–associated Ca2+ -binding protein 1
PCR	polymerase chain reaction
PD	plasmodesmata
PEG	polyethylene glycol
PEMV	*Pea enation mosaic virus*
PepMV	*Pepino mosaic virus*
PERK	RNA dependent protein kinase like ER kinase
PIC	43S pre-initiation complex
PIPO	pretty interesting Potyviridae ORF
PlAMV	*Plantago asiatica mosaic virus*
Poly(A)	polyadenylate
pot-1	*Potato virus Y and Tobacco etch virus* resistance *in tomato*
PRRs	pattern recognition receptors
PVA	*Potato virus A*
PVMV	*Pepper veinal mottle virus*
pvr1²/pvr6	*Pepper veinal mottle virus* and *Chili veinal mottle virus* resistance in pepper
PVX	*Potato virus X*
QDO	quadruple dropout
RT-qPCR	Reverse transcription quantitative PCR
RCNMV	*Red clover necrotic mosaic virus*
RdRp	RNA-dependent RNA polymerase (virus)
Retr01	*Turnip mosaic virus* resistance in Chinese cabbage
RNA	ribonucleic acid

RNAi	RNA interference
RP	right genomic primer
rpm	revolutions per minute
RSV	*Rice Stripe Virus*
RubisCO	ribulose-1,5-bisphosphate carboxylase/oxygenase
Rym-7	*Barley yellow mosaic virus* resistance in barley
RYMV	*Sobemovirus Rice yellow mottle virus*
S1P/S2P	site-1/site-2 proteases
SBD	substrate binding domain
sbm1	*Pea seed-borne mosaic virus* pathotype P1 resistance in pea
sbm2	*Pea seed-borne mosaic virus* pathotype L1 resistance in pea
SCE1	SUMO-Conjugating Enzyme 1
sgRNA	a single guide RNA
SNARE	soluble N-ethylmaleimide-sensitive-factor attachment protein receptor
SUMO3	small ubiquitin-related modifier 3
TALEN	transcription-activator-like effector nuclease
TBSV	*Tomato bushy stunt virus*
T-DNA	transfer DNA
TEV	*Tobacco etch virus*
TGBp3	triple gene block proteins 3
TILLING	targeted induced local lesions IN genomes
TuMV	*Turnip mosaic virus*
TYLCV	*Tomato Yellow Leaf Curl Virus*
UPR	unfolded protein response
UTR	untranslated region
UV	ultraviolet
va	*Potato virus Y* resistance in tobacco
VPg	the viral genome-linked protein
VRC	viral replication complex
wlv	*Bean yellow mosaic virus* resistance in pea
Y2H	yeast two-hybrid
YFP	yellow fluorescent protein
ZNF	zinc finger nuclease
zym	*Zucchini yellow mosaic virus* resistance in watermelon

Chapter 1: Introduction

1.1 An overview of *Turnip mosaic virus* and the *potyvirus* genus

1.1.1 Taxonomy, host range, and importance of *Turnip mosaic virus*

Viruses are among the major plant pathogens that cause crop losses greater than 30 billion US dollars annually around the world (Yang et al, 2021). *Potyviridae* is the largest family of agriculturally important RNA viruses that is comprised of over 200 species (Yang et al, 2021). *Turnip mosaic virus* (TuMV) infects a wide variety of crop species and belongs to the *Potyvirus* genus, the largest genus in the *Potyviridae* family. TuMV infection causes symptoms such as mosaic, mottling, chlorosis, necrosis, and deformation of the plant organs, loose of heading and stunting or withering of the plant (Nellist et al, 2022). Harsh environmental conditions may further worsen the symptoms, resulting in total loss of harvest. TuMV has a wider host range than any other known potyviruses, infecting over 300 species of plants in 156 genera of 43 families (Nellist et al, 2022). The most notable hosts of TuMV are from the family *Brassicaceae*, which includes economically important vegetable, oilseed, forage, and biofuel crops cultivated all over the world (Li et al, 2019; Sánchez et al, 2003; Walsh & Jenner, 2002). TuMV also infects model plants such as *Arabidopsis thaliana* and *Nicotiana benthamiana*. As it is an important plant pathogen, TuMV has become a widely studied virus, even considered to be a model *Potyvirus* for understanding the molecular pathology of potyviruses.

1.1.2 Potyvirus genome organization and viral protein function

Potyviruses possess a positive-sense single-stranded RNA [(+)ssRNA] genome that has a long open reading frame (ORF) encoding one large polyprotein of around 350 kDa (Yang et al, 2021). As shown by Fig. 1A, the polyprotein is processed by three viral proteases into 10 mature proteins (White, 2015). All potyviruses also encode an additional small ORF named PIPO (pretty interesting *Potyviridae* ORF) embedded in the P3 cistron. (Chung et al, 2008). This ORF encoding P3N-PIPO is actually present in a small percentage of progeny viruses due to transcriptional slippage during viral replication (Olspert et al, 2015; Rodamilans et al, 2015). The transcriptional slippage occurs at a conserved motif in the P3 cistron and causes frameshift, enabling the

translation of P3N-PIPO. Moreover, alternative ORFs have been discovered in some of other potyviruses (other than TuMV) (Hagiwara-Komoda et al, 2016; Mingot et al, 2016).

Therefore, the majority potyviruses including TuMV encode a total of 11 proteins. Starting from the N-terminus of the potyviral polyprotein, P1 (the first protein) is a serine endopeptidase self-released by *cis* cleavage at its C-terminus (Verchot et al, 1991). The cleavage of P1 is vital for potyvirus infection (Pasin et al, 2014). P1 is involved in RNA silencing suppression and enhances virus infection independent of RNA silencing suppression (Revers & García, 2015; Shan et al, 2018; Verchot & Carrington, 1995). Except for the conserved proteinase domain at its C-terminal region, P1 is highly variable in length and amino acid sequence, which may contribute to species adaptation of potyviruses (Charon et al, 2016; Nigam et al, 2019; Cui and Wang, 2019).

HC-Pro (the helper component–protease) is also a cysteine protease that self-cleaves at its C-terminus (Revers & García, 2015). HC-Pro was the first characterized viral suppressor of RNA silencing (VSR) of plant viruses (Kasschau & Carrington, 1998). Apart from that, HC-Pro plays multiple roles in diverse potyvirus infection stages such as in aphid transmission, genome replication, and virus long-distance movement (Cui & Wang, 2019; Hasiów-Jaroszewska et al, 2014; Rodamilans et al, 2018). The C-terminal domain of HC-Pro is the determinate of its proteolytic activity (Guo et al, 2011), whereas its N-terminal and central domains interact with aphid stylet and virion, respectively, bridging the vector and the virus for transmission (del Toro et al, 2018; Gadhave et al, 2020; Valli et al, 2018). HC-Pro interacts with almost all other virus proteins and many host proteins. However, the biological relevance of most of those interactions remains unclear.

The central region of the potyvirus polyprotein contains four potyviral proteins: P3 (the third protein), 6K1 (the first 6-kDa peptide), CI (the cylindrical inclusion), and 6K2 (the second 6-kDa peptide). In addition, as mentioned above, the coding sequence of P3N-PIPO is embedded in the P3 cistron. P3 and 6K1 are poorly characterized potyviral proteins (Cui & Wang, 2016; Cui et al, 2010). P3 includes two hydrophobic domains and the one located in the C-terminal is responsible for P3 targeting to endoplasmic reticulum (ER) (Cui et al, 2010; Eiamtanasate et al, 2007). The inclusion bodies formed by P3 associate with Golgi bodies and are trafficked to replication vesicles (Clavel et al, 2017; Cui et al, 2010). P3 is essential for virus replication and is related with viral

pathogenicity and symptom development (Jenner et al, 2003; Klein et al, 1994). P3 interacts with viral protein CI, NIb, and NIa (Yang et al, 2021). The proteolytic splitting between P3 and 6K1 is not a necessity for virus infectivity but has a regulatory role, and it is believed that P3-6K1, rather than P3 and 6K1, is the main functional product (Riechmann et al, 1995). However, 6K1 can be detected independently, and disrupting 6K1 disables the virus (Cui & Wang, 2016). 6K1 locates at replication vesicles as punctate structures and may be associated with the formation of the replication vesicles (Cui & Wang, 2016). Potyviral P3N-PIPO is located at the plasmodesmata (PD), a specialised intercellular organelle unique to the plant kingdom that establishes cytoplasmic continuity between neighbouring cells (Wang, 2015). P3N-PIPO interacts with CI to target it to PD structures (Wei et al, 2010b). P3N-PIPO is required for virus cell-to-cell movement, but not for virus replication (Cui et al, 2017; Vijayapalani et al, 2012; Wei et al, 2010b; Wen & Hajimorad, 2010).

CI is the largest potyviral protein and forms the cylindrical inclusions in the shape of pinwheel in the cytoplasm of infected cells (Sorel et al, 2014). CI self-interacts and forms conical structures at the PD to support virus cell-to-cell movement in collaboration with P3N-PIPO (Revers & García, 2015). CI is multifunctional as well, having ATPase and RNA helicase activities, which are associated with the C-terminal of the protein and are needed for virus genome replication (Deng et al, 2015).

6K2 is a small integral membrane protein targeting to the ER and induces ER proliferation as well as the formation of the virus replication vesicles at ER exit sites (Laliberté & Sanfaçon, 2010; Schaad et al, 1997; Wei & Wang, 2008). The N-terminal domain of 6K2 is essential for the induction of ER remodeling (González et al, 2019; Jiang et al, 2015). 6K2 is also found to play a part in virus systematic movement and symptomatology (González et al, 2019; Jiang et al, 2015; Spetz & Valkonen, 2004). 6K2 exists also in the form of a variety of polyprotein precursors, indicating that 6K2 may have other functions yet unknown (Yang et al, 2021).

The C-terminal region contains highly conserved NIa (the nuclear inclusion "a" protein), NIb (the nuclear inclusion "b" protein), and CP (coat protein). NIa forms crystalline inclusions that locate mostly in the nucleus of infected cells (Revers & García, 2015; Yang et al, 2021). NIa is processed to produce VPg and NIa-Pro (Jiang & Laliberté, 2011). VPg (viral protein genome-linked) is

intrinsically disordered and highly flexible, rending it to participate in diverse processes and interact with most other potyvirus proteins including itself (Jiang & Laliberté, 2011; Rantalainen et al, 2011), as well as several host factors such as eIF4E and eIF(iso)4E, poly(A)-binding protein (PABP), eukaryotic elongation factor eEF1A (Beauchemin & Laliberté, 2007; Huang et al, 2009; Wang, 2015; Wang & Krishnaswamy, 2012). In virion, VPg is covalently linked to the 5' end of virus genomic RNA. As a mimic of the mRNA cap structure but with higher affinity towards eukaryotic translation initiation factor (eIF), VPg is involved in initiating the translation of viral RNA and suppressing the translation of host RNA to promote viral RNA translation (Eskelin et al, 2011; Jiang & Laliberté, 2011). VPg also functions as a viral genome replication primer with its conserved NTP-binding site that can be uridylylated by NIb (Puustinen & Mäkinen, 2004). VPg contains nuclear localization signals, when VPg is not processed from NIa, it mainly localizes in the nucleus (Cotton et al, 2009; Rajamäki & Valkonen, 2009). When VPg is a part of the precursor 6K2-VPg-NIaPro, it is targeted to 6K2-induced virus replication vesicles and plays a role in viral RNA replication (Beauchemin et al, 2007). The dual role of VPg in both translation and replication of the viral genome makes it highly challenging to separate the processes and study them independently.

NIa-Pro is a cysteine protease responsible for proteolytic processing of the central and C-terminal regions of the viral polyprotein (Mann & Sanfaçon, 2019). The protease efficiencies of NIa-Pro at different cleavage sites are different, suggesting that it is a regulator potyviral polyprotein maturation (Revers & García, 2015; Yang et al, 2021). NIa-Pro has nonspecific DNase activity beside its proteinase activity; therefore, it might degrade host DNA during infection to alter the host gene expression (Anindya & Savithri, 2004). It has been recently shown that NIa-Pro interferes with the host DNA methylation to suppress host antiviral defenses (Gong et al, 2020).

NIb is also part of the nuclear-localized crystalline inclusion mentioned above (Knuhtsen et al, 1974). It is the viral RNA-dependent RNA polymerase (RdRp) that is obligatory for viral genome replication (Shen et al, 2020). A conserved GDD sequence motif is essential for NIb's RdRp activity (Shen et al, 2020). NIb contains nuclear localization signals, and the nuclear translocation is essential for viral viability (Yang et al, 2021). NIb interacts with viral proteins VPg, NIa, and CP. NIb is targeted to the membranous viral replication complex through domains on 6K2-VPg-NIaPro (Dufresne et al, 2008). The interaction of NIb with host eEF1A, PAPB, Hsc-3, AtRH8,

and small ubiquitin-like modifier-conjugating enzyme 1 (SCE-1) contributes to the formation of virus replication complex and subsequent virus proliferation (Tang et al, 2020).

CP is the last potyviral protein on the C-terminus of the polyprotein. About 2000 CP molecules helically encapsidate the viral genomic RNA to form a rod-like virion of approximately 11-13 nm in diameter and 689-900 nm in length (Kežar et al, 2019; Revers & García, 2015). The N-terminal arm of CP is variable and exposed on the virion surface, the core domain is highly conserved and binds to viral RNA to form the core of the virus particles, and the C-terminal is also exposed on the surface (Cuesta et al, 2019; Kežar et al, 2019; Zamora et al, 2017). CP is not required for viral genome replication, but plays indispensable role in virus cell-to-cell movement (Dai et al, 2020). However, CP regulates the assembly and disassembly of the virus particle and possibly regulates translation and replication through exposing or enclosing the genome (Hafrén et al, 2010). CP is also necessary for the aphid-transmission of the virion by interaction with HC-Pro through a conserved DAG motif in the N-terminal (Blanc et al, 1997). Additionally, CP is involved in seed transmission and host adaptation (Martínez-Turiño & García, 2020). Several types of post-translational modifications have been found on CP such as phosphorylation (Ivanov et al, 2003), ubiquitination (Hafrén et al, 2010), and O-GlcNAcylation (Martínez-Turiño et al, 2018), which may regulate the function of CP in different infection stages.

1.1.3 Infection cycle of potyvirus

The infection cycle of potyvirus can be divided into host cell entry, virion disassembly, translation of the viral genome, replication of the viral genome, virus particle assembly, cell-to-cell movement, and systematic movement shown in Fig. 1B. Due to the existence of cell wall in plant cells, plant viruses enter the host cell with the help of vector or through mechanical breaches of the cell. Once the virus particle is within the host, the change in cellular environment triggers the decoating of CP subunits, making space for the attachment of translation machinery, which further peels CP subunits from the viral RNA as it proceeds in translation (Culver, 2002; Saxena & Lomonossoff, 2014; Wang, 2015). The translation of potyviral RNA is located on the rough ER and will be specified below.

The potyviral polyprotein is processed co-translationally or post-translationally into functional products. The interplay between viral proteins and genomic RNA, as well as the host membrane

system and proteins induce the formation of membrane-anchored virus replication complexes (VRC) (Laliberté & Sanfaçon, 2010; Lõhmus et al, 2016; Wang, 2015). This special membranous compartment provides a microenvironment with concentrated materials for viral genome replication and for keeping away from host antiviral mechanisms (He et al, 2023). The 6K2 or 6K2-VPg-NIaPro is responsible for ER proliferation and VRC formation at endoplasmic reticulum exit sites (ERES) (Grangeon et al, 2012; Schaad et al, 1997; Wei & Wang, 2008), which may be trafficked to other organelles for vigorous replication (Li et al, 2020; Wei et al, 2010a; Wei et al, 2013). The secondary structures in the 3' end of viral RNA, including UTR and part of CP-coding region, with the help of PABP, direct NIb to the 3' end of genome to initiate negative-strand RNA synthesis (Haldeman-Cahill et al, 1998; Wang et al, 2000). This complementary strand RNA is then used as the template for producing progeny positive-strand viral RNA. Potyviral CI, an ADP-dependent helicase, unwinds complementary RNA strands in 3'-5' direction (Fernández et al, 1997), therefore the synthesis of progeny RNA also starts at the 3' end. The progeny viral RNA may repeat translation/replication step or might proceed to the virion assembly and movement. However, what events trigger the transition of viral RNA between these stages remains unknown (Yang et al, 2021).

Little is known about how CP subunits package viral RNA into a virion, but packaging might be a functionally connected process with replication (Gallo et al, 2018). The potyvirus crosses the cell wall barrier through plasmodesmata most likely in the form of virions (Wang, 2021). Potyviral P3N-PIPO mediates CI to assemble into a cone-shaped cylindrical structure at plasmodesmata, which is essential for the passage of the virus (Wei et al, 2010b). Moreover, viral cell-to-cell movement requires the cooperative action of other viral proteins such as CP (Dai et al, 2020), CI and P3N-PIPO (Wei et al., 2010b), along with many host proteins that dwell in the plasmodesmata such as expansin NbEXPA1 and plasma membrane protein PCaP1, as well as some dynamin-like proteins (Geng et al, 2014; Park et al, 2017; Vijayapalani et al, 2012; Wu et al, 2018; Wu et al, 2020). For long-distance movement, potyvirus enters bundle sheath cells from mesophyll cells, then sequentially enter phloem parenchyma, companion cells, phloem sieve element, and is finally passively carried to distant sites through the source-to-sin flow of photoassimilates (Wang, 2015). The process of potyviral long-distance movement is not well studied. Several host factors have been found to be involved in this process (Contreras-Paredes et al, 2013; Dong & Ronald, 2019; Jiang et al, 2015; Tang et al, 2020).

A

| 5'-UTR | P1 | HC-Pro | P3 | 6K1 | CI | 6K2 | VPg | NIa-Pro | NIb | CP | 3'-UTR |

P3N-PIPO

B
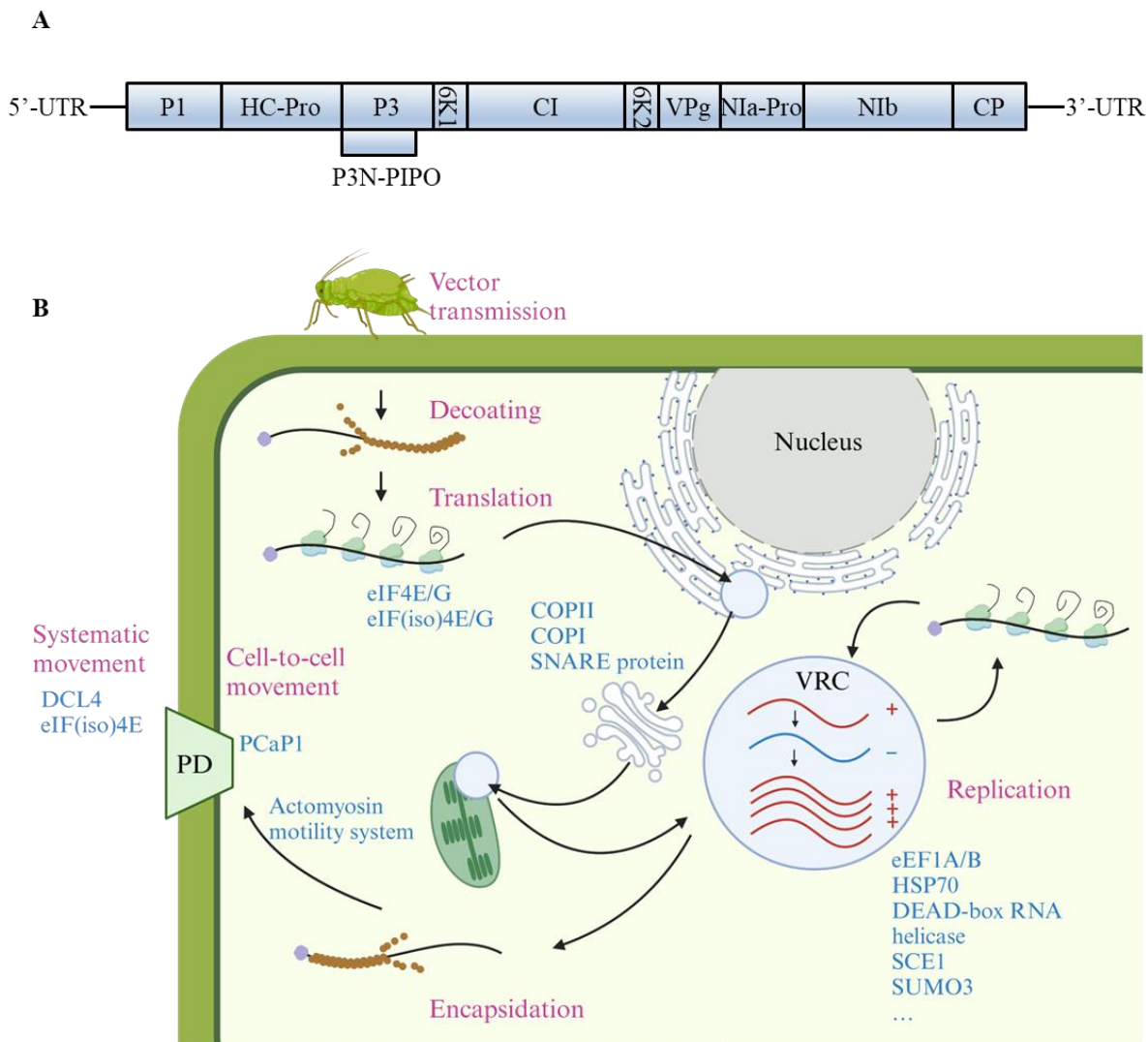
Figure 1. TuMV genome structure and potyvirus infection cycle

(A) TuMV genome structure indicating the viral proteins encoded.

(B) Potyvirus infection cycle shown with example host factors hijacked by the virus (shown in blue, as reviewed in Tang et al, 2020), picture produced with BioRender.

1.2 eIF4E/eIF(iso)4E as a host factor for virus infection

Viruses are obligate cellular parasites that accomplish their infection cycle by hijacking various cellular structural and functional components. Loss-of-function in essential host factors may alter the outcome of virus-host interactions, even conferring recessive resistance towards the virus (Hashimoto et al, 2016; Tang et al, 2020; Wang, 2015). This phenomenon is commonly found in natural resistant variants and is being utilized to develop virus-resistant cultivars by technologies such as breeding, mutagenesis, genetic modification, and genetic editing (Schmitt-Keichinger, 2019). Therefore, the research on host factors essential for virus infection may facilitates the development of genetic resistance, which is one of the means to help to combat virus outbreaks throughout the world to avoid huge agricultural losses.

The eukaryotic translation initiation factor 4E (eIF4E) or its isoform eIF(iso)4E with similar biological functions, are key host factors for the infection of the *Potyviridae* family and some other +ssRNA viruses (Schmitt-Keichinger, 2019; Shopan et al, 2020). In the evolution arms race between plants and viruses, together with the selection force of human intervention, virus resistance has been maintained in many cultivated crops. In the majority of those cases, the characterized naturally existing recessive resistance, mostly against viruses in the *Potyviridae* family, could be attributed to mutations in *eIF4E* or *eIF(iso)4E*, depending on which one is recruited by the virus for infection (Sanfaçon, 2015). The only known exception is resistance against *Chilli veinal mottle virus* (ChiVMV) and *Pepper veinal mottle virus* (PVMV) in pepper, in which mutation in both *eIF4E* and *eIF(iso)4E* is needed (Hwang et al, 2009; Ruffel et al, 2006). Some resistance alleles, though designated different names, were mapped to the same gene with only minor differences or even identical, as in the case of *sbm-1*, *wlv*, and *cyv-2* resistant alleles in pea (Andrade et al, 2009; Borgstrøm & Johansen, 2001; Gao et al, 2004b). There are recessive resistance alleles whose identity remains unknown, some of them nevertheless closely linked with either *eIF4E* or *eIF(iso)4E*, such as *sbm-2*, *cyv-1*, *rym-7* (Choi et al, 2012; Gao et al, 2004a; Kim et al, 2013; Yang et al, 2013).

Some naturally existing eIF4E/eIF(iso)4E-based resistances originate from eIF4E/eIF(iso)4E loss of function caused by a premature stop codon or large chunks of truncation, such as resistance conferred by recessive genes *retr01*, *va*, and *pvr1²/pvr6* (Hwang et al, 2009; Lee et al, 2017; Michel

et al, 2019; Nellist et al, 2014). However, most characterized resistances are attributed to mutations in the cap binding pocket of eIF4E/eIF(iso)4E, which disrupt eIF4E/eIF(iso)4E-VPg interaction and impair viral RNA translation. Examples of such mutations include *pot-1* in tomato, some *pvr* alleles in pepper, *mo1* alleles in lettuce, *zym* in watermelon, and some *rym* alleles in barley (Abdul-Razzak et al, 2009; Charron et al, 2008; German-Retana et al, 2008; Hwang et al, 2009; Kyle & Palloix, 1997; Kühne et al, 2003; Kanyuka et al, 2004; Kang et al, 2005; Kanyuka et al, 2005; Ling et al, 2009; Li et al, 2016; Lee et al, 2017; Moury et al, 2004; Nicaise et al, 2003; Perovic et al, 2014; Ruffel et al, 2005; Ruffel et al, 2006; Stein et al, 2005; Shi et al, 2019; Yeam et al, 2007). One functional study on the pepper *pvr1* allele identified the essential amino acid substitution G107R around the eIF4E cap-binding pocket that affects the binding to both VPg and the cap structure, while another crucial amino acid substitution L79R at an external loop disables VPg binding (Yeam et al, 2007). Another research showed that pepper eIF4Es from resistant cultivars retain their normal cellular function in yeast (Charron et al, 2008). Likewise, eIF4E's cap-binding ability in *Lettuce mosaic virus* (LMV) resistance alleles *mo1* is not affected (German-Retana et al, 2008). In melon, *nsv* confers resistance to non-potyvirus *Melon necrotic spot virus* (MNSV), which relies on the Cap-Independent Translation Elements (CITE) structure for translation. The mutated eIF4E interacts properly with the cap and eIF4G (Nieto et al, 2006). These findings indicate that eIF4E/eIF(iso)4E is capable of interacting with VPg or the viral virulence determinant using different modularity from its cap-binding domains, thus enabling the fine-tuning of eIF4E/eIF(iso)4E-mediated resistance without negative effects on plant regular growth and development. The list of mutations from eIF4E/eIF(iso)4E-based natural resistance inspires great ideas to study the role of eIF4E/eIF(iso)4E in virus infection and guide intelligent design of resistance cultivars.

1.2.1 Roles of eIF4E in eukaryotic cells

eIF4E family proteins have a cap-interacting domain highly conserved in a wide range of eukaryotic organisms (Dinkova et al, 2016; Hernández & Vazquez-Pianzola, 2005; Joshi et al, 2005). Plants possess an additional isoform of eIF4E: eIF(iso)4E. Belonging to the best characterized class of eIFs, eIF4E and eIF(iso)4E share structural similarity and some degree of amino acid identity, as well as overlapping functions (Duprat et al, 2002; Gallois et al, 2010; Joshi et al, 2005; Kropiwnicka et al, 2015; Nicaise et al, 2007; Patrick & Browning, 2012; Piron et al,

2010). In some cases, mutants in either eIF4E or eIF(iso)4E lack visible phenotypes, and knocking out one of the pair increases the expression level of the other (Combe et al, 2005; Duprat et al, 2002; Piron et al, 2010; Yoshii et al, 2004). In some others, down-regulation of eIF(iso)4E does not increase eIF4E expression (Combe et al, 2005; Rodríguez-Hernández et al, 2012). Some studies suggested that eIF4E isoforms have non-complementary functions and they are likely responsible for selective mRNA translation (Kawaguchi & Bailey-Serres, 2002; Kropiwnicka et al, 2015; Martínez-Silva et al, 2012), or have specific functions in plant development (Dinkova et al, 2011; Mayberry et al, 2009; Rodriguez et al, 1998), virus infection (Robaglia & Caranta, 2006; Sanfaçon, 2015), and stress resistance (Martínez-Silva et al, 2012; Salazar-Díaz et al, 2021). Other cap-binding proteins within the eIF4E family that have recently been identified include the novel cap-binding protein (nCBP), and *A. thaliana* eIF4E1b and eIF4E1c. The biological functions of these eIF4E-related proteins and their interaction partners are yet to be investigated (Joshi et al, 2005; Kropiwnicka et al, 2015; Patrick et al, 2014).

Structural biology studies reveal that eIF4E displays a crescent-shaped conformation formed by a strongly bent beta sheet consisting of eight antiparallel β-strands (Miras et al, 2017; Monzingo et al, 2007). The dorsal surface is formed by three α-helices which surround the convex side of crescent (Miras et al, 2017; Monzingo et al, 2007). The ventral surface, or concave side, contains the cap-binding pocket supported by two highly conserved Trp residues (Miras et al, 2017; Osborne & Borden, 2015; Volpon et al, 2019). eIF4G binds to the dorsal surface of eIF4E by two domains (Grüner et al, 2016; Osborne & Borden, 2015; Volpon et al, 2019). The ventral surface of eIF4E also contains different or overlapping binding domains for RNA structures, viral VPg, and chemical inhibitor (Borden & Volpon, 2020). Additionally, other proteins, such as Eukaryotic translation initiation factor 4E (eIF4E)-binding protein (4EBP), interact with eIF4E mainly on the dorsal side to regulate its function (Borden & Volpon, 2020).

1.2.1.1 eIF4E/eIF(iso)4E initiates cap-dependent translation

The canonical role of eIF4E/eIF(iso)4E, as indicated by their names, is to initiate mRNA translation by recognising the methyl-7-guanosine (m^7G) cap structure on the 5' end of mRNA (Borden & Volpon, 2020; Shopan et al, 2020). All plant mRNA possess a methyl-7-guanosine (m^7G) cap structure. When eIF4E binds to the mRNA cap structure, it recruits the core scaffolding protein eIF4G to assemble the eIF4F complex. The eIF4F complex then assembles DEAD-box

helicase eIF4A, and associates with the 43S pre-initiation complex (PIC) via the interaction with eIF3 (Borden & Volpon, 2020; Hinnebusch, 2014; Shopan et al, 2020). After the translation initiation complex is assembled, 43S PIC scans from 5'UTR until it meets a start codon, then it recruits the 60S ribosome subunit to form the 80S ribosome, and subsequently translation sets off. In the translation initiation complex, eIF4G also interacts with the poly(A) binding protein (PABP) to promote translation by binding to the RNA poly(A) tail in 3'UTR (Hinnebusch, 2014). The poly(A) tail is another feature that plant mRNA possess. This move circularizes mRNA as well as stabilizes the eIF4E-cap interaction (Hinnebusch, 2014). Similarly, eIF(iso)4E forms the eIF(iso)4F complex with eIF(iso)4G, which initiates translation in an identical process as its counterpart complex eIF4F (Sanfaçon, 2015; Wang, 2015).

1.2.1.2 eIF4E regulates mRNA processing and translation

Apart from its essential role in eukaryotic mRNA translation, eIF4E is also a regulator of the process. eIF4E is found in both cytoplasm and nucleus and forms nuclear bodies in many organisms. As reviewed by Borden & Volpon (2020) and Mars et al (2021), nuclear localized eIF4E plays roles in mRNA capping (Culjkovic-Kraljacic et al, 2020), 3' end processing (Davis et al, 2019), and nuclear export of specific mRNAs through a direct interaction with mRNA cap or interactions with other cap-binding proteins (Cohen et al, 2001; Culjkovic & Borden, 2009; de Sousa Abreu et al, 2009; Jeong et al, 2019; Lee et al, 2016). eIF4E may have a wider variety of roles in translation regulation through interactions with RNA modalities other than the cap (Liu et al, 2011; Martin et al, 2011). It also shows regulation roles in mRNA translation (Feoktistova et al, 2013), RNA cleavage (Davis et al, 2019), splicing (Ghram et al, 2022), as well as nuclear export through interactions with other proteins (Culjkovic-Kraljacic et al, 2012). Unfortunately, the functions of eIF4E or eIF(iso)4E beyond translation initiation are still not clear in plants. In *A. thaliana* cells, the nuclear localization of eIF4E changes with the phases of the cell cycle, while eIF(iso)4E distributes to both the cytoplasm and nucleus (Bush et al, 2009), indicating that the isoforms may have divergent roles in plant development. The nuclear localization of eIF4E and eIF(iso)4E in plant cells supports the assumption that plant eIF4E and eIF(iso)4E are also involved in mRNA nuclear export and processing as observed in other organisms.

1.2.2 eIF4E is a host factor for virus infection

Viruses hijack host translation machinery to synthesize their proteins with non-canonical strategies. Unlike cellular mRNA, the genomic RNA of +ssRNA viruses recruits the cellular translation machinery via specific structures, such as Internal Ribosome Entry Site (IRES) located in the 5'UTR or intergenic region, and CITEs found on the 3' UTR or even within ORF of viral RNA (Au & Jan, 2014; Martin et al, 2011; Sanfaçon, 2015; Simon & Miller, 2013; Yamamoto et al, 2017).

Some plant viruses, especially viruses from the *Potyviridae* family, hijack the host translation machinery by their VPg, which is a small protein covalently linked to the 5' end of their RNA (Sanfaçon, 2015; Tang et al, 2020; Wang, 2015). A universal property of VPgs in these viruses is that they are intrinsically disordered for versatility in interaction with different host partners (Sanfaçon, 2015). To date, the best model to explain the indispensability of eIF4E/eIF(iso)4E for the infection of potyviruses is that VPg acts as a m^7G cap mimic that binds to the eIF4E/eIF(iso)4E cap-binding pocket to initiate the assembly of the eIF4F/eIF(iso)4F complex and the cascade of events leading to viral RNA translation as shown in Fig. 2 (Wang & Krishnaswamy, 2012). VPg can outcompete the cellular mRNA m^7G cap, thus prioritizing the translation of viral RNA (Coutinho de Oliveira et al, 2019b; Eskelin et al, 2011; Khan et al, 2008; Michon et al, 2006).
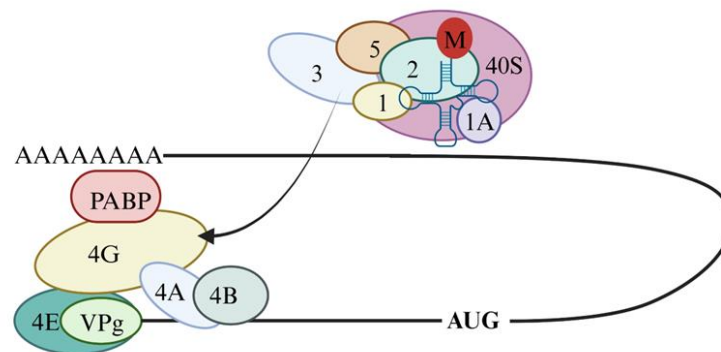
Figure 2. eIF4E/eIF(iso)4E as indispensable host factor for potyvirus RNA translation

VPg acts as mRNA cap structure mimic to interact with eIF4E/eIF(iso)4E for recruiting the host translation machinery, 4A, 4B, 4E, 4G, 1, 1A 2, 3, 5 indicate eukaryotic translation initiation factors. Picture produced with BioRender.

However, eIF4E/eIF(iso)4E binding to VPg as a cap mimic to initiate viral RNA translation alone may not fully explain the critical role of this host factor. First, eIF4E/eIF(iso)4E is host factor not only for potyviruses but also for some non-potyviruses (Atarashi et al, 2020; Nieto et al, 2007; Yoshii et al, 1998). Some of these non-potyviruses do not even possess a VPg. One example is *Melon necrotic spot virus* (MNSV, a member of *Carmovirus*) that infects melon or cucumber (Atarashi et al, 2020; Nieto et al, 2007; Wang & Krishnaswamy, 2012; Yoshii et al, 1998). In this case, eIF4E targets the CITE structure (Nieto et al, 2006; Nieto et al, 2007). Consistently, MNSV resistant mutations in eIF4E are not found in the cap-binding domain as most potyvirus resistance mutations (Nieto et al, 2006; Nieto et al, 2007). VPgs from non-potyviruses have no sequence or structural similarity with potyviral VPgs (Coutinho de Oliveira et al, 2019a; Coutinho de Oliveira et al, 2019b). They may interact with eIF4G instead of eIF4E for translation initiation, as in the case of the *Sobemovirus Rice yellow mottle virus* (RYMV) (Albar et al, 2006; Hébrard et al, 2010).

Second, translation initiation does not necessarily depend on eIF4E/eIF(iso)4E in potyviruses. For example, the RNA of *Tobacco etch virus* (TEV) has a translational enhancer structure that recruits eIF4G directly to form an eIF4F complex for translation initiation (Gallie, 2001). However, TEV still requires a functional eIF(iso)4E for infection in *A. thaliana* and eIF4E in tomato (Gallie, 2001; Mazier et al, 2011). eIF4E/eIF(iso)4E from susceptible cultivars do not necessarily interact with the VPg of viruses infecting them (Gallois et al, 2010; Gao et al, 2004b; Hébrard et al, 2010). Reversely, eIF4E/eIF(iso)4E from resistant cultivar may still retain its interaction with VPg, as in the case of TuMV resistance allele ConTR01 in Chinese cabbage, which is mapped to eIF(iso)4E. However, the resistance conferred by ConTR01 is dominant, while nearly all other eIF4E/eIF(iso)4E-associated resistances are recessive (Rusholme et al, 2007). eIF(iso)4Es isolated from resistant and susceptible cultivars all interact with VPg by yeast two hybrid assay (Nellist et al, 2014).

Third, mutations in other viral proteins rather than VPg are responsible for resistance breakage in some cases. For instance, a single nucleotide substitute in virus P1 of *Clover yellow vein virus* (ClYVV) is sufficient to overcome *cyv-2* resistance (Nakahara et al, 2010). In the case of LMV, mutations in CI account for breakdown of *eIF4E*-mediated resistance (Abdul-Razzak et al, 2009; Roudet-Tavert et al, 2007; Tavert-Roudet et al, 2012).

Fourth, eIF4E/eIF(iso)4E may play diverse roles in the virus infection cycle through direct or indirect interaction with other viral proteins. eIF(iso)4E is found in the membrane associated vesicles of infected cells with NIa-Pro, supporting its possible role in viral RNA replication (Beauchemin et al, 2007; Beauchemin & Laliberté, 2007; Dinkova et al, 2016; Thivierge et al, 2008). eIF(iso)4E interacts with CP of TEV in *A. thaliana* to promote viral movement (Contreras-Paredes et al, 2013). Moreover, eIF4E/eIF(iso)4E interacts with other potyviral proteins such as HC-Pro, P1 and VPg (Ala-Poikela et al, 2011; Nakahara et al, 2010; Shopan et al, 2020). These viral proteins play multifunctional roles such as genome amplification, RNA silencing suppressing, and host adaptation.

Finally, since the affinity of eIF4E/eIF(iso)4E for VPg is higher than that for mRNA cap (Khan et al, 2008; Léonard et al, 2000; Plante et al, 2004), eIF4E/eIF(iso)4E depletion by VPg might decrease cellular mRNA translation and favor viral RNA translation (Eskelin et al, 2011; Sanfaçon, 2015). In most cases, viral VPg preferably binds to either eIF4E or eIF(iso)4E (Sanfaçon, 2015; Wang and Krishnaswamy, 2012). eIF4E and eIF(iso)4E may be differentially regulated and subcellularly distributed subject to cell types, developmental stages, stress conditions, etc. (Bush et al, 2009; Salazar-Díaz et al, 2021). Therefore, the shift in the proportion of eIF4E/eIF(iso)4E available to host cell might be associated with altering cellular gene expression profile to favor the propagation of the virus (Khan et al, 2008; Léonard et al, 2000).

However, we are far from understanding the exact mechanics of how eIF4E/eIF(iso)4E regulates virus infection beyond translation. Results from reverse genetics studies added more complexity to the functions of eIF4E/eIF(iso)4E and their dependence on VPg as well as other viral and host factors in facilitating virus infection. As evident in dominant negative resistance, overexpressing a mutated eIF4E with disabled VPg interaction confers resistance (Cavatorta et al, 2011; Duan et al, 2012; Gutierrez Sanchez et al, 2020; Kang et al, 2007). On the other hand, transforming susceptible eIF4E into a resistant plant disrupts resistance, even when the susceptible eIF4E is derived from a different plant species (Estevan et al, 2014; Li & Shirako, 2015). As mentioned, potyvirus translation and replication are likely a coupled process (Wang, 2015), making it difficult to specify the role of eIF4E/eIF(iso)4E other than that in translation. Thereby, studying eIF4E/eIF(iso)4E associated host factors may provide a unique angle to understand the complex functions of eIF4E/eIF(iso)4E in the entire virus life cycle.

1.2.3 The application of eIF4E/eIF(iso)4E-based resistance

eIF4E/eIF(iso)4E-based resistance has great potential in agricultural practices as it is the essential host factor for a large plant virus family that includes so many agriculturally important viruses. Infection by these viruses relies on either eIF4E or eIF(iso)4E, mutating one of them does not affect plant physiology and viability thanks to their redundant function. Moreover, the functional domain of eIF4E/eIF(iso)4E as a virus host factor may not overlap with that for its regular functionality in plant. Therefore, it is possible to develop resistance targeting to eIF4E/eIF(iso)4E to achieve broad spectrum resistance without compromising yield (Bastet et al, 2017; Wang, 2015).

1.2.3.1 Conventional breeding and mutagenesis

Plant virus resistance occurring in nature falls into two categories: dominant and recessive. Dominant resistance is highly specific, most of dominant resistance genes belong to the nucleotide binding site-leucine rich repeat (NBS-LRR) genes and proteins encoded by these genes recognise pathogen virulence factors in a "gene-for-gene" manner (Maule et al, 2007). However, in rare cases, dominant resistance is conferred by mutations in eIFs, possibly in a dominant-negative mode (Rubio et al, 2019; Rusholme et al, 2007). Most of the recessive resistance genes characterized to date encode translation initiation complex components, such as eIF4E/eIF(iso)4E and eIF4G, with a few exceptions (Albar et al, 2006; Lee et al, 2010; Rubio et al, 2019; Shopan et al, 2017).

Though the naturally existing recessive resistances conferred by mutations in host factors are not restricted to mutations in eIFs, the non-eIF host factor-based resistance usually is less effective and has narrower spectrum resistance compared with eIF4E/eIF(iso)4E-based resistance as reviewed by Hashimoto et al (2016). However, pyramiding eIF4E/eIF(iso)4E-based resistance by knocking out or mutating both will cause growth defect in plants (Bastet et al, 2017; Callot & Gallois, 2014; Gauffier et al, 2016; Patrick et al, 2014; Rodríguez-Hernández et al, 2012). Stacking resistance with other host factor-based resistance may overcome this barrier to achieve broad-spectrum resistance.

With many existing eIF4E-based virus-resistant alleles identified, introgressing them into cultivars by breeding is a straightforward process. Moreover, conventional breeding (or traditional breeding) is still by now the only crop improvement approach accepted by nearly the entire general public (Pavan et al, 2010). However, this type of breeding is a time-consuming and laborious process.

In practice, TILLING (Targeted Induced Local Lesions IN Genomes) technology, chemical mutagenesis followed by screening with primers targeting to the desired locus, is being used to obtain novel resistance genes (Fondong et al, 2016; McCallum et al, 2000; Schmitt-Keichinger, 2019). EcoTILLING is an adaptation of TILLING being used to identify polymorphisms in natural populations (Comai et al, 2004). TILLING and EcoTILLING are less time-consuming and more cost-efficient ways to develop cultivars that contains eIF4E-based resistance to potyviruses in both crop cultivars and model plants. These techniques are not restricted by the plant's genome size and ploidy (Kurowska et al, 2011) and not based on genetic modification, and therefore is not subject to GMO regulations. However, the weakness of TILLING and EcoTILLING is that it is highly difficult to identify mutants from gene families sharing similar sequences and functions, as well as those near simple sequence repeats (Gauffier et al, 2016; Ülker & Weisshaar, 2011).

1.2.3.2 Genetic transformation

Genetic transformation is the most common way to introduce desirable traits into crops. Compared with breeding and mutagenesis, genetic transformation saves much time and labor. Moreover, the transgene is not necessarily from the same species, and transgene does not change the genetic composition of the cultivar (Niraula & Fondong, 2021). However, some species is recalcitrant to genetic transformation, and most importantly, genetic modified crops are surrounded by controversies and public concerns. Some of the concerns are not unbased, such as the leakage of transgene into other organisms in the environment, even into plant-infecting viruses by recombination, and the potential toxic effect of the transgene on consumers (Niraula & Fondong, 2021; Voloudakis et al, 2021). It is not surprising that genetically modified plant products often encounter strict regulations and oppositions in the market.

Virus resistance engineering strategies include incorporating resistance genes, expressing a part of the viral genome to induce RNA silencing, silencing an essential host factor for virus infection, and expressing a loss-of-function variant of host factor to generate dominant-negative resistance (Niraula & Fondong, 2021; Voloudakis et al, 2021). To date, RNAi directly targeting viral genomic RNA is the most common strategy used by commercialised genetically modified cultivar with virus resistance (Niraula & Fondong, 2021; Voloudakis et al, 2021). However, many virus resistances based on eIF4E or its isoform have been successfully generated in cultivars, such as plum (Wang et al, 2013), Chinese cabbage (Kim et al, 2014), tomato (Atarashi et al, 2020; Kuroiwa

et al, 2022; Moury et al, 2020; Yoon et al, 2020), potato (Miroshnichenko et al, 2020), soybean (Gao et al, 2020), cucumber (Chandrasekaran et al, 2016), wheat (Rupp et al, 2019), and so on.

1.2.3.3 Targeted genome editing

Genome editing is a young yet fast-developing technology. Theoretically, genome editing systems could induce precise deletions, insertions, and specific modifications in the genome of a transformable plant (Schmitt-Keichinger, 2019). After the desired mutations are introduced, the genome editing system components can be segregated from the cultivar, the resulting crop is no different to mutated or natural variant. Moreover, genetic editing system components can be delivered directly, to further reduce the concerns about whether the edited plants are classified as genetic modified plants (Kanchiswamy et al, 2015; Woo et al, 2015).

The first-generation genome editing technique was built upon chimeric proteins consisting of programmable, specific DNA-binding motif and non-specific nuclease to cleave genome at desired sites, such as zinc finger nucleases (ZNFs) and transcription-activator-like effector nucleases (TALENs) (Zhao et al, 2020b). Another application of these genome-editing systems is to confer virus resistance in plants by expressing the DNA-binding domains that target to conserved viral motifs (Cheng et al, 2015; Ordiz et al, 2010; Sera, 2005; Zhao et al, 2020b).

However, designing ZNFs and TALENs is not an easy task. As a result, these techniques quickly made way for the newer generation of genome editing technique: the CRISPR/Cas (clustered, regularly interspaced, short palindromic repeat associated protein) system, which is composed of an endonuclease Cas protein and a single guide RNA (sgRNA). sgRNA contains a Cas protein binding structure, and a spacer sequence of about 20-nt that can be designed to target to the desired sequence (Cong et al, 2013; Mali et al, 2013). Like ZNF and TALEN component, the CRISPR/Cas system can also be adapted to target viral genome directly to attain resistance (Makarova et al, 2018; Zhao et al, 2020b). Nevertheless, this antiviral strategy requires introducing foreign genes into the plants through genetic transformation, thus misses out on the advantage of genetic editing. Another antiviral approach via genome editing is to precisely edit essential host factors like eIF4E and its isoform. This approach holds great promise as it may get away from GMO regulations.

Existing host factor-based virus resistance generated by genetic editing techniques is mostly based on knocking out the host factor by deletions (Atarashi et al, 2020; Chandrasekaran et al, 2016;

Duprat et al, 2002; Kuroiwa et al, 2022; Lellis et al, 2002; Pyott et al, 2016; Sato et al, 2005; Takakura et al, 2018; Yoon et al, 2020; Yoshii et al, 1998; Zhao et al, 2020). To tap the full potential of genetic editing technology, more studies on the structures of the host translation initiation proteins, their paralogs, and interaction partners are needed. The availability of such information, combined with knowledge obtained from natural resistant variants, will allow for more precise and accurate editing of the host factors for broad spectrum, durable resistance without compromising plant viability.

1.2.4 The significance of studying eIF4E-associated host factors

As a decisive plant host factor for infections by many potyviruses as well as some non-potyviruses, eIF4E/eIF(iso)4E-based mutations are present in natural resistant variants, and eIF4E/eIF(iso)4E is frequently edited/modified to achieve virus resistance in crops or model plants (Bastet et al, 2017; Sanfaçon, 2015; Wang and Krishnaswamy, 2012). Mutations in eIF4E/eIF(iso)4E possibly confer broad-spectrum resistance because viruses hijack them by similar translation strategies. Despite the advantages of targeting eIF4E/eIF(iso)4E for resistance and the successes achieved, relying exclusively on eIF4E/eIF(iso)4E-based mutations as sole source of recessive resistance is risky. Resistance breakage is already existing in nature and constantly evolving. Viruses can shape their eIF4E/eIF(iso)4E interaction motif in order to fit into the resistant version for compatible interaction, or to adapt to the other isoform (Jenner et al, 2010; Takakura et al, 2018). As mentioned, simultaneous mutation in eIF4E and eIF(iso)4E to pyramid resistance is impossible because of developmental defects (Bastet et al, 2017; Hashimoto et al, 2016). Therefore, to expand the resistance spectrum further, constant efforts should be made to look for substitute host factors as new targets of recessive resistance.

A promising approach is to search for eIF4E/eIF(iso)4E-associated host factor(s) for virus infection. Indeed, eIF4E/eIF(iso)4E-interacting translation initiation complex components such as eIF4G and its isoform have also been found to play essential roles in virus infection.

1.3 HSP70 family proteins

Heat shock proteins (HSPs) are a group of highly conserved, stress-responsive molecular chaperones widely present in living organisms from bacteria to plants and mammals (Singh et al, 2019; Usman et al, 2017). HSPs were discovered in *Drosophila* after exposure to heat stress in

1960s, and were studied in yeast, *E. coli*, and plants as early as in 1980s (ul Haq et al, 2019). Since then, there is a large volume of literature on HSPs in different organisms, especially in the context of human diseases and aging as well as environmental and climate changes (Rana et al, 2018; Rosenzweig et al, 2019; Singh et al, 2019; ul Haq et al, 2019). In plants, they are known to play housekeeping roles in growth and development under normal conditions, and vital roles in diverse stress conditions such as heat stress, cold stress, drought, high salinity, oxidative stress, heavy metal stress, as well as biotic stresses (Guo et al, 2014; Singh et al, 2016; Timperio et al, 2008; ul Haq et al, 2019). Plant HSPs are located in different cellular compartmentations including the nucleus, plastid, mitochondria, ER, and cytoplasm (Karlin & Brocchieri, 1998). HSPs can be classified into six major groups based on their molecular weight: HSP100, HSP90, HSP70, HSP60, HSP40, and small HSPs.

HSP70 is the major and most conserved family of protein chaperones present in all living organisms with molecular weight between 68-78 kDa (Lindquist, 1986). The HSP70 superfamily in *A. thaliana* consists of 18 members, with 14 of them being the DnaK subfamily and 4 belonging to the HSP110/SSE subfamily (Sung et al, 2001a; Sung et al, 2001b). It is predicted that among the DnaK subfamily of HSP70 in *A. thaliana*, one of them is supposedly a pseudogene whose location is unknown, 5 are cytosolic, 3 reside in the ER lumen, 2 locate in mitochondria, and 3 in plastid (Sung et al, 2001a; Sung et al, 2001b).

1.3.1 Structure and functions of HSP70

HSP70 family protein is composed of a highly conserved N-terminal ATPase domain (also named as the nucleotide binding domain, NBD) of about 44 kDa, and a substrate binding domain (SBD) of about 18 kDa connected to NBD by a flexible linker domain (Lu et al, 2014; Rosenzweig et al, 2019; Sarkar et al, 2013). At the C-terminus of the SBD, sometimes classified as a part of SBD, is a variable C-terminal lid of about 10 kDa (Sarkar et al, 2013). In the extreme ends of HSP70 are N- and C- terminal variable regions containing optional targeting or retention signals determining its subcellular localization (Lin et al, 2001). Fig. 3A shows the functional domains and the number of amino acids of each functional domain.

The ATPase domain acts by ATP hydrolysis-driven conformational change to regulate the substrate binding and release of the SBD, which binds to short linear stretches of hydrophobic

residues (Dragovic et al, 2006; Lund, 2001; Rosenzweig et al, 2019; Sharma & Masison, 2009). Two co-chaperones: HSP40/J-domain proteins and nucleotide exchange factors (NEF) assist HSP70 to function properly (Mayer, 2010; Mayer et al, 2001; Sarkar et al, 2013). A chaperone cycle of HSP70 starts with the binding of ATP to the NBD. In this state, the C-terminal lid remains open, and the substrate binds to or releases from the SBD (Mayer, 2010). This is followed by the hydrolysis of ATP into ADP catalyzed by both J-domain proteins and NEFs (Sarkar et al, 2013). Once HSP70 is bound by ADP, the C-terminal lid is closed, trapping the substrate protein in the SBD for processing or submission to targeted site (Mayer et al, 2001; Rosenzweig et al, 2019). Finally, NEFs facilitate the discharge of ADP from the NBD and the binding of a new ATP, starting a new HSP70 chaperone cycle (Mayer, 2010; Mayer et al, 2001; Rosenzweig et al, 2019; Sung et al, 2001a). Fig. 3B is a graphic representation of HSP70 cycle of substrate binding and release.

Working with co-chaperones and various other cellular machineries, and operating in different modes, HSP70s perform multiple functions such as *de novo* protein folding and refolding of non-native proteins, handing substrates to protein quality control machineries, protein disaggregation, protein complex assembly and disassembly, and protein translocation to subcellular compartments such as mitochondria and chloroplast (Rana et al, 2018; Rosenzweig et al, 2019). With such a variety of functions, HSP70 is associated with plant growth and development, and plant responses under many stressful situations.

A

N terminal variable domain with optional targeting signal

C terminal variable domain with optional retention signal

	ATPase domain	Peptide binding domain	

3~81   ~370   ~210~260   ~30

B

JDP

Pi

ADP

NBD

Low affinity "Open"

NBD
ATP
SBD

SBD

High affinity "Closed"

ADP   NEFs   ATP
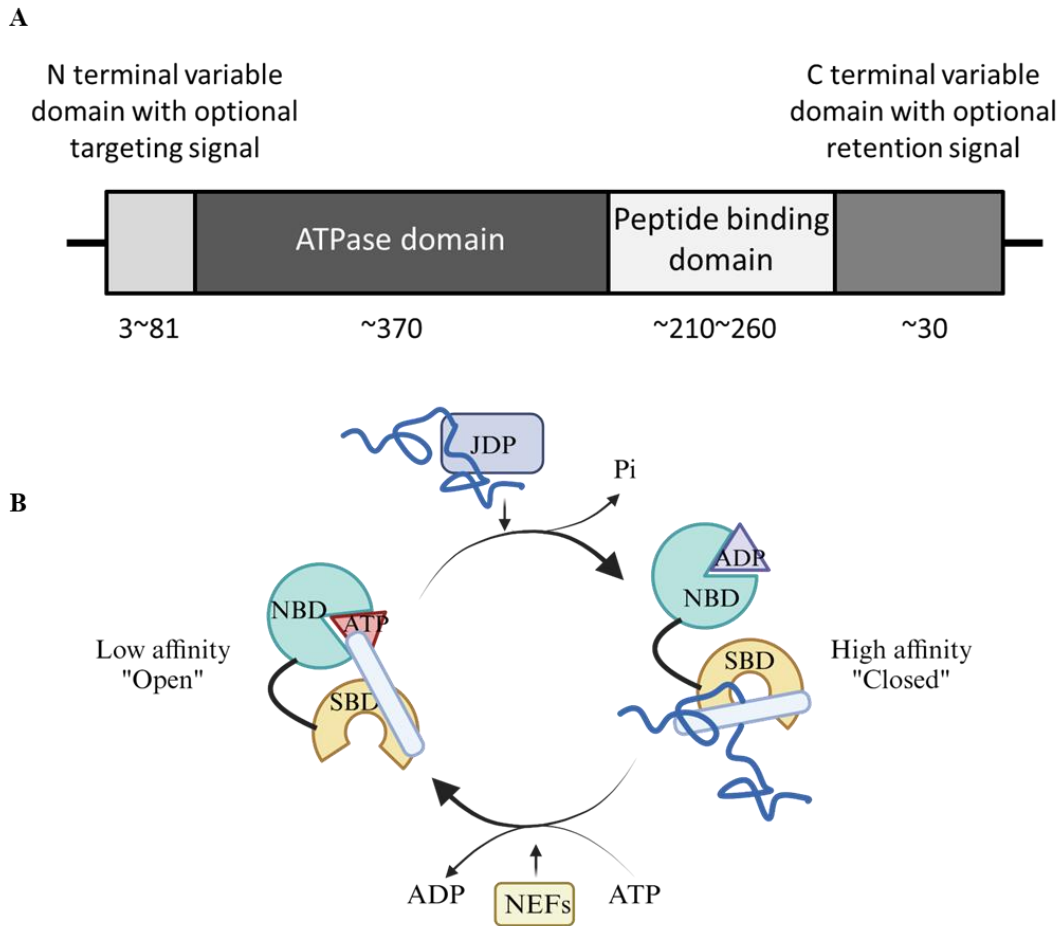
Figure 3. Functional domains of *A. thaliana* HSP70 and HSP70 cycle

(A) Functional domains of *A. thaliana* showing N-terminal variable domain (NVD), ATPase or nucleotide-binding domain (NBD), peptide or substrate binding domain (SBD), and C-terminal variable domain (CVD). The approximate number of amino acids for each domain is shown.

(B) HSP70 cycle of substrate binding and release. Picture produced with BioRender.

1.3.2 HSP70 in plant growth and development

It is important to note that HSP70s are not just induced upon stress to protect plant under a critical environment. As a matter of fact, they are constitutively and ubiquitously expressed, and are associated with different plant organs in different developmental stages (Gupta & Golding, 1993; Sarkar et al, 2013; Sung et al, 2001a). In plant cells, they maintain protein homeostasis by promoting correct folding, preventing protein aggregation in normal conditions, helping the transportation of proteins to their destination such as PD, mitochondria, and plastid or across membranes (Aoki et al, 2002; Ueki & Citovsky, 2011; Wang et al, 2004), and facilitating protein degradation by proteasome or lysosome pathways (Hartl et al, 2011; Kotak et al, 2007). In human cells, HSP70 is involved in modulating signal transduction pathways through interactions with signal transduction line protein kinase A, protein kinase C, and protein phosphatase (Ding et al, 1998). In plants, HSP70s participate in regulating the expression of signal transduction pathway genes in both stress and normal conditions (Wang et al, 2004). HSP70s are important for plant development and seed germination (He et al, 2008; Jung et al, 2013; Maruyama et al, 2010; Maruyama et al, 2014; Ohta et al, 2013; Rowarth et al, 2019; Su & Li, 2008; Sung et al, 2001a; Wakasa et al, 2011). HSP70s, especially those with organelle localization, are indispensable for the biogenesis and development of plant organelles such as mitochondria and chloroplast (Dudley et al, 1997; Haynes & Ron, 2010; Kim & An, 2013; Shi & Theg, 2010; Wang et al, 2004).

1.3.3 HSP70 association with abiotic stress

As reviewed in (Ray et al, 2016; ul Haq et al, 2019), the expression of HSP70 in a number of plant species is up-regulated in nearly all abiotic stress conditions. Heat shock response (HSR), or the transcriptional regulation of heat shock proteins, is regulated by heat shock factors (HSF), transcription factors which bind to heat shock elements (Akerfelt et al; PIRKKALA et al, 2001). Compared with other eukaryotes, plants possess diverse HSFs (Virdi et al, 2015), and their HSR show considerable complexity and uniqueness, helping them to survive through continuous environmental fluctuations (Bokszczanin et al, 2013).

The HSFA class of HSFs is responsible for regulating HSPs cycle (Yoshida et al, 2011). Under normal conditions, HSFs are maintained in the inactive monomer state in the cytoplasm. Upon stress conditions, stress signals are generated by different stress sensors, and then converge into

signal transduction cascades involving secondary messengers (such as Ca^{2+}, H_2O_2 and NO), kinases (such as CDPKs and MAPKs), phosphatases, and transcriptional regulators [such as DREB2 (dehydration responsive element binding) family transcription factors] (Dong et al, 2015; Mittler et al, 2012; Qin et al, 2011; Ray et al, 2016). Following the signal transduction cascades, HSFA is phosphorylated and activated to form homo-trimer that binds to Heat shock elements (HSE) in the promoter region (Ali et al, 1998; Zou et al, 1998), and activates the expression of HSPs and a "transcriptional relay" of HSFAs to maintain a strong and prolonged HSR by positive feedback loop (Calderwood et al, 2010; Yoshida et al, 2011). HSP70/90 and possibly other chaperones regulate the HSR in a negative feedback manner as stated by a "chaperone titration model" (Guo et al, 2001; Volkov et al, 2006), as free HSP70/90 (without binding to an unfolded/misfolded client) sequesters HSFs to regulate HSR in a fine-tuned manner (Hahn et al, 2011; Meiri et al, 2010).

HSP70 plays important roles for plants to cope with various abiotic stresses such as heat, drought, salinity, cold, UV radiation, etc. (Alvim et al, 2001; Anaraki et al, 2018; Cho & Choi, 2009; Jacob et al, 2017; Jungkunz et al, 2011; Kim & An, 2013; Lee et al, 2009; Liu et al, 2014; Park & Seo, 2015; Ré et al, 2017; Sarkar et al, 2013). Overexpressing HSP70 could improve plant tolerance to a wide range of abiotic stresses and could be used as one of the strategies for engineering stress tolerance in crop cultivars (Singh et al, 2019). Due to crosstalk between different stress pathways, HSP70s are also involved in stress priming and plant memory of pre-exposure to various abiotic conditions (Goswami et al, 2010; Nair et al, 2022).

1.3.4 HSP70 association with UPR

HSP70s residing in the ER are also named Binding immunoglobulin protein (BiP). They have another mode of transcriptional regulation by the unfolded protein response (UPR). ER stress is imposed by external stimuli from biotic or abiotic stresses, which cause disruption of cellular redox equilibrium and calcium homeostasis, followed by increase in protein synthesis and dysfunctional post-transcriptional modifications. The result is accumulation of mis-folded or unfolded protein in the ER lumen, triggering UPR (Iwata & Koizumi, 2012; Kleizen & Braakman, 2004; Ye et al, 2011). UPR initiates a complex signaling cascade, resulting in the adaptation to ER stress or apoptosis if unable to cope with ER stress (Chen & Brandizzi, 2013; Hetz, 2012; Walter & Ron, 2011; Wang et al, 2014; Williams et al, 2014).

In plants, there are three known UPR pathways: the most conserved IRE1-bZIP60 (basic leucine zipper) branch, analogous to the mammalian inositol-requiring transmembrane kinase/endonuclease (IRE1) pathway; a branch involving S1P/S2P (site-1/site-2 proteases)-bZIP17/bZIP28, analogous to mammalian activating transcription factor 6 (ATF6) pathway (Deng et al, 2011; Gao et al, 2008; Liu & Howell, 2010; Liu et al, 2007; Nagashima et al, 2011); and a recently discovered branch governed by GCN2 (General Control Non-repressible 2) kinase, corresponding to the mammalian branch consisting of GCN2 and PERK (RNA dependent Protein Kinase like ER kinase) (Kørner et al, 2015; Liu et al, 2019; Wek et al, 2006). IRE1 senses ER stress through the luminal domain and transmits signals through its kinase and RNase domains to the effector domain on the cytoplasmic side (Walter & Ron, 2011). Activated IRE1 dimerizes, trans-autophosphorylates, and mediates the alternative splicing of bZIP60 mRNA, producing an active transcription factor that translocate to the nucleus to up-regulate UPR target genes (Afrin et al, 2019; Zhang & Wang, 2012). Plant GCN2 kinase activation mechanism is unknown, and plants do not contain homolog of the mammalian ER stress sensor PERK. However, it has been known that GCN2 responds to ER stress-related stimuli, as well as various biotic and abiotic stresses (Faus et al, 2015; Lageix et al, 2008; Li et al, 2018c; Liu et al, 2015; Monaghan & Li, 2010).

bZIP17/bZIP28 are membrane-tethered transcription factors retained in the ER by BiPs. In plants, ER stresses deplete BiPs and unleash bZIP17/bZIP28, and free bZIP17/bZIP28 traffic to the nucleus via Golgi body to transcribe UPR genes (Iwata & Koizumi, 2012; Wahyu Indra Duwi et al, 2013). In mammalian cells, IRE1 is regulated by BiP in the same negative feedback cycle (Bertolotti et al, 2000; Herath et al, 2020; Srivastava et al, 2013). These discoveries suggest that BiP, as a downstream gene in UPR response, is not only an effector in alleviating ER stress but also a negative regulator of both UPR pathways in plants.

ER stress signaling is much less studied in plants than that in animals and yeast. In plants, ER stress is associated with multiple abiotic stress conditions, infections by viruses, fungi, and bacteria, plant physiology and pollen development, as reviewed in (Park & Park, 2019; Pastor-Cantizano et al, 2020; Singh et al, 2021; Verchot & Pajerowska-Mukhtar, 2021). In plants, BiP expression level is altered under stress, but not unanimously upregulated as for cytosolic HSP70s (Henriquez-Valencia et al, 2015; Wang et al, 2017). BiP contributes to defense against various abiotic stresses (Alvim et al, 2001; Srivastava et al, 2013; Valente et al, 2008; Wang et al, 2017). However, the

role of UPR and BiP in pathogen infection is ambiguous, especially in virus infection (Herath et al, 2020; Park & Park, 2019; Park & Seo, 2015; Verchot & Pajerowska-Mukhtar, 2021; Zhang & Wang, 2012). For example, previous studies have demonstrated that infection by a number of plant viruses, including TuMV, *Potato virus X* (PVX), and *Plantago asiatica mosaic virus* (PlAMV) can induce bZIP60 mRNA splicing and their membrane-associated proteins such as 6K2 or TGBp3 (triple gene block proteins 3) are the effector to trigger the UPR in plant cells (Zhang & Wang, 2016). Silencing or knock-out of the IRE1-bZIP60 branch inhibits viral infection (Gayral et al, 2020; Li et al, 2021; Li et al, 2020; Li et al, 2018b; Luan et al, 2016; Zhang et al, 2015). However, in another study with IRE1 mutant plants, TuMV infection was higher in inoculated leaves and both TuMV and PlAMV systematic movement were increased by IRE1 knockout (Gaguancela et al, 2016). Apart from the IRE1/bZIP60 pathway, *rice stripe virus* (RSV) induces UPR through the bZIP17/28 branch, and that UPR plays dual roles in the infection of the virus through mediating the accumulation of movement protein (Li et al, 2021; Li et al, 2022).

1.3.5 HSP70 association with biotic stress

Unlike animals that possess immune system with specified organs and cells dedicated to defense against invading pathogens, plants deal with invading pathogens with their genetically encoded and intertwined barricade of pathways mediated by membrane-bond pattern recognition receptors (PRRs), intracellular effector recognition receptors, phytohormones, and stress-related molecules including HSPs.

HSP70s are up-regulated in some viral and fungal infections probably through the induction of oxidative stress or UPR by pathogens (Jacob et al, 2017; Piterková et al, 2013; ul Haq et al, 2019), but whether its protective or harmful for the plan during infection is case by case (Ray et al, 2016). The reduced expression level of HSP70 is associated with increased growth of certain bacterial pathogens (Jelenska et al, 2010; Kanzaki et al, 2003; Kim & Hwang, 2014), suggesting its contribution to plant basal defense. HSP70 is also potentially involved in innate resistance by modulating HSP90, which is known to play a direct role in plant immunity by stabilizing resistance proteins, as in the case where a Heat-shock cognate 70 that down-regulates resistance protein mediated resistance (Noël et al, 2007). In the ER, BiPs are important regulators of plant immunity. As reviewed in (Park & Seo, 2015), they participate in (1) the biogenesis, maturation, and correct

folding of membrane PRRs; (2) the production and secretion of defense-related proteins; (3) pathogen-induced hypersensitive response.

HSP70 is hijacked through a direct interaction with *Pseudomonas syringae* type III effector HOPI1. HOPI1 transports HSP70 to the chloroplast and forms a complex with it that is essential for infection (Jelenska et al, 2010). In the infection of powdery mildew in sunflowers, it's found that HSP70 expression and accumulation level is higher in resistant genotypes compared with susceptible ones, indicating HSP70's contribution to resistance (Kallamadi et al, 2018). However, this does not hold true in tomato where HSP70 expression level is up-regulated in susceptible cultivars while remains unchanged in resistant cultivars (Kubienova et al, 2013), illustrating the ambiguous role of HSP70 in plant disease resistance.

In virus infection, it's plausible to hypothesize that HSP70 promote plant resistance by improving the performance of defense-related protein and regulating plant stress response. Indeed, heat treatment that induces HSP70 expression is an established way to eliminate viruses in seeds and vegetative tissues (Hýsková et al, 2021). However, in the majority of the cases, plant viruses have evolved to utilize HSP70 as a host factor for infection.

1.3.6 HSP70 as a host factor in virus infection

Plant virus infection usually upregulates HSP70 expression in its host (Aparicio et al, 2005; Aranda et al, 1996; Chen et al, 2008; Whitham et al, 2003; Yang et al, 2007). HSP70 induction is associated with the compatibility of the virus and the host (Makarova et al, 2018). The profile of HSP70 induction may be determined by many factors such as the virus strain, host species, symptom severity, and the duration of infection. Moreover, whether HSP70 acts against the virus or promotes the infection depends on the specific virus-host pathosystem (Hýsková et al, 2021). In some case where HSP70 may serve as a host factor, HSP70 inhibition or silencing may hinder virus infection. In some others, a fine-tuned heat treatment to induce a spectrum of HSPs as well as other defence mechanisms may help the plant to restrict virus infection. Here, HSPs promote innate immune response, maintain cellular homeostasis, and alleviate the stress posed by virus infection. Therefore, the functional role of HSPs in virus infection is quite complex.

For many plant viruses, HSP70 family proteins seem to play a proviral role. *Beet yellows virus*, a *closterovirus*, encodes its own HSP70 homolog, which functions in viral particle assembly,

intercellular movement, and systematic spread through interactions with viral and host components (Alzhanova et al, 2001; Peremyslov et al, 1999; Prokhnevsky et al, 2005; Prokhnevsky et al, 2002). Other viruses from distinct families have evolved to hijack host HSP70 for their infection. As summarised in Table 1, in general, HSP70 facilitates viral genome replication as a component of the VRC, regulates replication through mediating CP degradation, and participates in virus particle assembly through interaction with CP, and virus movement through interactions with MP. In potyviruses, a heat shock cognate has been found to play a role in virus replication as a component of the VRC, and an *A. thaliana* HSP70 family protein has been found to facilitate virus infection.

Table 1. The summary of existing research about the involvement of host HSP70 proteins in plant virus infection

Virus	Virus co-factor	Roles played	Reference
Cucumber necrosis virus (CNV, Tombusvirus)	Virus replication protein P33, Virion particle, Virus CP	Replicase complex component; facilitate virus replication; facilitate virion disassembly; Increase CP solubility, virus particle assembly, and CP chloroplast targeting.	(Alam & Rochon, 2016; 2017; Serva & Nagy, 2006)
Tomato bushy stunt virus (TBSV, Tombusvirus)	Viral replicase complex, RdRp	Replicase component; assembly of replicase complex; membrane insertion of the viral replication proteins; promote viral RNA synthesis.	(Pogany & Nagy, 2015; Pogany et al, 2008; Wang & Nagy, 2008; Wang et al, 2009a)
Red clover necrotic mosaic virus (RCNMV, Tombusvirus)	Viral replicase complex, virus replication protein p27	Virus replication and assembly of viral replicase complex.	(Mine et al, 2012; Mine et al, 2010)
Beet black scorch virus (BBSV, Tombusvirus)	Virus replication protein p23, capsid protein	Promote replication by alleviating CP's inhibition on replication.	(Wang et al, 2018)
Potato virus A (PVA, Potyvirus)	Co-chaperone CPIP/Viral CP	Regulation of replication through mediating CP degradation.	(Hafrén et al, 2010; Lõhmus et al, 2017)
Turnip mosaic virus	Virus replication protein NIb	Co-localize with VRC and associate with RdRp; facilitate virus infection.	(Dufresne et al, 2008; Jungkunz et al, 2011)
Bamboo mosaic virus (BaMV, Potexvirus)	Viral replicase complex	Replicase component; facilitate replication; involve in infection preference for older leaves.	(Huang et al, 2017)
Tomato Yellow Leaf Curl Virus (TYLCV, Begomovirus)	Virus CP	Co-localize with and promote the formation of nuclear viral DNA-CP aggregate; promote virus infection.	(Gorovits & Czosnek, 2017; Gorovits et al, 2016; Gorovits et al, 2013)
Rice Stripe Virus (RSV, Tenuivirus)	Virus replication protein	Co-localize with RdRp and promote virus infection.	(Jiang et al, 2014)

Abutilon mosaic virus (AbMV, Geminivirus)	Virus movement protein	Co-localize with movement protein oligomers at cell periphery and chloroplasts; viral transport and symptom induction.	(Krenz et al, 2010)
Pepino mosaic virus (PepMV, Potexvirus)	Virus CP	Interact with CP at both nuclear and cytoplasm, co-localize with viral particle at phloem	(Mathioudakis et al, 2012)
Chinese wheat mosaic furovirus (CWMV, Furovirus)	Virus replication protein	Recruited into the viral replication complex (VRC) to promote furoviral replication.	(Yang et al, 2017)
Various viruses		Virus infection induce HSP70; HSP70 facilitate virus infection.	(Chen et al, 2008)

1.4 Research objectives and goals

Identifying host factors for virus infection can advance knowledge about general virus-host interactions as well as plant virology. Though eIF4E/eIF(iso)4E as an essential host factor for potyvirus infection is well established, the exact role that eIF4E/eIF(iso)4E plays in the virus infection cycle within the plant is still not very clear. The highly coupled viral genome translation and replication makes it almost impossible to examine the role of eIF4E/eIF(iso)4E in either translation or replication. Studying eIF4E/eIF(iso)4E-associated host factors may help better elucidate the underlying mechanism by which eIF4E/eIF(iso)4E function as an essential host factor and advance general knowledge about molecular virus-plant interactions. Moreover, identifying novel host factors, especially those associated with essential host factors or vital host machinery for virus infection, increases our selection pool of possible antiviral targets when it comes to developing genetic recessive resistance. Though the majority of developed or natural genetic resistance are still based on eIF4E/eIF(iso)4E, it is important to continuously looking for new options to counter emerging resistance breaking variants and increase the spectrum of resistance in cultivars.

To look for eIF4E/eIF(iso)4E-associated host factors for potyvirus infection, immunoprecipitation of the eIF(iso)4E complex followed by mass spectrometry (IP-MS) to identity the components present in the complex was performed using the TuMV-*A. thaliana* pathosystem. Since several HSP70 family proteins were identified from the eIF(iso)4E complex, I proposed to screen *A. thaliana* T-DNA insertion mutants with disrupted HSP70 expression for their TuMV susceptibility. The hypothesis for my project is: One or more HSP70 family proteins are host factors that facilitate TuMV infection. The specific objectives of this project are:

(1) To investigate whether HSP70 proteins, particularly those identified from our IP-MS experiment, facilitate TuMV infection through reverse genomic approach by screening TuMV infection in HSP70 knockout/knockdown and overexpression *A. thaliana* lines;

(2) To determine the step(s) of the TuMV infection process in which HSP70s are involved;

(3) To identify TuMV proteins that interact with HSP70s;

(4) To explore the molecular mechanisms by which HSP70s are involved in virus infection.

2. Materials and Methods

2.1 Plant material and growth conditions

Unless otherwise specified, *A. thaliana* and *N. benthamiana* plants were grown with Pro-Mix Mycorrhizae peat-based growth medium in greenhouse conditions at 60% relative humidity, with 16 h light (22°C)/8 h dark (18°C) regime. *A. thaliana* plants were kept under light intensity of 120 µmol/m^2, *N. benthamiana* were kept under light intensity of 70 µmol/m^2. After being seeded, *A. thaliana* seeds were placed at 4°C to break dormancy before being transferred to regular growth condition. Plants were watered and fertilized (20-8-20 [N-P-K]) as needed.

Seeds for *A. thaliana* T-DNA insertion mutants were obtained from the Arabidopsis Biological Resources Center (ABRC) at Ohio state university, Columbus, Ohio USA.

2.2 Virus constructs

The TuMV infectious clones pCambiaTunos/6Kmcherry for visualization of VRC and pCambiaTunos/GFP for protoplast transformation were gifted by Dr. Jean-François Laliberté at INRS, Laval, Québec, Canada (Cotton et al, 2009). TuMV infectious clone pCBTuMV-GFP/mCherry for virus cell-to-cell movement observation and virus infection assay in *A. thaliana* plants were constructed by Dr. Zhaoji Dai (Dai, 2018).

2.3 Bacterial and yeast strains

Escherichia coli strain DB3.1 was used for propagation of Gateway donor vectors and Gateway destination vectors, and *E. coli* strain Top10 was used for propagation of expression clone plasmids. *Agrobacterium tumefaciens* strain GV3101 was used for all binary vector transformation into plants. All bacteria were cultured in standard LB medium with antibiotics added according to the selection markers that they harbor. *E. coli* transformants containing HSP70 constructs were cultured at 28°C due to the instability of the construct. Otherwise, *E. coli* strains were grown under 37°C and *A. tumefaciens* strains were grown under 28°C.

Yeast strain AH109 (clontech) and NMY51 (Dualsystems Biotech) used for Y2H assay were maintained on YPDA medium (Takara Bio) at 30°C.

2.4 Plasmid construction

All plasmid constructs used in this study were generated by Gateway technology (Invitrogen) except plasmid constructs for Membrane Yeast two-Hybrid system. Polymerase chain reactions (PCR) to amplify coding sequences for cloning purpose were performed using Phusion™ High-Fidelity DNA Polymerase (Thermo Scientific). Colony PCR and genotyping PCR were performed using 2X Taq FroggaMix (FroggaBio). All vector constructs were verified by DNA sequencing (Eurofins Genomics), primers for this study were ordered from the same company.

Protein coding sequences of *A. thaliana* eIF(iso)4E (AT5G35620), HSP70-1 (AT5G02500), HSP70-2 (AT5G02490), HSP70-8 (AT2G32120), HSP70-11 (AT5G28540), and HSP70-12 (AT5G42020) were amplified from *A. thaliana* total cDNA. TuMV protein coding sequences were amplified from plasmid pCambiaTunos/GFP. The primers used for gene amplification is listed in Table S1. To amplify HSP70-1, HSP70-2, and HSP70-8 with the HDEL ER localization signal, a sequence of 12 nucleotides encoding HDEL was added to the reverse primer. To amplify HSP70-11 and HSP70-12 without HDEL ER localization signal, a reverse primer that omitted the HDEL sequence was used. The PCR fragments were transferred into pDONR™221 (Invitrogen) using BP Clonase™ Enzyme Mix (Invitrogen) following the user's manual to generate entry clones.

To generate expression clones for the Matchmaker Gold Yeast Two-Hybrid system (Clontech), protein coding sequences on entry clones were further transferred into gateway compatible destination vectors pDESTG-BKT7 (BK) or pDEST-GADT7 (AD) (Lu et al, 2010) by recombination reaction using LR Clonase™ Enzyme mix (Invitrogen) following the user's manual. Similarly, the expression clones for bimolecular fluorescence complementation (BIFC) assay were constructed using destination vectors pEarleyGate201-YN (YN) and pEarleyGate202-YC (YC) provided by Dr. Yuhai Cui, Agriculture and agrifood Canada, London research and development center (Lu et al, 2010). To generate expression clones with fluorescence tag, destination vectors pEarleyGate101, pEarleyGate102, pEarleyGate103, pEarleyGate104, designated herein as 101, 102, 103, 104 for convenience, were used. Binary Gateway compatible destination vector pBA-Flag-4×Myc-DC (Zhu et al, 2011), designated herein as pBA, was used to generate expression clone containing Flag and Myc tag at protein N-terminal.

The vectors containing HSP70 family genes coding region, eIF(iso)4E, TuMV NIb and CP for the Split-Ubiquitin Based Membrane Yeast Two-Hybrid system (Dualsystems Biotech) were constructed by PCR amplification from the constructed pDONR entry clones with primers containing SfiI restriction site as shown in Table S2. PCR fragments, vectors pBT3-STE and pPR3-N (Dualsystems Biotech) were digested by SfiI (NEB) at 50°C overnight. Subsequently, the cut PCR products were constructed onto the vectors using T4-DNA ligase (NEB).

2.5 Y2H assay

Matchmaker Gold Yeast Two-Hybrid System was used to detect protein-protein interaction localized to the yeast nucleus. Yeast cells (strain AH109) were transformed following the protocol provided by the supplier (Clontech protocol PT3024-1). The amount of plasmid used was bait (BK-): 50μg, prey (AD-): 100 μg. Transformed yeast cells were seeded on selective medium DDO (Double dropout media, Clontech). Three days later, colonies grown on DDO were transferred onto high stringency selective medium QDO (Quadruple dropout media, Clontech). The vector pair BK-VPg and AD-eIF(iso)4E served as a positive control and the vector pair BK-T7-Lam and AD-T7-T (commercially available from Clontech) was used as a negative control.

For detecting membrane protein interactions, Split-Ubiquitin Based Membrane Yeast Two-Hybrid system was used. Bait vector (pBT3-) and prey vector (pPR3N-) were mixed at 50 μg:100 μg and transformed into yeast cells (strain NMY51), transformation and selection followed the same procedure as above. Vector pair pBT3-CP and pPR3N-CP was used as positive control, empty vector pair pBT3-STE and pPR3-N (the vectors were commercially available from Dualsystems Biotech) was used as negative control.

2.6 BiFC and subcellular localization study

Bimolecular fluorescence complementation (BiFC) assay was performed to detect protein-protein interactions in planta. BiFC assay was performed following procedures described (Tang et al, 2022). Briefly, *A. tumefaciens* GV3101 was transformed with vector expressing the YN- or YC-tagged protein of interest. *A. tumefaciens* cells harboring appropriate expression vectors were harvested by low-speed centrifugation, washed and mixed with the infiltration buffer (10 mM MES PH 5.6, 10 mM MgCl2 and 100 μ acetosyringone) at a final dilution of OD600 0.3 for each *A. tumefaciens*. Subsequently, the *A. tumefaciens* suspension mix was infiltrated into *N. benthamiana*

leaves, fluorescence was detected at 48 hpi (hours post infiltration) with Olympus FV1200 Confocal microscope.

To visualize protein subcellular localization, *A. tumefaciens* harboring plant expression vector constructed to express proteins of interest (fused with a fluorescence protein) was infiltrated into *N. benthamiana*, following similar procedures as BiFC: *A. tumefaciens* was infiltrated at OD600 0.3 (in the case of co-infiltration of multiple *A. tumefaciens* transformants, the OD600 for each *A. tumefaciens* in the mix is 0.3) and observation was made 48 hpi with Olympus FV1200 Confocal microscope. pCambiaTunos/6Kmcherry was used as VRC marker and infiltrated at OD600 0.2. Nucleus marker (NLS-mCherry) was constructed by PCR amplification of mCherry with AvrII and SpeI restriction site from mCherry-harboring infectious clone (Primer F/R, 5'-3': GCCCTAGGATGGTGAGCAAGGGCGAGGAG/GAACTAGTCTACTTGTACAGCTCGTCC ATG), and PCR amplification of NLS signal using overlapping primers with XhoI and AvrII restriction site (Primer F/R, 5'-3': CTCTCGAGATGGCTCCCAAGAAGAAGACAAAGGTAATGGAGCCAGGA/ GCCCTAGGTAGTGATTGTCCTCCTGGTGATCCTGGCTCCATTACCTT) followed by restriction enzyme digestion of the PCR fragments with respective restriction enzymes and ligation to pEarleyGate201 digested with XhoI and SpeI. ER marker (mCherry-HDEL) was constructed by Gateway technology into pEarleyGate201 starting with mCherry amplification using primers containing HDEL signal and attB recognition site (Primer F/R, 5'-3': GGGGACAAGTTTGTACAAAAAAGCAGGCTTCATGGTGAGCAAGGGCGAGGAG/ GGGGACCACTTTGTACAAGAAAGCTGGGTCCTA**AAGCTCATCATG**CTTGTACAGCT CGTCCATG).

2.7 Co-immunoprecipitation assay

Co-immunoprecipitation (Co-IP) assay was performed to confirm protein-protein interactions. 104-HSP70-11, 104-HSP70-12, pBA-NIb, pBA-CP, pBA-eIF(iso)4E were transformed into *A. tumefaciens* strain GV3101 and further infiltrated into *N. benthamiana* leaves at OD600 0.4. Co-IP was performed following the protocols specified in (Win et al, 2011) with some adaptations. Briefly, leaf samples were collected at 72 hpi and grinded into fine powder in liquid nitrogen. 2 ml of extraction buffer (25 mM Tris HCl, pH 7.5, 10% glycerol, 1 mM EDTA, 150 mM NaCl, 10 mM DTT, 2% w/v polyvinylpolypyrrolidone (PVPP), 1×EDTA-free protease inhibitor cocktail

cOmplete (Roche REF. 11697498001), 0.1% Tween 20) was added to 2 g of grinded leaf powder to homogenate the sample. The homogenate was then incubated at 4°C on a vertical shaker for 30 min. Centrifuge at 12, 000 rpm for 10 min at 4°C to remove leaf pellet (repeat centrifuge if supernatant was not clear of leaf pellet), take 100 μl of protein extract and add 20 μl of 5× SDS-PAGE loading buffer (5g SDS, 15.1g tris-base, 72g glycine in 1000ml water, add 0.5% β-mercaptoethanol before use) as Co-IP input sample. 40 μl of anti-Flag M2 affinity gel (Sigma, Cat. A2220) washed 3 times with IP buffer (25 mM Tris HCl, pH 7.5, 1mM EDTA, 150 mM NaCl, 10% glycerol, 0.1% Tween 20) was added to 2mL protein extracts and incubated at 4 °C on vertical shaker for 3 h. Pellet the agarose beads at 800 g for 30 s at 4 °C, discard the supernatant and wash the beads with IP buffer for 5 times. In the last wash, remove as much supernatant as possible and add 100 μl of IP buffer with 20 μl of SDS-PAGE loading buffer.

After boiling the samples at 95°C for 5 min, the protein samples were used to perform western blotting. The primary antibodies used were polyclonal anti-c-Myc antibody produced in rabbit (Sigma, Cat. C3956) to detect protein expressed by pBA vector, and polyclonal anti-GFP, N-terminal antibody produced in rabbit (Sigma, Cat. G1544) to detect protein expressed by 104 vector (YFP can also be recognised by this anti-GFP antibody). Anti-rabbit IgG peroxidase antibody produced in goat (Sigma, Cat. A6154) was used as secondary antibody. Protein bands were visualized using Immobilon Western Chemiluminescent HRP substrate (Millipore, Kit No. WBKL S0100) under UV light.

Immunoprecipitation of 101-NIb for the detection of ubiquitination was performed with 20 μl of ChromoTek GFP-Trap® Agarose (ChromoTek, Cat. Gta) for each reaction following the same procedure. Anti-Ubiquitin antibody produced in rabbit (Sigma, Cat. AB1690) was used as the primary antibody to detect ubiquitination.

2.8 Protein transient expression analysis in *N. benthamiana*

To determine the effect of transient expression of HSP70s on the protein level of its interaction partners, *A. tumefaciens* carrying pBA-HSP70 or pBA empty vector as a control (at OD600 of 0.4) were co-infiltrated with *A. tumefaciens* carrying 101-NIb, 101-CP, or 101-eIF(iso)4E (at OD600 of 0.3). A vector expressing the viral RNA silencing suppressor from *Tomato bushy stunt virus* 35S-P19 (Xiong et al, 2019) was also co-infiltrated at OD600 of 0.1. To determine the effect of

transient expression of HSP70s on TuMV local infection in *N. benthamiana*, *A. tumefaciens* carrying pBA-HSP70 or pBA empty vector as a control (at OD600 of 0.4) were co-infiltrated with *A. tumefaciens* carrying TuMV infectious clone pCBTuMV-GFP/mCherry (at OD600 of 0.1).

pBA-HSP70 and pBA empty vector control were infiltrated at each half of the same *N. benthamiana* leaf to control other independent variables caused by the plant. Samples were taken 3 days post infiltration (dpi) by circular cutter 8 mm in diameter. 5 pieces of leaf tissues were taken for each sample, the control group leaf tissues were cut in symmetrical locations relative to HSP70 group. Four zirconia beads (BioSpec Products, Cat. 11079125z) were put into each 2 ml microtube (Diamed) with the leaf samples. The samples were frozen in liquid nitrogen and then grounded in TissueLyser II (Qiagen®) at 30/s for 3 min 30 s. 250 μl of SDS-PAGE loading buffer was added to each sample. After boiling the samples at 95°C for 5 min, the protein samples were used to perform western blotting. The same antibodies were used to detect Myc-tagged HSP70 expressed by pBA vector and YFP-tagged protein expressed by 101 vector.

For protein expression assay after treatment with ubiquitin-proteasome pathway inhibitor, 50 μM of MG-132 (MilliporeSigma, Cat. 474790, 5mM 100× stock in DMSO, dilute in infiltration buffer before infiltration) were infiltrated in plants 16 h prior to sample collection.

For evaluation of mRNA level of transiently expressed NIb, the samples were frozen in liquid nitrogen and then grounded in TissueLyser II at 30/s for 3 min. Extract RNA using 5M LiCL: 600 μl of extraction buffer (20 mM Tris-HCl pH 7.8, 200 mM NaCl, 1% w/v SDS, 50 mM EDTA) was added to the grounded sample and vortex to homogenate, then 600 μl of Phenol:Chloroform:Isoamylalcohol (25:24:1) was added to the sample and vortex for 5 min. Centrifuge at 12,000 rpm for 30 min at 4°C. Pipette 500 μl of top-layer supernatant in a new 1.5 ml microtube and add 500 μl of 4M LiCl, vortex for 5 min. Let it sit overnight at 4°C. Centrifuge at 12,000 rpm for 30 min at 4°C and discard supernatant. Wash the pellet with 75% ethanol three times and dissolve the final pellet in 50 μl of Rnase free water. 1 μg of RNA from each sample was digested in Dnase I (Invitrogen), following reverse transcription by SuperScript™ III Reverse Transcriptase according to manufacturer's instruction. Finally, quantitative PCR (qPCR) was performed using SensiFAST™ SYBR® No-ROX Kit (Meridian Bioscience®, Cat. No. BIO-98050) according to the user's manual on CFX96 real-time PCR system (Bio-Rad). qPCR primers

(YFP-qPCR-F/R, 5'-3': CACCGGCAAGCTGCCCGTGCC/ GAAGATGGTGCGCTCCTGGAC) and *N. benthamiana* actin qPCR primers (NbAct-qPCR-F/R: GGGATGTGAAGGAGAAGTTGGC/ATCAGCAATGCCCGGGAACA) were used. NIb mRNA level was calculated by $2^{-\Delta\Delta Ct}$ method, briefly, NIb mRNA levels in both pBA-HSP70 group and pBA empty vector group were normalized with actin and NIb mRNA level in pBA empty vector group was taken as a control.

2.9 Characterization of T-DNA insertion *A. thaliana* lines

A. thaliana T-DNA insertion mutant lines for HSP70-1 (SALK_135531C), HSP70-2 (SALK_085076C), HSP70-3 (SALK_013280C), HSP70-4 (SALK_029571C), HSP70-6 (SALK_140810), HSP70-7 (SALK_095715C), HSP70-8 (SALK_069187C), HSP70-11 (SALK_001435C), HSP70-12 (SALK_047956C), HSP70-13 (SALK_024133C) were grown until four week old. Leaf samples collected from these plants were used for genomic DNA extraction with the method described previously (Edwards et al, 1991). T-DNA insertion zygosity was determined using a PCR-based genotyping method described by Salk Institute Genome Analysis Laboratory (http://signal.salk.edu/tdnaprimers.2.html). Briefly, each sample was subjected to PCR by two sets of primers: LP+RP and LB+RP (LB: primer specific to the left border of T-DNA; LP: left genomic primer; RP: right genomic primer). All genotyping primer sequences were designed based on instructions from Salk Institute Genome Analysis Laboratory. In wild-type or heterozygous plants, a PCR product of about 1kb should be detected with LP+RP primers. In homozygous and heterozygous plants, a PCR product of about 600bp should be detected with LB+RP primers. Seeds were collected from homozygous plants for future use. If no homozygous plants were found in the first screening, the seeds from heterozygous plants were collected and seeded, and the zygosity in the second generation was screened. Homozygous plants could be obtained from the second generation if the T-DNA insert is not lethal.

HSP70 mRNA level was further evaluated in these *A. thaliana* mutant lines. RNA was extracted from homozygous T-DNA insert lines and wild-type line using the Plant Total RNA Mini Kit (Geneaid) following the supplier's instructions. Dnase digestion and reverse transcription as well as qPCR were performed as described above. The primers to detect each HSP70 gene are listed in Table S3. HSP70 expression levels were calculated by $2^{-\Delta\Delta Ct}$ method. Verified HSP70 knockout or knockdown lines with a reduction in HSP70 mRNA level were used for TuMV infection assay.

2.10 Generation of double knockout/knockdown mutant

The HSP70-11/HSP70-12 double knockdown *A. thaliana* mutant was generated by crossing the homozygous HSP70-11 and HSP70-12 single knockdown lines. F1 seeds were collected and heterozygosity of both HSP70-11 and HSP70-12 was confirmed by PCR-based genotyping. Successfully crossed F1 plants should be heterozygous on both loci. Self-pollinated seeds of the F1 generation were collected as F2 generation. F2 plants were subjected to genotyping to identify plants homozygous on both HSP70-11 and HSP70-12 loci, and their seeds were collected as F3 generation. F3 seeds were kept for use in future assays as HSP70-11/HSP70-12 double knockdown mutant (named as *hsp70-11/hsp70-12*). The HSP70-1/HSP70-2 double knockout *A. thaliana* mutant (named as *hsp70-1/hsp70-2* for convenience) was obtained from ABRC (SALK_087844). This single T-DNA insertion mutant happened to disrupt the expression of both HSP70-1 and HSP70-2 genes due to the close proximity of the genes (Jungkunz et al, 2011). RNA extraction, reverse-transcription, and qPCR were performed to confirm the reduction of HSP70-1 and HSP70-2 mRNA level in *hsp70-1/hsp70-2* line and the reduction of HSP70-11 and HSP70-12 mRNA level in *hsp70-11/hsp70-12* line. The verified lines were used for future experiments such as TuMV infection assay.

2.11 Generation of HSP70 overexpression transgenic plants

pBA-HSP70-1, pBA-HSP70-2, pBA-HSP70-8, pBA-HSP70-11, pBA-HSP70-12 were introduced into *A. tumefaciens* and further transformed into *A. thaliana* (Col-0 ecotype) by the floral dip method (Zhang et al, 2006). The resulting *A. thaliana* seeds (F1 generation) were sowed. Transgenic plants were selected by spraying herbicide Basta (250 mg/L, Sigma, Cat. 45520) at 8, 9, and 10 days after sowing (counting 3 days under cold treatment). Survived seedlings were further analyzed by western blotting (with antibody against Myc tag) to confirm the expression of the transgene. Three transgenic plants for each HSP70 were selected and seeds collected from them were designated as F2 generation. F2 plants were again seeded and screened by Basta and verified by western blotting, seeds were collected from positive F2 plants as F3 generation, which can be used in future TuMV infection assays.

2.12 TuMV infection assay

A. thaliana HSP70 knockout/knockdown or transgenic lines and wild-type (Col-0) plants were seeded and transplanted at 12 days after sowing. Three weeks after transplantation, *A. thaliana* seedlings were infiltrated with *A. tumefaciens* harboring TuMV infectious clone pCBTuMV-GFP/mCherry. Three fully extended leaves were infiltrated on each plant. *A. tumefaciens* cells were diluted with the same infiltration buffer as described above for the BiFC experiment at OD600 of 0.3 for infiltration of knockout/knockdown lines and control; or OD600 of 0.03 for infiltration of HSP70 transgenic lines and control for better sensitivity. 16 plants were infiltrated for each line in each repeat. At 14 dpi, the tip of stalks of the plants was sampled. The samples were frozen in liquid nitrogen and then grounded in TissueLyser II with zirconia beads at 30/s for 2 min. RNA was extracted from the grounded samples, followed by synthesis of cDNA by reverse transcription as described above. qPCR was performed using TuMV qPCR primers (TuMV-qRT-F/R, 5'-3': TGGCTGATTACGAACTGACG/CTGCCTAAATGTGGGTTTGG) and *A. thaliana* Actin8 qPCR primers. TuMV level in each line was calculated by $2^{-\Delta\Delta Ct}$ method. Briefly, TuMV level in each line was normalized by actin and TuMV level in wild-type line was taken as a control.

To evaluate HSP70 expression in TuMV-infected plant, about 0.5 g of stalk tip flower sample and stalk leaf sample were taken from TuMV-infected and mock infected plants (infiltrated with *A. tumefaciens*) at 7 dpi and 14 dpi. RT-qPCR was performed using HSP70 qPCR primers and *A. thaliana* Actin8 qPCR primers. HSP70 level in each line was calculated by $2^{-\Delta\Delta Ct}$ method.

2.13 Protoplast isolation and transfection

A. thaliana plants used for mesophyll protoplast isolation were kept under 8 hours light (22°C)/16 hours dark (18°C) regime after transplantation of the seedlings. Protoplast isolation and transfection were performed by following the procedure as described previously (Dai & Wang, 2022). In brief, *A. thaliana* leaves from 4-5 week old plant peeled of lower epidermal surface were digested with enzyme solution (1% cellulase OnozukaTM R-10, 0.25% MacerozymeTM R-10, 0.4 M mannitol, 10 mM CaCl2, 20 mM KCl, 20 mM MES, 0.1% BSA, pH 5.7) under dark for 2 h. Stop reaction by washing protoplasts in W5 buffer (154 mM NaCl, 125 mM CaCl2, 5 mM KCl, 5 mM glucose, 2 mM MES, pH 5.7) to remove enzyme solution. The isolated protoplasts were placed on ice for 30 min before transformation. For transformation, W5 buffer was removed, and

protoplasts were suspended in MMg buffer (0.4 M mannitol, 15 mM MgCl2, 4 mM MES, pH 5.7) at a density of $2–5\times10^5$/mL. The plasmid for transformation was extracted from *E. coli* harboring pCambiaTunos/GFP cultured at 28°C using Maxi Plasmid Kit Endotoxin Free (Geneaid, Cat. PME25). For each *A. thaliana* line, 3 transformation reactions were performed in each repeat. 6×10^5 isolated mesophyll protoplasts were used in each transformation reaction, 50 µg of plasmid DNA was transfected by PEG reagent (40% PEG 4000, 0.1 M CaCl2, 0.2 M mannitol) in 13 ml tube (SARSTEDT). After transformation, the protoplasts were washed with W5 buffer three times and divided into two wells in a 12-well plate (Greiner bio-one CELLSTAR, Cat. 665180) after gentle mixing. The transformed protoplasts were maintained in W5 buffer in dark, one well from each reaction was collected at 24 hours post transformation (hpt), and the other well was collected at 48 hpt. RNA was extracted from protoplasts and TuMV RNA level was evaluated by RT-qPCR as described above.

2.14 TuMV cell-to-cell movement assay

To determine the effect of HSP70 overexpression on TuMV cell-to-cell movement in *N. benthamiana*, *A. tumefaciens* harboring pBA-HSP70 vectors as well as pBA empty vector were co-infiltrated with *A. tumefaciens* harboring pCBTuMV-GFP/mCherry infectious clone. pBA-HSP70 and control pBA empty vector *A. tumefaciens* were infiltrated on opposite halves on the same leaf at OD600 of 0.4 to eliminate independent variables caused by the plant. *A. tumefaciens* containing virus infectious clone was co-infiltrated at OD600 of 0.002. At 84 hpi, the movement of the virus from primary infected cell was observed by Olympus FV1200 Confocal microscope. The primary infected cell emits both green and red fluorescence while the secondary infected cells emit only green fluorescence.

2.15 Statistical analysis

All RNA levels were quantified by $2^{-\Delta\Delta Ct}$ method. RNA levels in both treatment group and control group were normalized with *A. thaliana* or *N. benthamiana* actin, and RNA level in control group was set to 1. Protein blots were quantified using ImageJ with the protein level of control samples set to 1. Bar graphs were plotted with the average of relative RNA or protein level from 3 or 5 repeats. Error bars represent standard deviation. Two-tailed, two sample equal variance unpaired

student's t test was used to test the difference between treatment samples and control samples. All calculations were performed with Excel.

3 Results

3.1 Identification of *A. thaliana HSP70* genes involved in TuMV infection

3.1.1 Screening for homozygous T-DNA insertion lines of HSP70 genes in *A. thaliana*

The TuMV-*A. thaliana* pathosystem was used as a model to study host proteins involved in virus infection. As an indispensable host factor required for a successful infection, eIF(iso)4E may interact with other host factors to exert its multi-functional roles during TuMV infection. To identify these host factors, we previously conducted an immunoprecipitation-mass spectrometry (IP-MS) analysis using proteins isolated from the TuMV-infected *A. thaliana* leaves. Briefly, GFP-tagged eIF(iso)4E was stably expressed in eIF(iso)4E-knockout T-DNA insertion *A. thaliana* mutant plants to restore their susceptibility to TuMV. Then, the plants were infected with TuMV by mechanical inoculation and total protein of the infected plants were extracted. Subsequently, immunoaffinity-purification using GFP affinity gel was carried out to isolate the eIF(iso)4E protein complexes from the total protein extract. Finally, liquid chromatography–tandem mass spectrometry (LC-MS/MS) was performed to identify proteins associated with eIF(iso)4E protein complexes. Three independent experiments were carried out. Four heat shock protein 70 (HSP70) family proteins, e.g., HSP70-1, HSP70-6, HSP70-7, HSP70-12, were amongst the proteins complexed with eIF(iso)4E (data not published).

The *A. thaliana* genome is predicted to contain 14 HSP70 genes of the DnaK subfamily (Table 2), which can be further divided into subgroups based on HSP70's subcellular localization (Lin et al, 2001). HSP70-18 is not included in the table as it is a pseudogene whose expression cannot be detected (Lin et al, 2001). HSP70-8 is not targeted to the chloroplast as predicted (Inoue et al, 2008) and tentatively grouped with cytoplasmic HSP70s. Based on their amino acid sequences, a phylogenetic tree of *A. thaliana* DnaK subfamily HSP70 proteins (excluding HSP70-18) was constructed using the neighbor-joining method (Fig. 4). HSP70s sharing the same subcellular localization are also more closely related in phylogeny analysis. HSP70-1, HSP70-2, HSP70-3, and HSP70-4 share over 95% amino acid sequence similarity with each other, and HSP70-5 shares over 90% amino acid similarity with HSP70-1, HSP70-2, HSP70-3, and HSP70-4 (Lin et al, 2001). HSP70-6 and HSP70-7 share over 95% amino acid sequence similarity with each other, and HSP70-11 and HSP70-12 share over 99% amino acid sequence similarity with each other (Lin et

al, 2001). HSP70-8 is exceptional and has only 25% similarity with other HSP70s (Lin et al, 2001). It would be interesting to find out whether HSP70-8 has certain special functions.

A. thaliana T-DNA insertion lines corresponding to HSP70 DnaK subfamily proteins localized in the cytoplasm, ER, and plastid were ordered from ABRC. Homozygous T-DNA insertion lines were obtained, and the reduction in HSP70 mRNA levels were confirmed. T-DNA insertion lines for TuMV infection assay are shown in Table 2. The homozygous T-DNA insertion mutant for HSP70-6 has serious phenotype including a withering appearance, slender and curved stalk, and smaller in size. HSP70-5 T-DNA insertion lines purchased either did not germinate or did not contain the T-DNA insertion. HSP70-5 was not included for TuMV infection assay.

Table 2. List of DnaK subfamily HSP70 genes and the corresponding T-DNA insertion mutants

Location	Gene Name	Locus	Mutants	Target Gene mRNA Level	Insertion
Cytoplasm	HSP70-1	AT5G02500	SALK_135531C	0	Exon
	HSP70-2	AT5G02490	SALK_085076C	0	Exon
	HSP70-3	AT3G09440	SALK_013280C	40%	5'UTR
	HSP70-4	AT3G12580	SALK_088253C	0	Exon
	HSP70-5	AT1G16030			
	HSP70-8	AT2G32120	SALK_069187C	0	Exon
Plastid	HSP70-6	AT4G24280	SALK_140810	0	Intron2
	HSP70-7	AT5G49910	SALK_095715C	0	Intron2
Mitochondria	HSP70-9	AT4G37910	SALK_140494	20%	promoter
	HSP70-10	AT5G09590	SALK_040792	30%	Promoter
ER	HSP70-11	AT5G28540	SALK_001435C	10%	5'UTR
	HSP70-12	AT5G42020	SALK_047956C	20%	Exon
	HSP70-13	AT1G09080	SALK_024133C	0	Exon
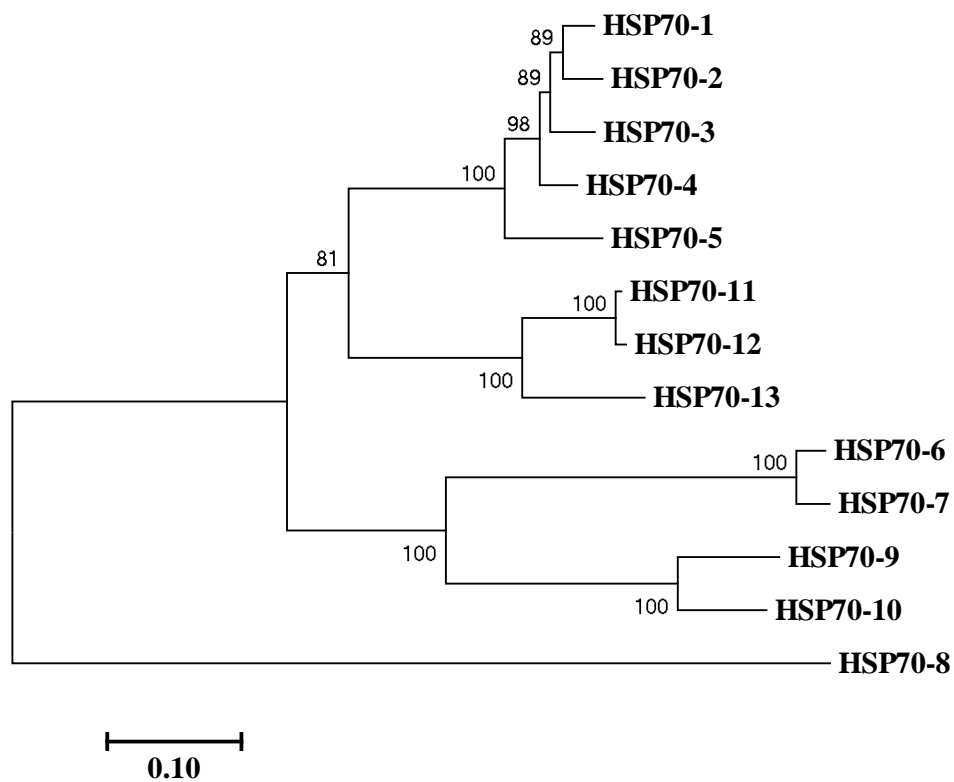
Figure 4. Phylogenetic analysis of *A. thaliana* **DnaK subfamily HSP70 proteins**

The tree was constructed by MEGA7 using the neighbor-joining algorithm. The bootstrap confidence values were generated by 1000 replications.

3.1.2 Identification of HSP70 genes associated with TuMV infection

TuMV infection was evaluated in the selected T-DNA insertion mutant *A. thaliana* lines in comparison with wild-type plants. Mutant *A. thaliana* plants and wild-type plants were inoculated with *A. tumefaciens* harboring the TuMV infectious clone pCBTuMV-GFP/mCherry, followed by observation of disease symptoms and quantification of TuMV RNA level at 14 dpi. I tested single HSP70 mutants including *hsp70-1*, *hsp70-2*, *hsp70-3*, *hsp70-4*, *hsp70-8*, *hsp70-6*, *hsp70-7*, *hsp70-11*, *hsp70-12*, *hsp70-13*. I was unable to obtain *hsp70-5* and did not test mitochondrial HSP70s because none of them was identified from the eIF(iso)4E complex. Among all the single HSP70 mutants tested, only HSP70-8 mutant (SALK_069187C, designated as *hsp70-8*) showed alleviated symptoms with reduced level of TuMV RNA accumulation compared to wild-type (Fig. S1). TuMV-induced symptoms and viral RNA levels in other HSP70 single knockout/knockdown lines including *hsp70-1*, *hsp70-2*, *hsp70-3*, *hsp70-4*, *hsp70-6*, *hsp70-7*, *hsp70-11*, *hsp70-12* and *hsp70-13* are shown in Fig. S1. In view of the very high amino acid sequence identity similarity between HSP70-1 and HSP70-2, between HSP70-6 and HSP70-7, and between HSP70-11 and HSP70-12, their corresponding double knockout/knockdown mutants are necessary to assess the effect of these genes on TuMV infection. The *A. thaliana* double knockout mutant of HSP70-1 and HSP70-2, designated as *hsp70-1/2*, was obtained from ABRC (SALK_087844), and the double knockout line for HSP70-11 and HSP70-12, designated as *hsp70-11/12*, was generated by crossing SALK_001435C and SALK_047956C followed by selfing. Despite at least three attempts, I failed to screen out a double knockout line for HSP70-6 and HSP70-7 from the F2 population after crossing HSP70-6 and HSP70-7 mutant lines followed by selfing. Most likely, HSP70-6 and HSP70-7 double knockout was lethal for *A. thaliana*. Compared with wild-type plants, *hsp70-1/2* showed more severe symptoms and increased TuMV RNA accumulation after TuMV infection, and *hsp70-11/12* showed alleviated symptoms and reduced TuMV RNA accumulation after TuMV infection. These data suggest that HSP70-1, HSP70-2, HSP70-8, HSP70-11, and HSP70-12 are involved in TuMV infection, which is consistent with our previous finding that HSP70-1, and HSP70-12 are present in the eIF(iso)4E complex. Thus, HSP70-1, HSP70-2, HSP70-8, HSP70-11, and HSP70-12 were selected for further analysis in their role in TuMV infection.

3.1.3 HSP70-1, HSP70-2, HSP70-8, HSP70-11, and HSP70-12 expression in response to TuMV infection

Infection by plant viruses, including TuMV, could induce the expression of HSP70 in its host (Aparicio et al, 2005; Aranda et al, 1996; Chen et al, 2008; Whitham et al, 2003; Yang et al, 2007). To confirm if TuMV infection upregulates HSP70-1, HSP70-2, HSP70-8, HSP70-11, and HSP70-12, I harvested stalk tip flowers and stalk leaves of TuMV-infected *A. thaliana* at 7 days and 14 days post inoculation and conducted RT-qPCR to profile mRNA levels of these five *HSP70* genes. The expression of HSP70-1 was not altered in both samples at 7 dpi, but showed an incremental increase in both samples at 14 dpi compared with the mock inoculated control (Fig. 5A). The expression of HSP70-2 showed a trend of increase in both samples at both time points, however, upregulation in some samples did not reach statistically significant levels (Fig. 5B). Among the five HSP70s, HSP70-8 was the least responsive to TuMV infection with only a slight increase in flower tissue at 14 dpi compared with the mock inoculated control (Fig. 5C). HSP70-11 and HSP70-12 exhibited a similar trend of change. Their expression levels in leaf samples were dramatically upregulated at 14 dpi (Fig. 5D & 2E) while the expression level in flower samples remained without significant difference. The expression level of HSP70-11 and HSP70-12 at 7 dpi in flower samples experienced a slight yet statistically significant decrease (Fig. 5D & 2E). These results confirmed previous findings that TuMV infection induces HSP70 expression.
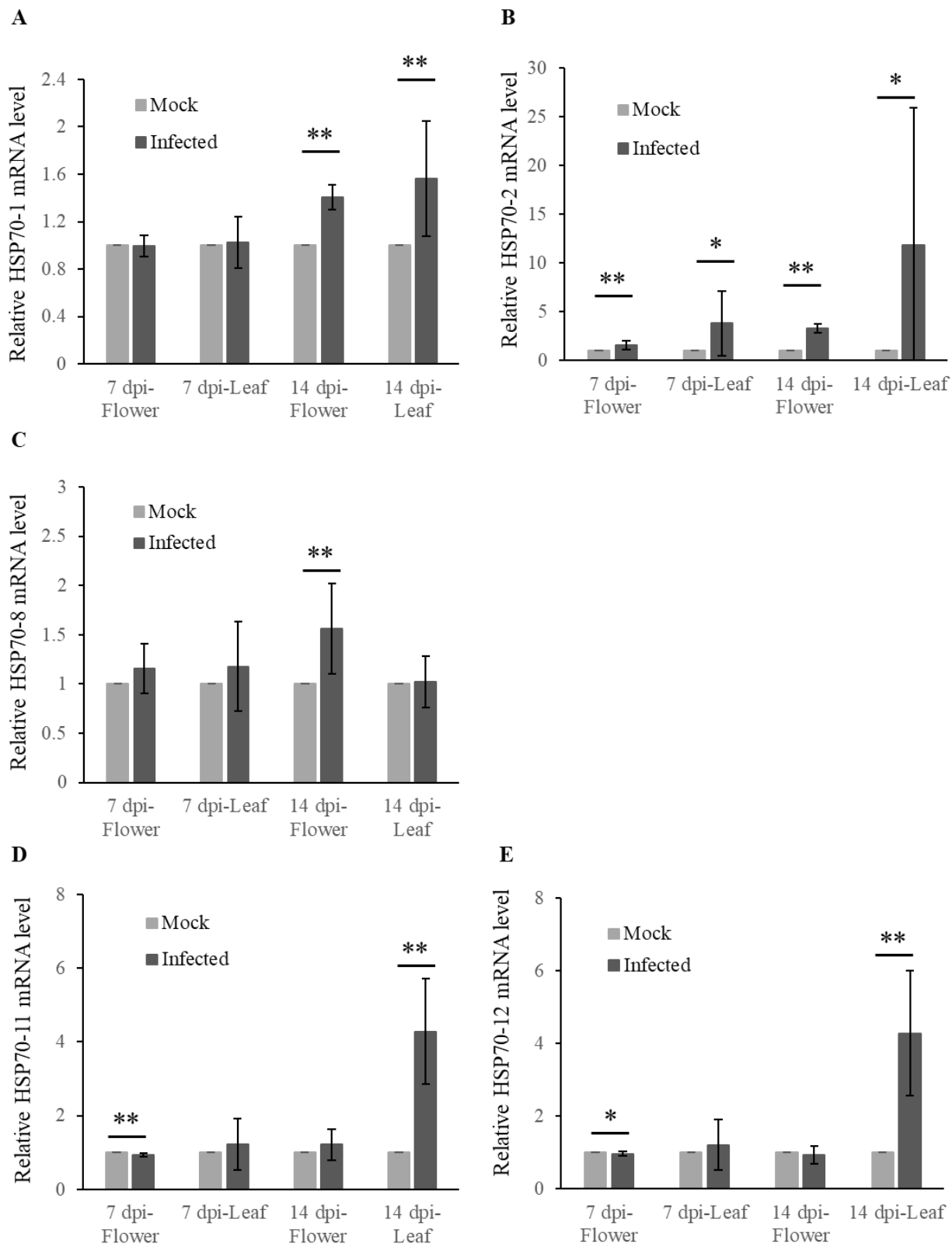
Figure 5. The expression level of HSP70-1 (A), HSP70-2 (B), HSP70-8 (C), HSP70-11 (D) and HSP70-12 (E) in response to TuMV infection

Relative fold changes of HSP70 mRNAs in *A. thaliana* flower and leaf tissue at 7 days and 14 days after TuMV inoculation compared with mock-infected control plant evaluated by RT-qPCR. The HSP70 mRNA levels of the mock-inoculated control was set to 1 at each time point. All HSP70 mRNA levels were normalized against Actin8 transcripts in the same sample. Data were collected from five independent experiments. Error bars represent standard deviation (n=5). ** $P<0.05$, * $P<0.1$, student's t test, two-tailed, unpaired.

3.2 Characterization of HSP70 mutant lines and their TuMV susceptibility

3.2.1 Verification of *A. thaliana* HSP70 T-DNA insertion lines *hsp70-1/2*, *hsp70-8*, *hsp70-11/12*

To study the function of HSP70 family proteins in TuMV infection through reverse genetics, T-DNA insertion lines were analyzed and verified. T-DNA insertion line SALK_087844 contains an insertion located in the second exon of HSP70-2, encoded by At5g02500, as well as deletion of about 10 kb upstream of HSP70-2, including gene At5g02490 encoding HSP70-1 (Jungkunz et al, 2011). Thus, SALK_087844 can be considered as a double deletion mutant for both HSP70-1 and HSP70-2 (Fig. 6A). Homozygosity of the insertion in *hsp70-1/2* was confirmed by two-step PCR: using gene-specific primer pair LP+RP to detect the absence of wild-type genotype, along with a gene-specific primer RP and a T-DNA specific primer LB to detect T-DNA insertion (Fig. 6D left panel). Loss of HSP70-1 and HSP70-2 transcripts in *hsp70-1/2* was confirmed by RT-qPCR analysis using HSP70-1 and HSP70-2 specific qPCR primers (Fig. 6F). T-DNA insertion line SALK_069187 contains an insertion located in the exon of HSP70-8 encoded by At2g32120 and is designated as *hsp70-8* (Fig. 6B). Homozygosity of the insertion in *hsp70-8* was confirmed by two-step PCR genotyping (Fig. 6D middle panel). Loss of HSP70-8 transcripts was determined by RT-qPCR analysis using HSP70-8 specific qPCR primers (Fig. 6G), confirming *hsp70-8* is a knockout mutant for HSP70-8. Similarly, SALK_001435 contains an insertion in the 5'UTR of HSP70-11 encoded by At5g28540 whereas SALK_047956 contains an insertion at the end of the last exon of HSP70-12 encoded by At5g42020 (Fig. 6C). Homozygosity of the lines was confirmed by two-step PCR genotyping. Double knockout mutant of HSP70-11 and HSP70-12 was generated by crossing SALK_001435 and SALK_047956 followed by selfing of F2 and screening the F3 by two-step PCR genotyping for homozygous double mutant (Fig. 6D right panel). RT-qPCR was performed on *hsp70-11/12* to quantify HSP70-11 and HSP70-12 transcripts. Low levels of HSP70-11 and HSP70-12 mRNA were detected in this double mutant (Fig. 6H), suggesting *hsp70-11/12* is actually a double knockdown mutant. The single and double mutants obtained showed no visible phenotypes under standard growth conditions (Fig. 6E).

A HSP70-1 qPCR Fragment HSP70-2 SALK_087844 qPCR Fragment

B HSP70-8 SALK_069187 qPCR Fragment

C HSP70-11 qPCR Fragment SALK_001435 HSP70-12 SALK_047956 qPCR Fragment

D LB+RP LP+RP LB+RP LP+RP LB+RP LP+RP LB+RP LP+RP mut wt mut wt mut wt mut wt mut wt mut wt mut wt mut wt 1kb 500bp 1kb 500bp

mut: *hsp70-1/2*
(SALK_087844)

mut: *hsp70-8*
(SALK_069187)

mut: *hsp70-11/12*
(SALK_047956 and SALK_001435)

E

F Relative HSP70-1 mRNA level *Col-0* *hsp70-1/2* Relative HSP70-2 mRNA level *Col-0* *hsp70-1/2*

G Relative HSP70-8 mRNA level *Col-0* *hsp70-8*

H Relative HSP70-11 mRNA level *Col-0* *hsp70-11/12* Relative HSP70-12 mRNA level *Col-0* *hsp70-11/12*

Figure 6. Verification of *A. thaliana* **HSP70 T-DNA insertion lines** *hsp70-1/2*, *hsp70-8*, *hsp70-11/12*

(A) Schematic representation of HSP70-1 and HSP70-2 gene structures and T-DNA insertion sites (triangle) for the mutant SALK_087844. Exons and introns are represented by filled boxes and lines, respectively. 5' UTR (left) and 3' UTR (right) are represented by open boxes. The positions of qPCR fragments are indicated by lines.

(B) Schematic representation of HSP70-8 gene structure and T-DNA insertion sites for the mutant SALK_069187.

(C) Schematic representation of HSP70-11 and HSP70-12 gene structure and T-DNA insertion sites for the mutants SALK_001435 and SALK_047956.

(D) Confirming the homozygosity of T-DNA insertions by PCR. PCR was conducted using genomic DNA from wild-type Col-0 genotype *A. thaliana* (wt) and mutant (mut) plants as template. Gene specific primer pair LP+RP were used to identify wild-type allele. A T-DNA specific primer LB and a gene specific primer RP were used to identify allele with insertion. Homozygous T-DNA insertion mutant is characterized by a band with LB+RP primer pair and no band with LP+RP primer pair. Left panel: mutant *hsp70-1/2* with wild-type; middle panel: mutant *hsp70-8* with wild-type; right panel: mutant *hsp70-11/12* with wild-type. wt: wild-type Col-0 genotype *A. thaliana*.

(E) Mutants and wild-type *A. thaliana* at 6 leaf stage (4-5 weeks old). 1, Col-0; 2, *hsp70-1/2*; 3, *hsp70-8*; 4, *hsp70-11/12*.

(F) HSP70-1 and HSP70-2 mRNA expression level in *hsp70-1/2* compared with Col-0.

(G) HSP70-8 mRNA expression level in *hsp70-8* compared with Col-0.

(H) HSP70-11 and HSP70-12 mRNA expression level in *hsp70-11/12* compared with Col-0.

3.2.2 TuMV infection symptoms and TuMV RNA accumulation were altered in HSP70 mutant lines

To evaluate TuMV infectivity in *hsp70-1/2*, *hsp70-8*, *hsp70-11/12* mutant lines, 3-week-old mutant and wild-type *A. thaliana* plants were agroinfiltrated with pCBTuMV-GFP/mCherry infectious clone. At 14 dpi, *hsp70-1/2* mutant line developed more severe symptoms than wild-type, including more severe dwarfing and curled bolts (Fig. 7A). In contrast, *hsp70-8* and *hsp70-11/12* mutant lines showed milder symptoms than wild-type *A. thaliana* (Fig. 7B and Fig. 7C). RT-qPCR was performed to quantify TuMV genomic RNA accumulation in stalk tip flower samples collected at 14 dpi. In consistency with symptoms, TuMV RNA accumulation showed a 40% increase in *hsp70-1/2* mutants (Fig. 7D), a 20% decrease in *hsp70-8* mutants (Fig. 7E), and a 40% decrease in *hsp70-11/12* mutants (Fig. 7F), compared with wild-type plants. These observations suggest that HSP70-1 and HSP70-2 have negative effect on TuMV infection in *A. thaliana*, while HSP70-8, HSP70-11, and HSP70-12 facilitate TuMV infection. HSP70-1 and HSP70-2, as well as HSP70-11 and HSP70-12 may have complimentary roles in TuMV infection because TuMV infection level was not altered in the single knockout or knockdown lines of these genes.

A
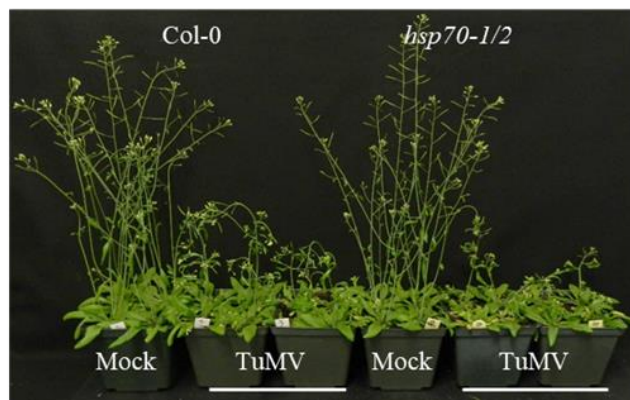
B
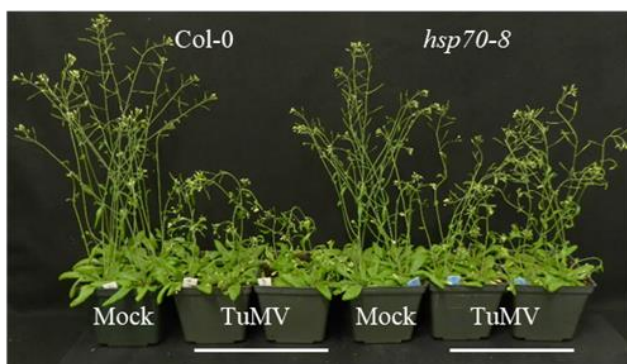
C
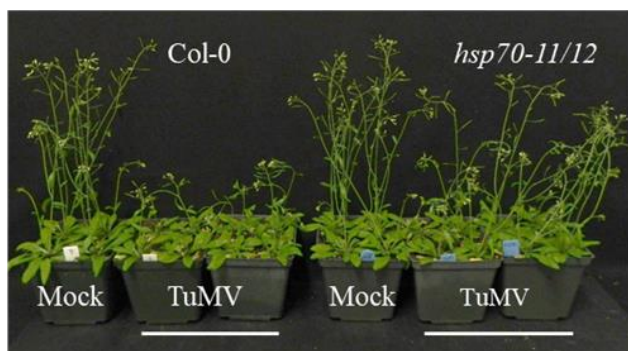
D
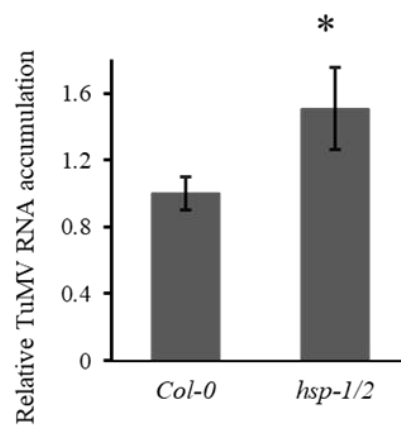
E
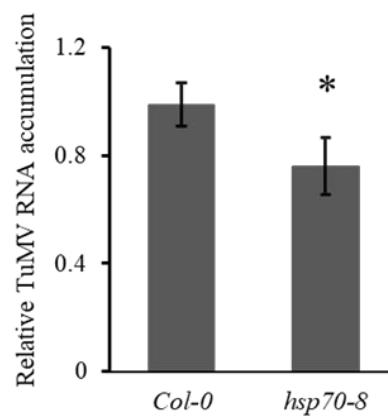
F
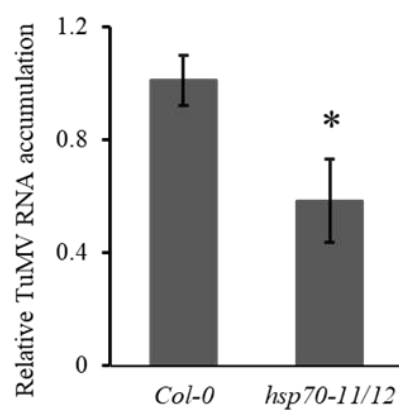
Figure 7. TuMV infection symptoms and TuMV RNA accumulation were altered in HSP70 mutant lines

(A) Symptom comparison between TuMV-infected *hsp70-1/2* mutants and Col-0 plants.

(B) Symptom comparison between TuMV-infected *hsp70-8* mutants and Col-0 plants.

(C) Symptom comparison between TuMV-infected *hsp70-11/12* mutants and Col-0 plants.

Above images were taken at 14 dpi. Mock, infiltrated with *A. tumefaciens*; TuMV, infiltrated with *A. tumefaciens* harboring TuMV infectious clone at OD600 of 0.3.

(D) Fold change of TuMV RNA accumulation in *hsp70-1/2* mutants compared with Col-0 plants evaluated by RT-qPCR.

(E) Fold change of TuMV RNA accumulation in *hsp70-8* mutants compared with Col-0 plants evaluated by RT-qPCR.

(F) Fold change of TuMV RNA accumulation in *hsp70-11/12* mutants compared with Col-0 plants evaluated by RT-qPCR.

The TuMV RNA level of Col-0 control were set to 1. All TuMV RNA levels were normalized against *A. thaliana* Actin8 transcripts in the same sample. RNA was extracted from stalk tip flowers at 14 dpi. Data were collected from five independent experiments. Error bars represent standard deviation (n=5). *$p<0.05$, student's t test, two-tailed, unpaired.

3.2.3 Verification of and evaluation of TuMV infection in *A. thaliana* HSP70-1, HSP70-2, HSP70-8, and HSP70-12 overexpression lines

To investigate the effect of stable overexpression of HSP70 proteins on TuMV infection in *A. thaliana*, the coding sequences of HSP70-1, HSP70-2, HSP70-8, HSP70-11, and HSP70-12 were cloned into the expression vector pBA-Flag-4×Myc-DC. Transgenic *A. thaliana* lines overexpressing HSP70-1, HSP70-2, HSP70-8, and HSP70-12 were successfully generated. However, Basta selection of the first-generation seeds from *A. thaliana* plants transformed with HSP70-11 failed to obtain viable offspring likely due to the lethal effect of overexpression of HSP70-11. Immunoblotting detection of transgene-encoded Flag-Myc-HSP70 fusion proteins in the *A. thaliana* transgenic lines were performed using anti-Myc antibodies (Fig. 8A). Transgenic HSP70-12 could not be detected in *A. thaliana* by immunoblotting at the correct size probably due to the low protein expression level and fast protein turnover rate. The HSP70-1, HSP70-2, HSP70-8 and HSP70-12 overexpression transgenic lines showed no phenotypic difference with their parental wild-type *A. thaliana* (Col-0) under given growth conditions (Fig. 8B). RT-qPCR confirmed increased HSP70s mRNA levels in the transgenic lines including HSP70-12 overexpression lines (Fig. 8C). TuMV infection assay were performed in the transgenic lines. However, no difference in TuMV infection symptom as well as TuMV RNA level in the overexpression lines was observed at 14 dpi when compared with control wild-type plants (Fig. 8D & Fig. 8E). These data suggest that overexpression of HSP70-1, HSP70-2, HSP70-8, and HSP70-12 does not affect TuMV infection in *A. thaliana* plants.

A

C-Myc

Actin

-72 KDa

-72 KDa

-17 KDa

B

C
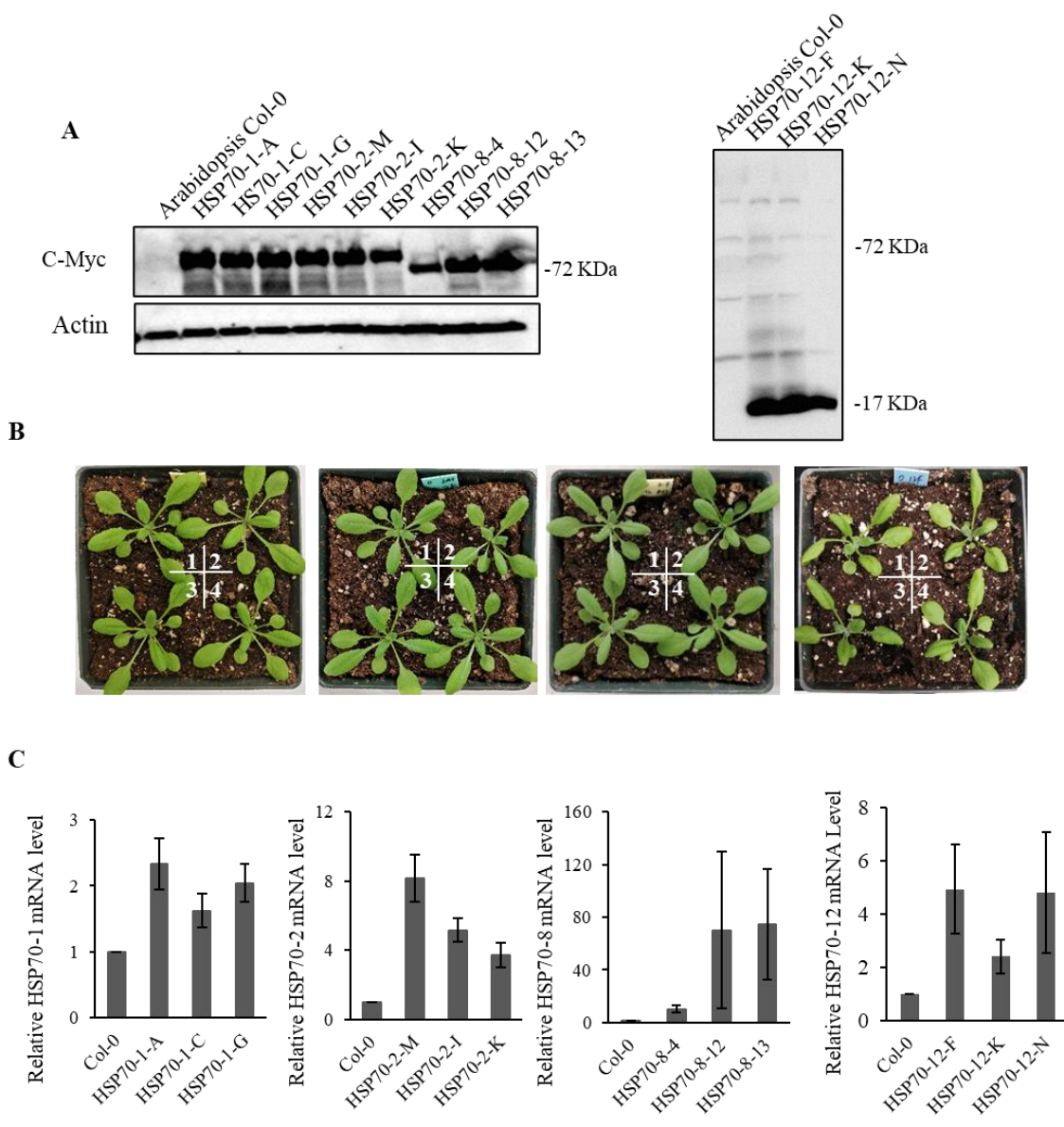
D
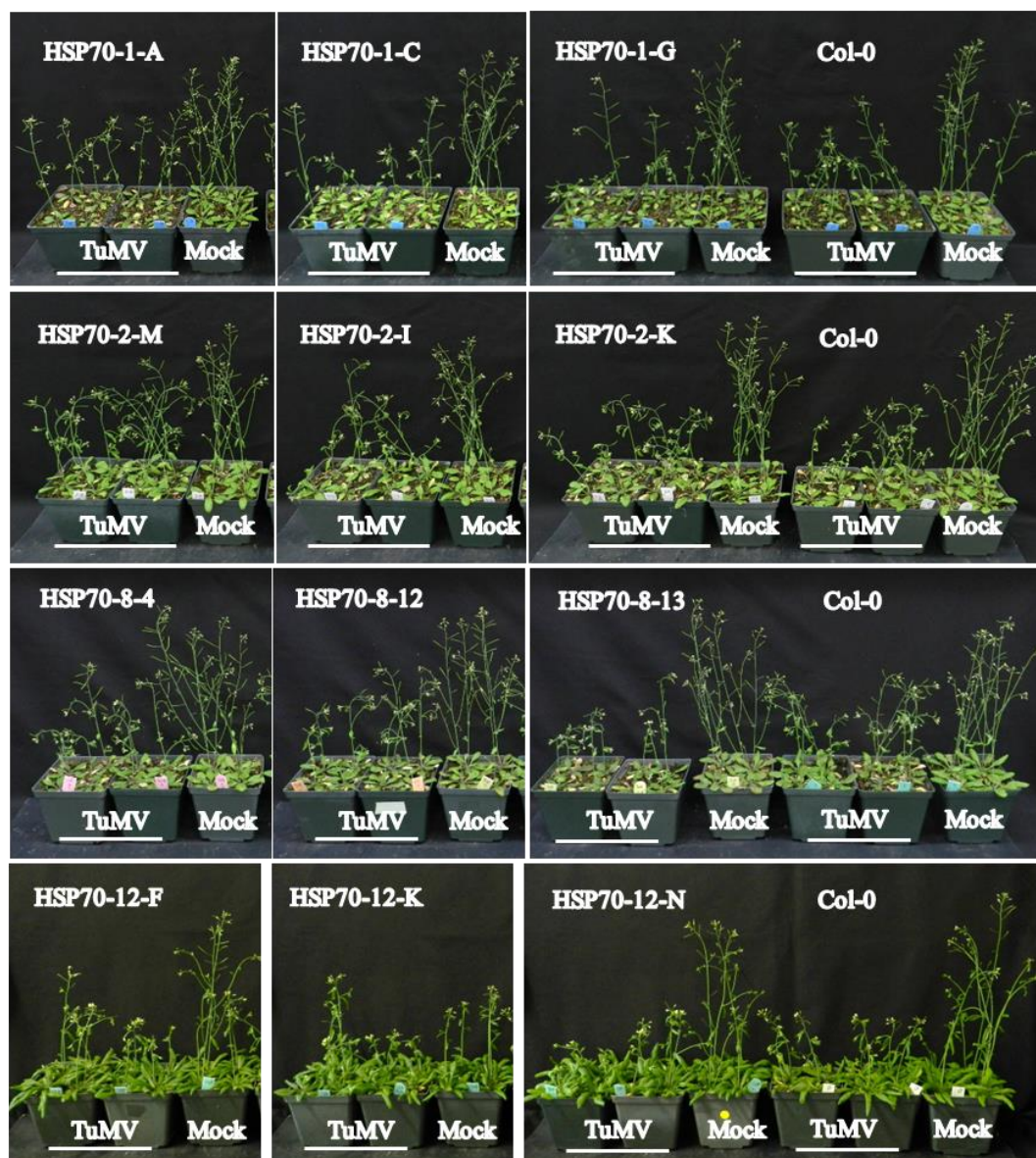
E
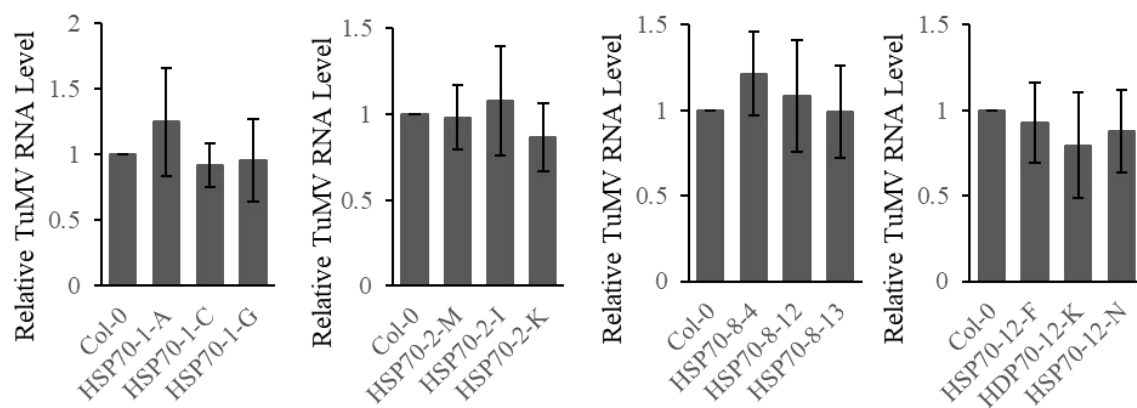
Figure 8. Verification of and evaluation of TuMV infection in *A. thaliana* HSP70-1, HSP70-2, and HSP70-8 overexpression lines

(A) Left panel, immunoblotting of HSP70-1, HSP70-2, and HSP70-8 in their corresponding overexpression plants. Right panel, immunoblotting with Myc antibody in HSP70-12 overexpression plants. Three independent lines for each of HSP70s were selected. Total protein was extracted from rosette leaves of 6-week-old plants. Anti-Myc antibodies were used to probe HSP70s tagged by Myc. Actin immunoblotted with anti-Actin antibodies is shown as a loading control.

(B) Overexpression lines and wild-type *A. thaliana* at 6-leaf stage (4-5 weeks old).

Left first panel, 1: Col-0; 2: HSP70-1-A; 3: HSP70-1-C; 4: HSP70-1-G. Left second panel, 1: Col-0; 2: HSP70-2-M; 3: HSP70-2-I; 4: HSP70-2-K. Left third panel, 1: Col-0; 2: HSP70-8-4; 3: HSP70-8-12; 4: HSP70-8-13. Right panel, 1: Col-0; 2: HSP70-12-F; 3: HSP70-12-K; 4: HSP70-12-N.

(C) RT-qPCR analysis of HSP70-1, HSP70-2, and HSP70-8 expression levels in their overexpression lines. Left first panel, in HSP70-1 overexpression lines in comparison with Col-0. Left second panel, in HSP70-2 overexpression lines in comparison with Col-0. Left third panel, in HSP70-8 overexpression lines in comparison with Col-0. Right panel, in HSP70-12 overexpression lines in comparison with Col-0. The HSP70 mRNA level of Col-0 control was set to 1. All HSP70 mRNA levels were normalized against Actin8 transcripts in the same sample. RNA was extracted from rosette leaves of 6-week-old plants. Data were collected from three independent experiments. Error bars represent standard deviation (n=3).

(D) Upper first panel, phenotype comparison between TuMV-infected HSP70-1 overexpression lines (labelled A, C, and G) and Col-0 plants. Upper second panel: phenotype comparison between TuMV-infected HSP70-2 overexpression lines (labelled M, I, and K) and Col-0 plants. Upper third panel, phenotype comparison between TuMV-infected HSP70-8 overexpression lines (labelled 4, 12, and 13) and Col-0 plants. Lower panel, phenotype comparison between TuMV-infected HSP70-12 overexpression lines (labelled F, K, and N) and Col-0 plants. Above Images were taken

at 14 dpi. Mock, infiltrated with *A. tumefaciens*; TuMV, infiltrated with *A. tumefaciens* harboring TuMV infectious clone at OD600 of 0.03.

(E) Left first panel: fold change of TuMV RNA accumulation HSP70-1 overexpression lines compared with Col-0 plants evaluated by qPCR. Left second panel: fold change of TuMV RNA accumulation in HSP70-2 overexpression lines compared with Col-0 plants evaluated by qPCR. Left third panel: Fold change of TuMV RNA accumulation in HSP70-8 overexpression lines compared with Col-0 plants evaluated by qPCR. Right panel: Fold change of TuMV RNA accumulation in HSP70-12 overexpression lines compared with Col-0 plants evaluated by qPCR. The TuMV RNA level of Col-0 control was set to 1. All TuMV RNA levels were normalized against Actin8 transcripts in the same sample. RNA was extracted from stalk tip flowers at 14 dpi. Data were collected from five independent experiments. Error bars represent standard deviation (n=5).

3.3 Understanding of the possible role of HSP70s in the TuMV infection cycle

3.3.1 Evaluation of TuMV multiplication in protoplasts isolated from HSP70 mutant lines

To explore the possible roles of host genes of interest in viral infection, one may isolate mesophyll cell protoplasts of plants of the corresponding gene mutant and conduct a transfection/replication assay to determine if viral replication is affected or not (Dai & Wang, 2022). This is because protoplasts have disrupted PD structures and after transfection with a viral infectious clone, viral genome multiplication is contained within transfected protoplast (individual, disconnected cells) without viral cell-to-cell movement. Protoplasts were isolated from *hsp70-1/2*, *hsp70-8*, *hsp70-11/12* mutant plants and wild-type Col-0 plants, and then transfected with the TuMV infectious clone pCambiaTunos/GFP using the PEG method (Fig. 9A). RNA extraction followed by RT-qPCR was performed at 24 hpt and 48 hpt to evaluate TuMV RNA level. Protoplasts from mutant plants did not exhibit observable phenotypic difference before or after transformation compared with wild-type protoplasts. RT-qPCR results indicated that TuMV RNA level in *hsp70-1/2*, *hsp70-8*, and *hsp70-11/12* mutant protoplasts were reduced at 48 hpt (Fig. 9B). This result suggests that HSP70-1, HSP70-2, HSP70-8. HSP70-11, and HSP70-12 might be proviral host factors facilitating TuMV genome replication.

3.3.2 TuMV cell-to-cell movement is not affected in *N. benthamiana* with transient HSP70 expression

To observe the effect of HSP70 overexpression on TuMV cell-to-cell movement, the model plant *N. benthamiana* and the double-cassette infectious clone pCBTuMV-GFP/mCherry were used. This clone contains two expression cassettes, one for the expression of the mCherry fluorescent protein fused with an ER retention signal and the other for the transcription of a recombinant TuMV genome with GFP coding sequence embedded (Dai et al, 2020). After inoculation with this clone, the primarily infected cells would emit both GFP and mCherry fluorescence while secondarily infected cells would emit GFP fluorescence only. *A. tumefaciens* harboring pCBTuMV-GFP/mCherry (at OD600 of 0.002) was co-infiltrated into *N. benthamiana* leaf cells with either *A. tumefaciens* harboring pBA-HSP70 vector or pBA empty vector. At 84 hpi, the inoculated leaf was observed under a confocal microscope. It was found that in *N. benthamiana* leaf cells transiently overexpressing HSP70s and inoculated with the double-cassette infectious clone, the clusters of cells emitting green fluorescence only resulting from TuMV intercellular

spread from primary infection foci (emitting both green and red fluorescence) were of the similar size as those in with the control (overexpressing the empty vector pBA and inoculated with pCBTuMV-GFP/mCherry) (Fig. 10). This result indicates that overexpression of HSP70s does not affect TuMV cell-to-cell movement. Interestingly, I noticed that, in comparison to that in the control, the number of infection foci was apparently reduced in *N. benthamiana* leaves expressing HSP70-1, HSP70-2, or HSP70-8 but remarkably increased in the leaf expressing HSP70-11 or HSP70-12 (data not shown).
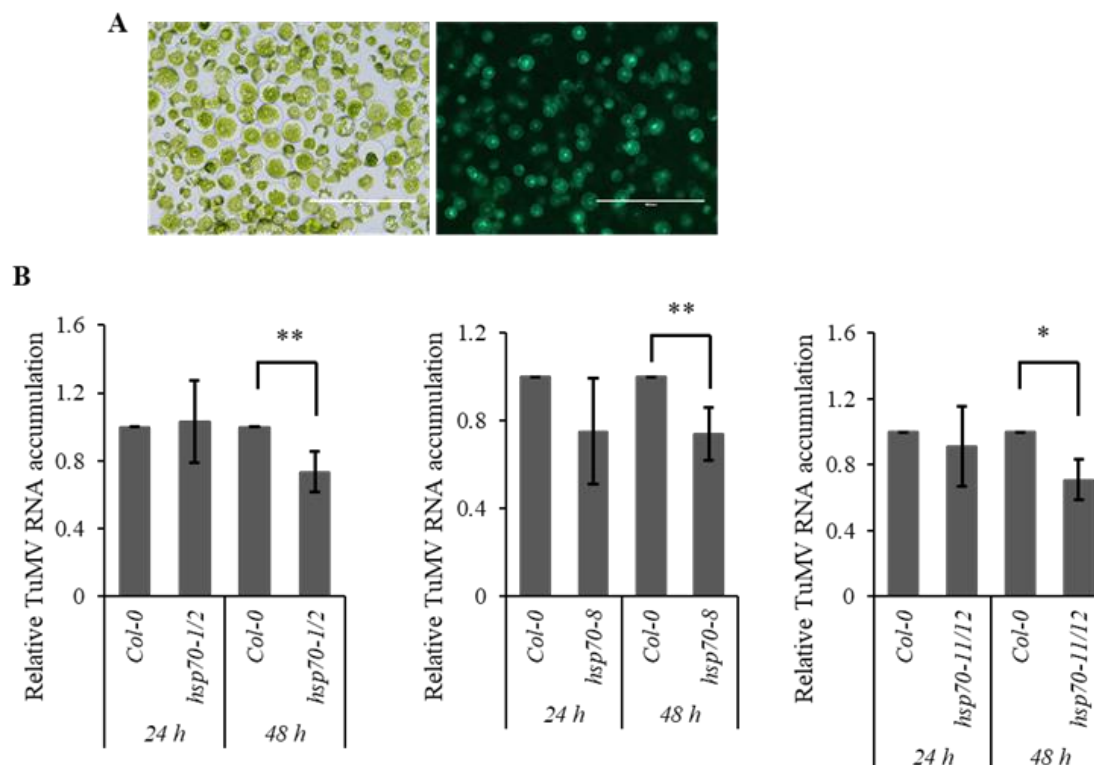
Figure 9. Evaluation of TuMV multiplication in protoplasts isolated from HSP70 knockout or knockdown lines

(A) Left panel: *A. thaliana* protoplast isolated from mesophyll cells. Right panel: protoplasts transformed with plasmid carrying GFP-labeled TuMV sequence. Bar=400 µm.

(B) Fold change of TuMV RNA accumulation in *hsp70-1/2* (left panel), *hsp70-8* (middle panel), and *hsp70-11/12* (right panel) protoplasts compared with control Col-0 protoplast at 24 hpi and 48 hpi evaluated by RT-qPCR. The TuMV RNA level of Col-0 control was set to 1 at each time point. All TuMV RNA levels were normalized against Actin8 transcripts in the same sample. Data were collected from five independent experiments. Error bars represent standard deviation (n=5), **P<0.05, *P<0.1, student's t test, two-tailed, unpaired.
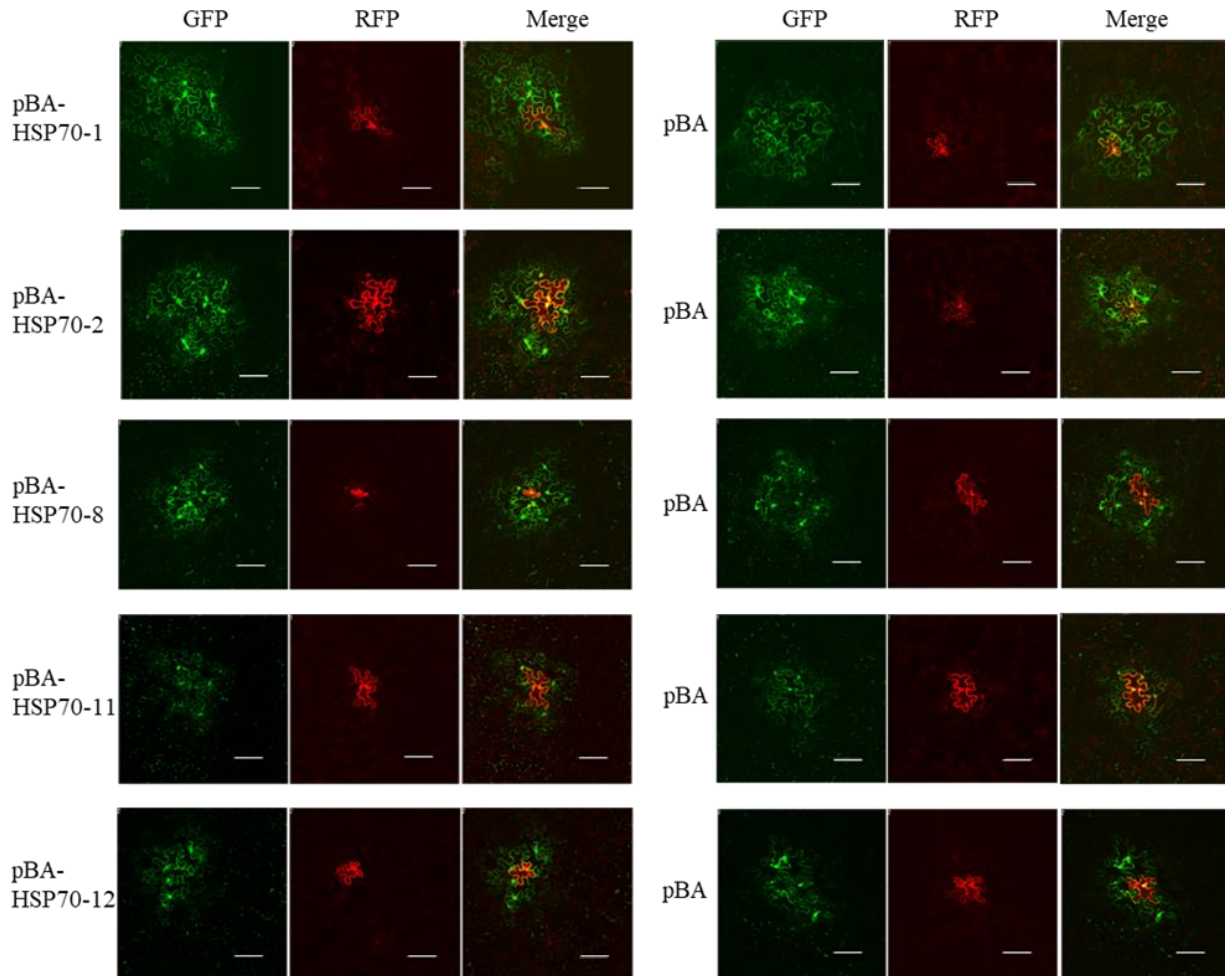
Figure 10. TuMV cell-to-cell movement is not affected in *N. benthamiana* with transient HSP70 expression

Analysis of cell-to-cell movement of TuMV infectious clone pCBTuMV-GFP/mCherry agroinfiltrated into *N. benthamiana* leaf epidermal cells transiently expressing HSP70s (left panel). *A. tumefaciens* harboring pBA empty vector was infiltrated on the same leaf as a control (right panel). Confocal images were taken at 84 hpi on infiltrated leaf. Primarily infected cells emit both green and red fluorescence and secondarily infected cells emit only green fluorescence. Bar = 100 μm.

3.3.3 TuMV local infection is affected in *N. benthamiana* transiently expressing HSP70s

In the TuMV infecting *A. thaliana* pathosystem, stable overexpression of HSP70s did not have an effect on TuMV infection, probably due to the redundancy of native HSP70s. To further evaluate the effect of HSP70 overexpression on TuMV infection, I determined viral CP accumulation in primarily infected cells in *N. benthamiana* transiently expressing HSP70s. Since cell-to-cell spread of the infiltrated TuMV infectious clone takes place between 3 and 4 dpi (Dai, 2018), viral CP accumulation in the inoculated leaf area at or before 3 dpi is attributed to primarily infected cells. *A. tumefaciens* harboring pCBTuMV-GFP/mCherry (at OD600 of 0.1) was co-infiltrated with either *A. tumefaciens* harboring one of pBA-HSP70 vectors or pBA empty vector. Finally, immunoblotting confirmed the expression of HSP70s *N. benthamiana* (Fig. 11A). Immunoblotting with anti-TuMV CP antibodies revealed that in *N. benthamiana* leaf transiently expressing HSP70-1, HSP70-2, and HSP70-8, TuMV local infection was significantly reduced as shown by reduced CP protein levels compared with *N. benthamiana* leaf infiltrated with pBA empty vector (Fig. 11B left panel, Fig. 11C; Fig. S2 left panel). On the contrary, transient expression of HSP70-11 and HSP70-12 enhanced TuMV infection (Fig. 11B right panel, Fig. 11C; Fig. S2 right panel), though the enhancement of TuMV by HSP70-11 did not reach statistical significance, TuMV CP level was increased in each of the three repeats. These results support that HSP70-11 and HSP70-12 are proviral factors for TuMV along with both infection assays with HSP70-11 and HSP70-12 double mutant plant and protoplast (Fig. 7C, Fig. 7F; Fig. 9B right panel). These data are also consistent with the data from the HSP70-1 and HSP70-2 double mutant plant that HSP70-1 and HSP70-2 inhibit TuMV infection but are contradictory to the data from the protoplast assay that HSP70-1, HSP70-2 and HSP70-8 promote TuMV multiplication.
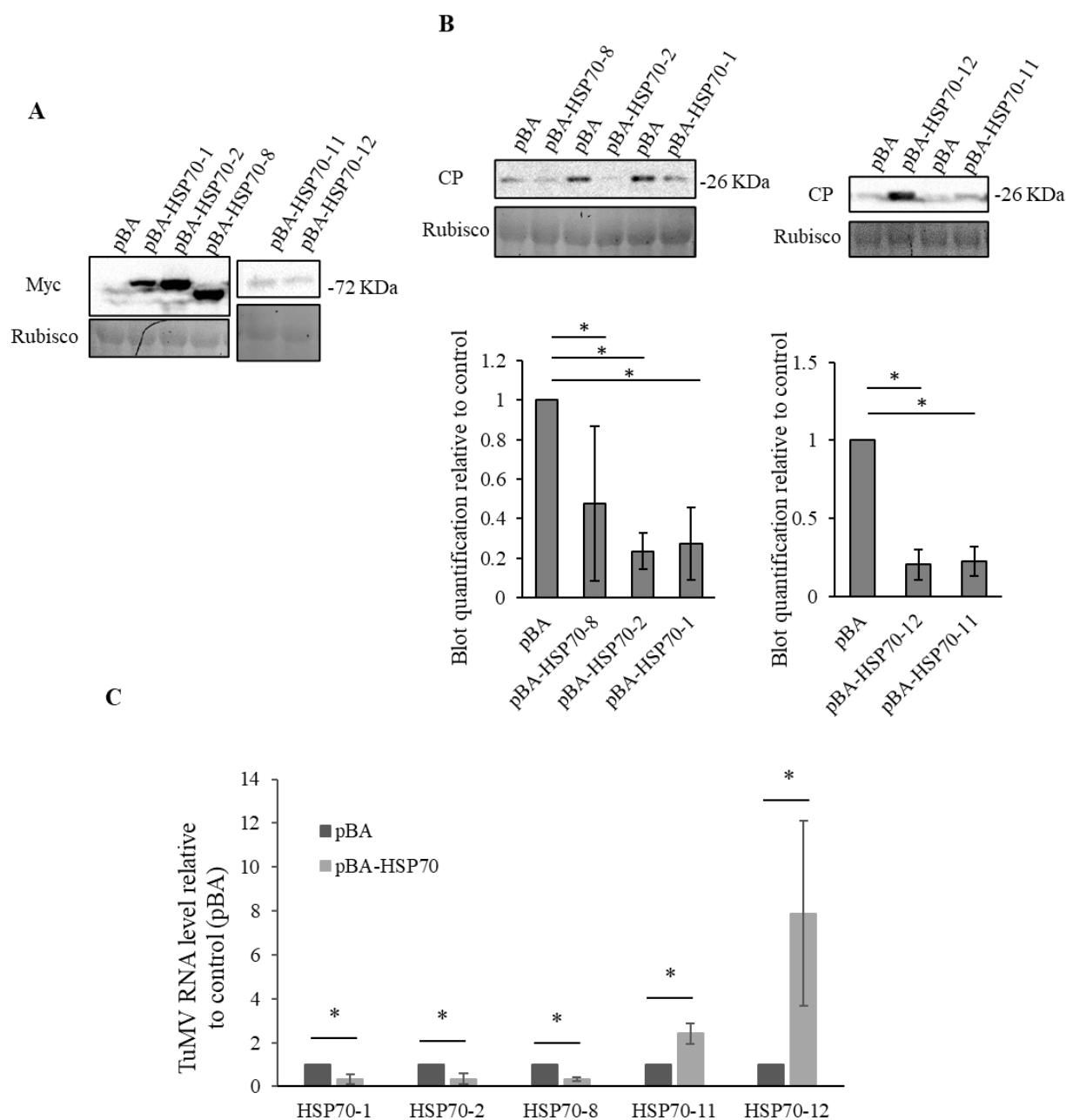
Figure 11. TuMV local infection is affected in *N. benthamiana* transiently expressing HSP70s

(A) The expression of HSP70 proteins in *N. benthamiana* by pBA expression vectors.

(B) Evaluation of TuMV accumulation in *N. benthamiana* transiently expressing HSP70s. *A. tumefaciens* harboring pBA empty vector was infiltrated in place of HSP70 expression vectors on

the same leaf as a control. Sample from the infiltrated leaf were taken at 3 dpi and immunoblotted with anti-TuMV CP antibodies. Rubisco large subunit is shown as a loading control. Experiments were repeated three times with similar results. The blots were quantified with ImageJ from three experiments using rubisco band as internal control and pBA control band intensity set to 1. * P<0.1, student's t test, two-tailed, unpaired.

(C) Fold change of TuMV RNA accumulation in *N. benthamiana* transiently expressing HSP70s. A. tumefaciens harboring pBA empty vector infiltrated in place of HSP70 expression vectors on the same leaf was used as a control with TuMV RNA level set to 1. All TuMV RNA levels were normalized against actin transcripts in the same sample. Data were collected from three independent experiments. Error bars represent standard deviation (n=3), **P<0.05, student's t test, two-tailed, unpaired.

3.4 Studying the interaction of HSP70s with virus and host factors

3.4.1 HSP70s interact with TuMV proteins NIb and CP

To investigate if HSP70s interact with TuMV viral proteins, yeast two hybrid (Y2H) was performed to detect possible interactions between HSP70 and TuMV viral proteins. In the Matchmaker Gold Yeast Two-Hybrid System, I screened the interaction of HSP70s with TuMV proteins, with each pair being switched between bait and pray. Positive interactions were only detected with HSP70s as prey (AD-HSP70s) and TuMV replicase protein NIb as the bait (BK-NIb). Yeast co-transformed with BK-NIb and AD-HSP70-1, AD-HSP70-2, AS-HSP70-8, AD-HSP70-11 or AD-HSP70-12 showed growth on high stringency selection plates (SD/-Ade/-His/-Leu/-Trp) (Fig. 12A). Yeast co-transformed with BK-NIb and AD empty vector and yeast co-transformed with AD-HSP70s with BK empty vector did not grow (Fig. S3), indicating BK-NIb and AD-HSP70s do not cause auto activation of reporter genes in the Matchmaker Gold Yeast Two-Hybrid System. The Split-Ubiquitin Based Membrane Yeast Two-Hybrid system was used to detect more possible interactions of HSP70s with TuMV proteins that occur on cellular membranes. Positive signals were detected between HSP70s and CP, NIb or eIF9(iso)4E (Fig. S5). However, autoactivation of reporter genes by HSP70s happened regardless of being used as a bait or prey (Fig. S4), rendering this system useless in determining the interaction of HSP70s.

BiFC assay was also employed to assess the interaction between HSP70s of interest and NIb as well as the TuMV coat protein CP, which is also involved in potyvirus multiplication and regulated by HSP70 (Hafrén et al, 2010; Lõhmus et al, 2017). The coding sequences of HSP70s and TuMV proteins NIb and CP were introduced into BiFC vectors that contain either the DNA sequences encoding N-terminal or C-terminal of YFP. Negative controls for BiFC are shown in Fig. S6. *A. tumefaciens* harboring YC-HSP70-1, YC-HSP70-2, or YC-HSP70-8 were co-infiltrated with *A. tumefaciens* harboring YN-NIb or YN-CP into *N. benthamiana* leaf, and yellow fluorescence signals were detected at 48 dpi using confocal microscope (Fig. 12B), suggesting positive interactions between three HSP70s (HSP70-1, HSP70-2, and HSP70-8) and two TuMV proteins (NIb and CP).

Since YN-HSP70-11, YN-HSP70-12, YC-HSP70-11 and YC-HSP70-12 proteins were barely detectable when transiently expressed in *N. benthamiana*, probably due to their fast turnover. Co-IP was employed to confirm the interaction between HSP70-11 and HSP70-12 with TuMV

proteins NIb and CP. *A. tumefaciens* harboring 104-HSP70-11 and 104-HSP70-12 that allow for the expression of HSP70-11 or HSP70-12 with YFP tag at its N-terminal were co-infiltrated with pBA-NIb or pBA-CP. An empty pBA vector co-infiltrated with 104-HSP70-11 or 104-HSP70-12 as well as 201-GFP co-infiltrated with pBA-NIb or pBA-CP served as controls. Protein extracts from infiltrated *N. benthamiana* leaves were directly subjected for immunoblotting analysis for input detection or incubated with anti-Flag M2 affinity gel for Co-IP. For Co-IP, the affinity gel beads were washed 5 times and subjected to western blot using anti-GFP and anti-Myc antibody, the result showed that HSP70-11 and HSP70-12 do interact with TuMV proteins NIb and CP *in planta* (Fig. 12C). Taken together, these data suggest that five HSP70s (HSP70-1, HSP70-2, HSP80-8, HSP70-11 and HSP70-12) examined here interact with TuMV proteins NIb and CP.

3.4.2 HSP70s interact with eIF(iso)4E

The initial IP-MS work from our lab identified HSP70-1, HSP70-6, HSP70-7, and HSP70-12 as components of the eIF(iso)4E complex in TuMV-infected *A. thaliana*. This prompted me to check if the five selected HSP70s interact with *A. thaliana* eIF(iso)4E. BiFC analysis confirmed the interaction of HSP70-1, HSP70-2, or HSP70-8 with eIF(iso)4E in *N. benthamiana* (Fig. 13A), and Co-IP verified the interaction of HSP70-11 or HSP70-12 with eIF(iso)4E in *N. benthamiana* as well (Fig. 13B).
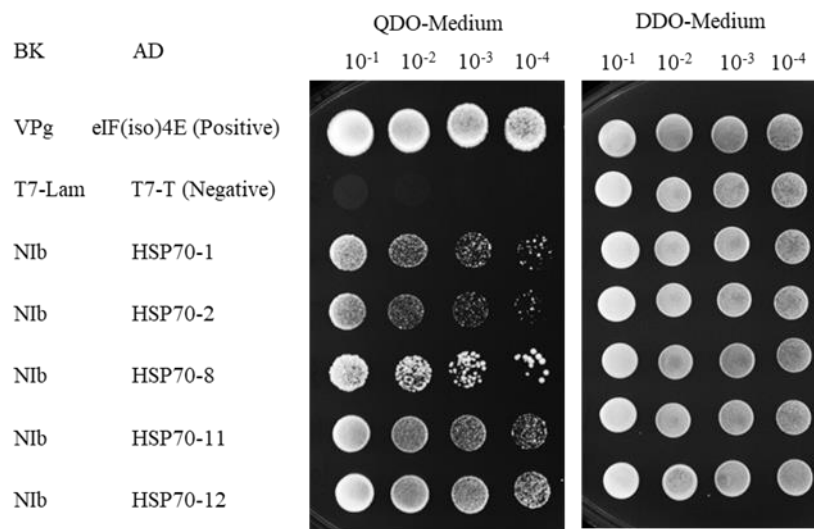
Matchmaker® Y2H system
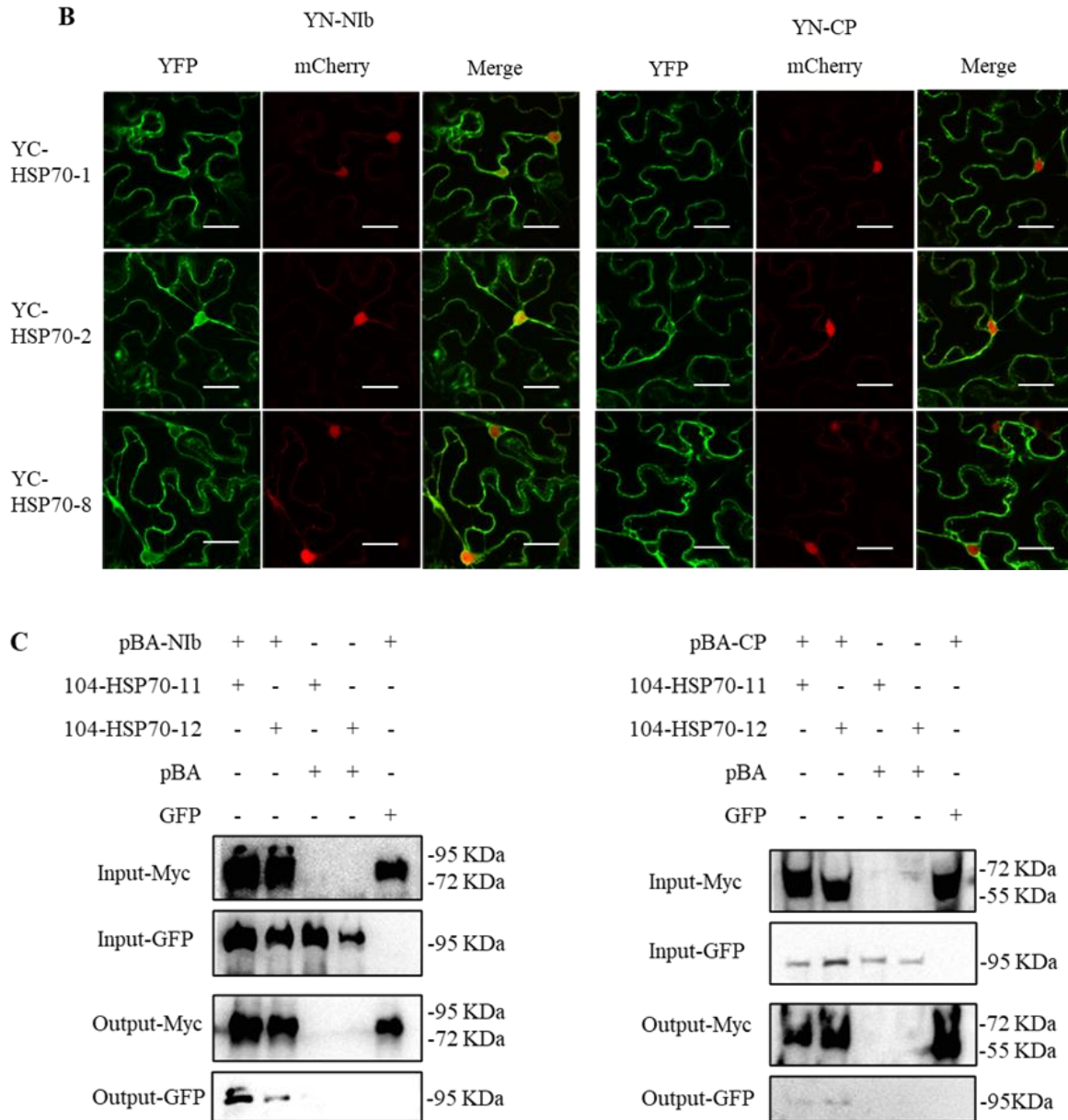
Figure 12. HSP70s of interest interact with TuMV proteins NIb and CP

(A) Y2H analysis of possible HSP70s and NIb interactions. Yeast competent cells co-transformed with bait and prey plasmids were plated on double dropout (DDO) media lacking tryptophan and leucine to select for double transformation. Successfully transformed colonies were plated on quadruple dropout (QDO) media lacking tryptophan, leucine, histidine and adenine to confirm protein interaction. Yeast co-transformed with AD-eIF(iso)4E and BK-VPg served as positive control.

(B) BiFC analysis of HSP70s interaction with TuMV NIb and CP *in planta*. Positive interactions were observed between HSP70-1, HSP70-2, HSP70-8 and NIb, as well as HSP70-1, HSP70-2, HSP70-8 and CP, respectively at 48 hpi. Cell nuclei were labelled with mCherry. Experiments were repeated three times with similar results. Bars=30 μm.

(C) Co-IP analysis of the interaction of HSP70-11 and HSP70-12 with TuMV proteins NIb and CP. HSP70-11 and HSP70-12 were fused to YFP-tagged expression vectors, NIb or CP were fused to Flag/Myc-tagged expression vectors. Protein extracts were incubated with anti-Flag M2 affinity gel. Protein samples before (Input) and after (Output) immunopurification were subjected to immunoblotting using Myc or GFP antibody.
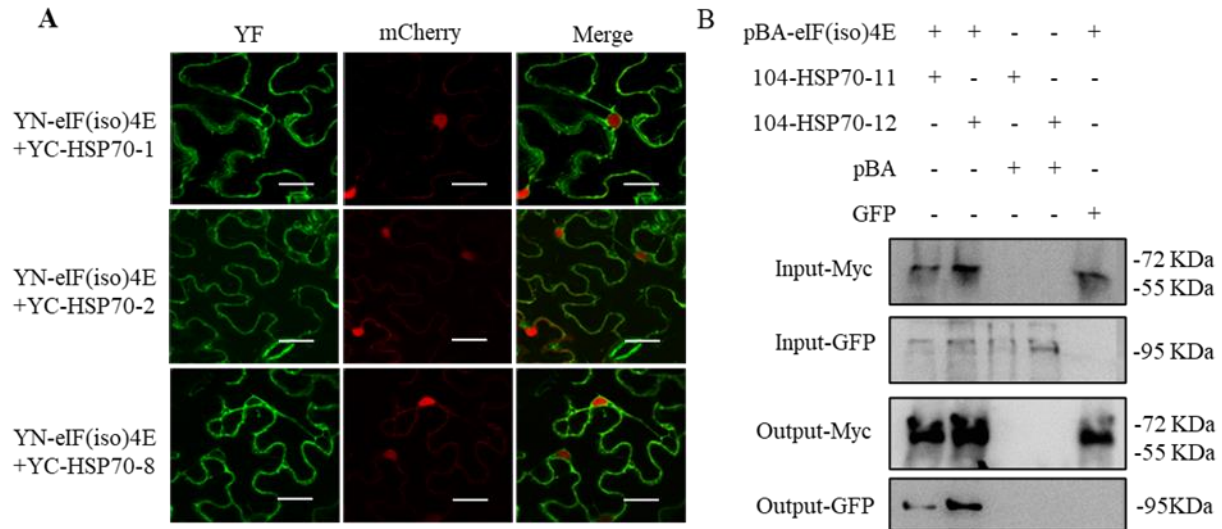
Figure 13. eIF(iso)4E interacts with HSP70-1, HSP70-2, HSP70-8, HSP70-11 and HSP70-12

(A) BiFC analysis of HSP70-1, HSP70-2, and HSP70-8 interaction with *A. thaliana* eIF(iso)4E in planta. Positive interactions were observed between HSP70-1, HSP70-2, HSP70-8 and eIF(iso)4E at 48 hpi. Cell nuclei were labelled with mCherry. Experiments were repeated three times with similar results. Bars=30 μm.

(B) Co-IP analysis of HSP70-11 and HSP70-12 interaction with *A. thaliana* eIF(iso)4E. HSP70-11 or HSP70-12 and eIF(iso)4E were fused to YFP and Flag/Myc-tagged expression vectors, respectively. Protein extracts were incubated with anti-Flag M2 affinity gel. Protein samples before and after immunopurification were subjected to immunoblotting using Myc or GFP antibody.

3.5 Subcellular localization of HSP70s and co-localization with VRC

3.5.1 Subcellular localization of 103-HSP70-1, 103-HSP70-2, 103-HSP70-8, 104-HSP70-11, and 104-HSP70-12

To gain insights into the molecular function of HSP70s, subcellular localization of GFP or YFP tagged HSP70s were visualized in *N. benthamiana* leaves. *A. tumefaciens* harboring 103-HSP70-1, 103-HSP70-2, 103-HSP70-8, 104-HSP70-11, and 104-HSP70-12 were co-infiltrated into *N. benthamiana* leaves with the nucleus marker NLS-mCherry or ER marker mCherry-HDEL. Subcellular localization of fusion proteins was visualized with confocal microscope at 48 hpi. HSP70-1, HSP70-2, and HSP70-8 were localized in the cytoplasm and nucleus (Fig. 14A), consistent with previous report (Inoue et al, 2008; Leng et al, 2017). HSP70-11 and HSP70-12 were evident in the cytoplasm as well as in the perinuclear region (Fig. 14B). A small proportion of fluorescence could also be detected within the nucleus. The ER marker mCherry-HDEL highlighted a web-shaped structure, indicating its localization in the cytoplasm is tightly associated with the ER network. HSP70-11 and HSP70-12 colocalized with mCherry-labeled ER web-shape structure (Fig. 14D). For HSP70-1, HSP70-2, and HSP70-8, though their fluorescence partially highlighted the ER, their fluorescence did not exhibit such a clear-cut and sharp edge as the fluorescence of HSP70-11 and HSP70-12 (Fig. 14C).

3.5.2 HSP70s co-localize with TuMV VRC in infected cell

HSP70 is a component of VRCs of diverse viruses including TuMV (Tang et al, 2020; Wang, 2015). To confirm whether HSP70s identified from this study also co-localize with VRC in TuMV-infected plants, fluorescent protein-tagged HSP70s were transiently expressed in *N. benthamiana* leaves together with pCambiaTunos/6K-mcherry by agroinfiltration at OD600 of 0.3. Subcellular localization of HSP70 fusion proteins were visualized by confocal microscopy at 3 dpi. VRCs were visualized as clustered vesicle structures with red fluorescence. Consistent with previous findings, yellow or green fluorescence emitted by fluorescent protein-tagged HSP70s was concentrated around VRC structures (Fig. 15).

| | GFP | mCherry | Merge |

A

103-HSP70-1
+ mCherry-NLS

103-HSP70-2
+ mCherry-NLS

103-HSP70-8
+ mCherry-NLS

| | YFP | mCherry | Merge |

B

104-HSP70-11
+ mCherry-NLS

104-HSP70-12
+ mCherry-NLS

| | GFP | mCherry | Merge |

103-HSP70-1 + mCherry-HDEL

103-HSP70-2 + mCherry-HDEL

103-HSP70-8 + mCherry-HDEL

| | YFP | mCherry | Merge |

104-HSP70-11 + mCherry-HDEL

104-HSP70-12 + mCherry-HDEL
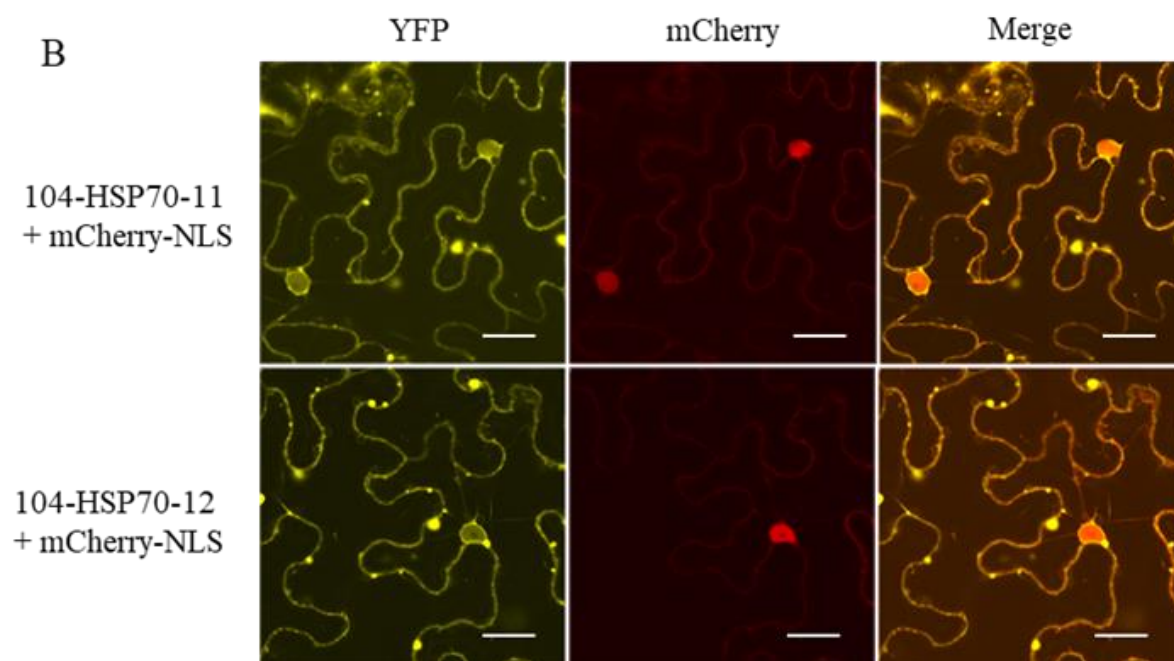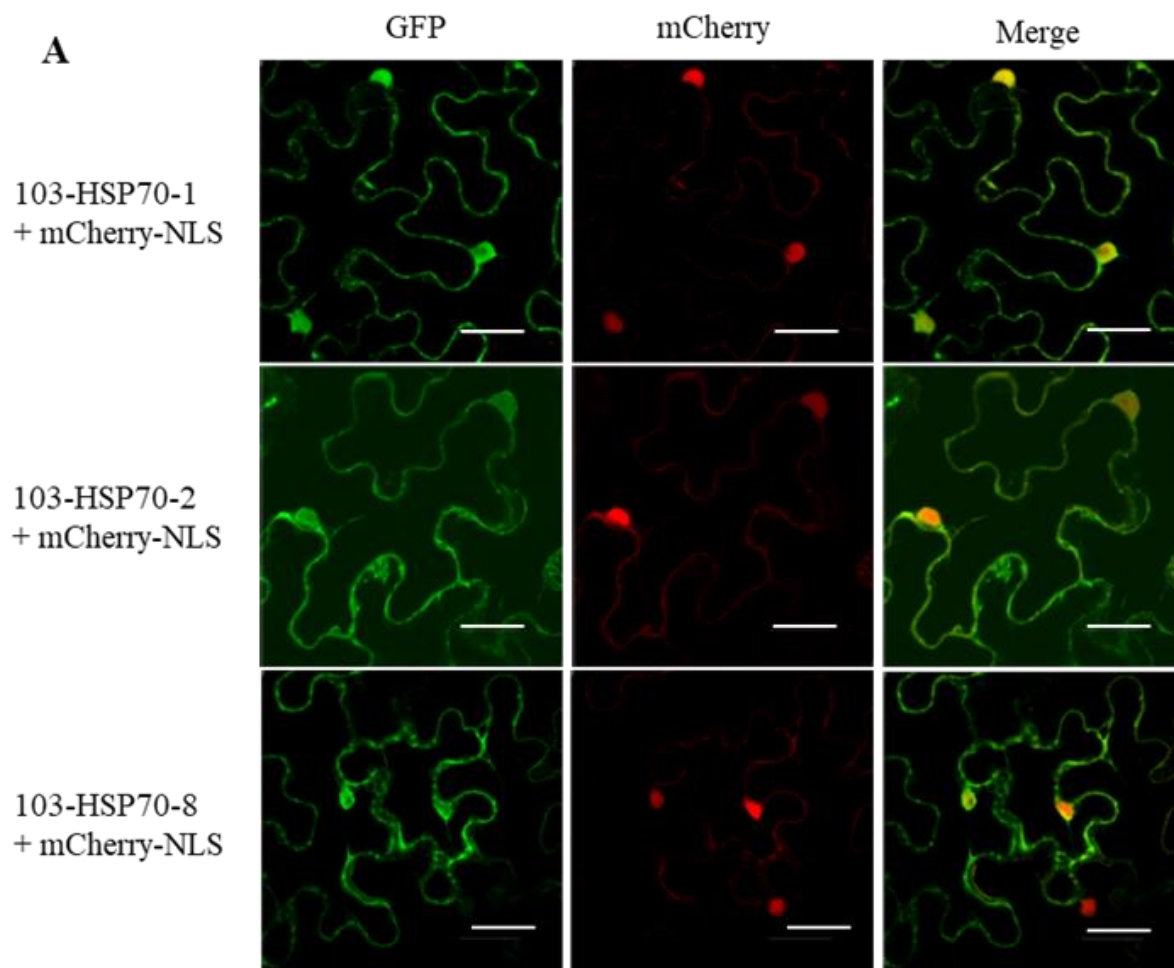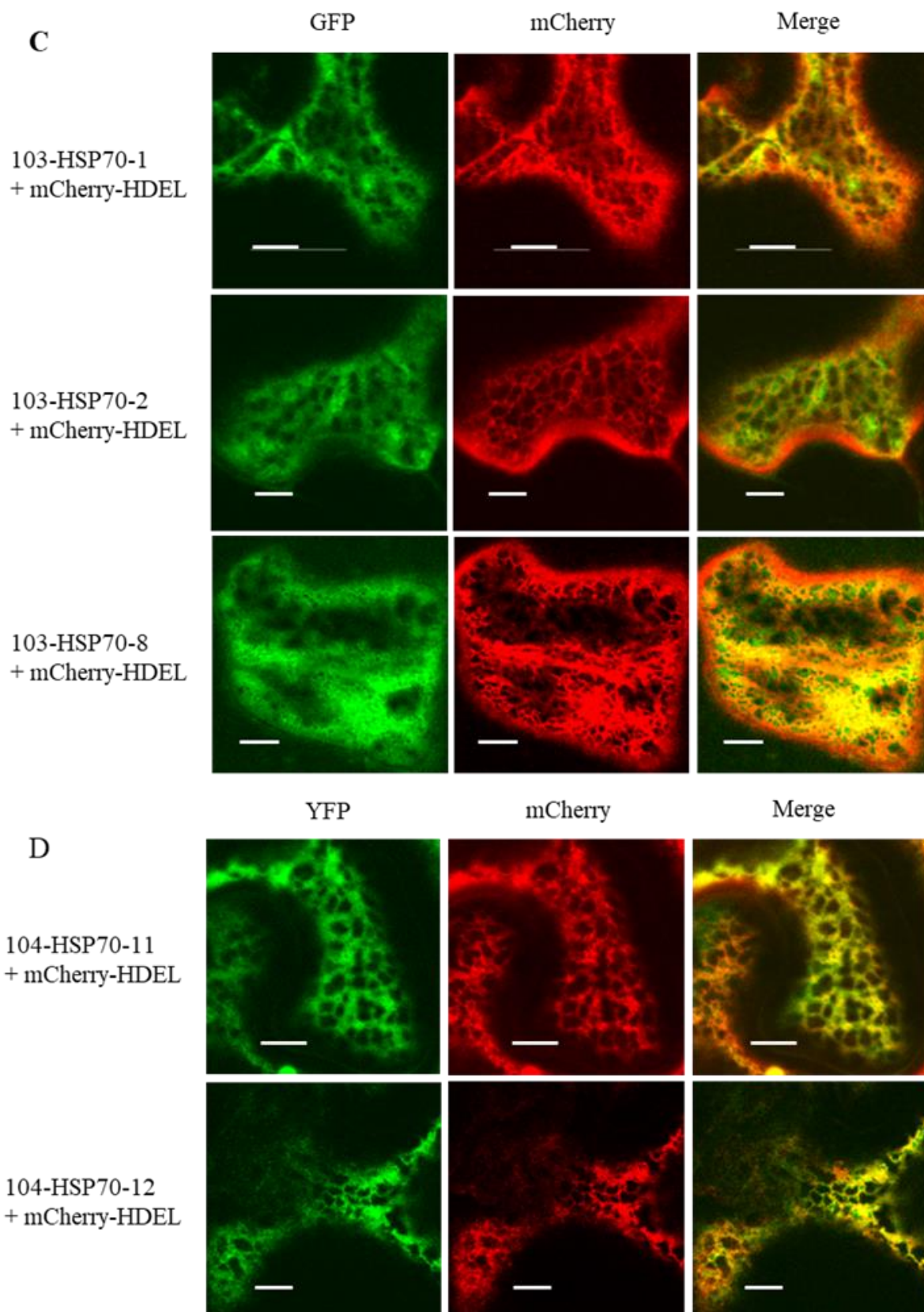
Figure 14. Subcellular localization of fluorescent-protein tagged HSP70s

(A) Co-expression of fluorescent protein-tagged HSP70-1, HSP70-2, and HSP70-8 with mCherry labelled cell nucleus *in planta*. Photos were taken 48 hpi using confocal microscope. Bar=30 μm.

(B) Co-expression of fluorescent protein-tagged HSP70-11 and HSP70-12 with mCherry labelled cell nucleus *in planta*. Photos were taken 48 hpi using confocal microscope. Bar=30 μm.

(C) Co-expression of fluorescent protein-tagged HSP70-1, HSP70-2, and HSP70-8 with mCherry labelled ER *in planta*. Photos were taken 48 hpi using confocal microscope. Bar=5 μm.

(D) Co-expression of fluorescent protein-tagged HSP70-11 and HSP70-12 with mCherry labelled *ER in planta*. Photos were taken 48 hpi using confocal microscope. Bar=5 μm.
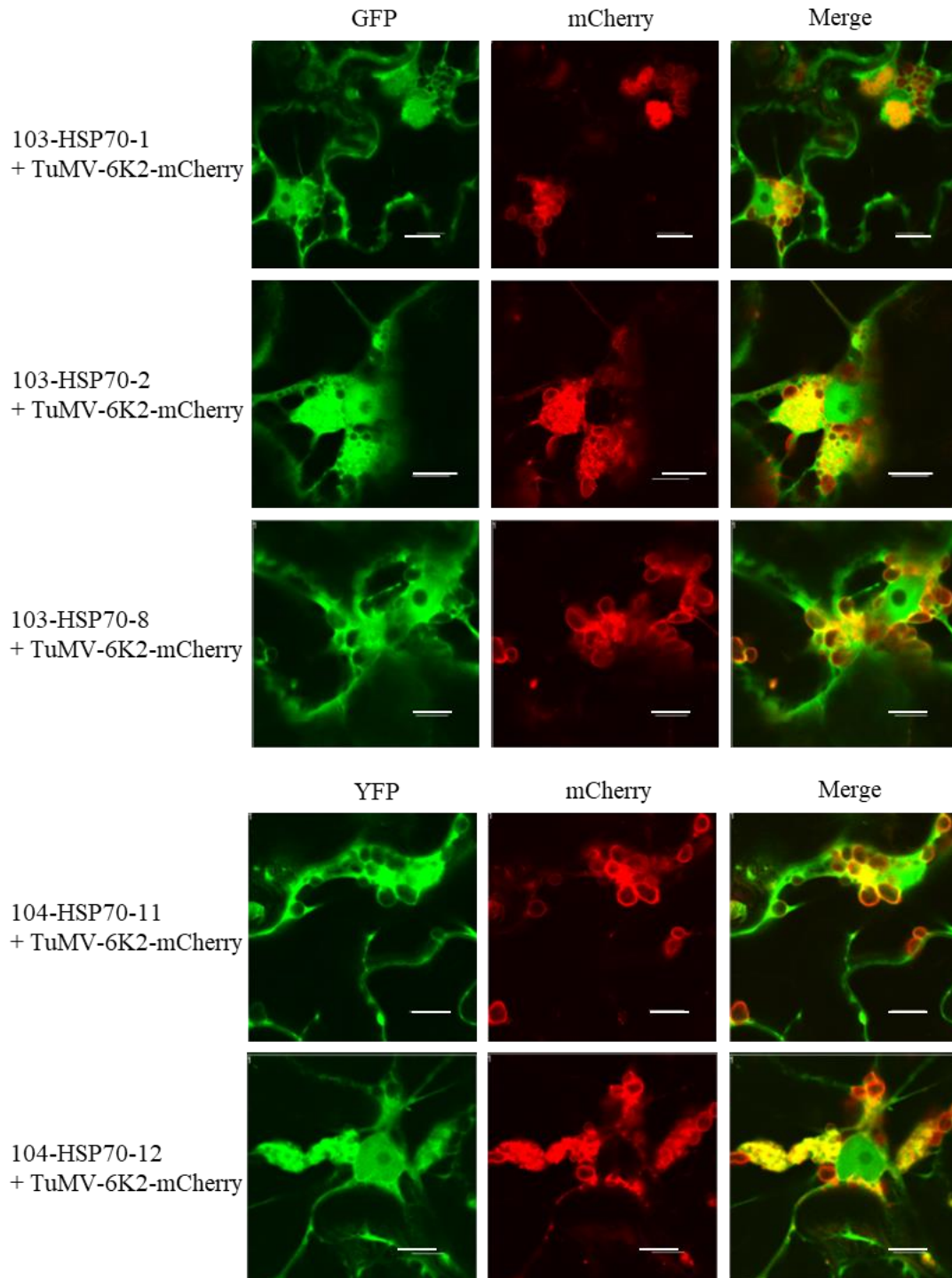
Figure 15. HSP70s co-localize with TuMV VRC in infected cells

Fluorescent protein-tagged HSP70s colocalized with mCherry labeled VRCs in TuMV-infected *N. benthamiana* leaf cells. Photos were taken 3 dpi under a confocal microscope. Bar=10 μm.

3.6 HSP70s mediate interaction partners by altering their turnover

3.6.1 HSP70s do not change the subcellular localization of its interaction partners

To investigate if transient expression of HSP70s in *N. benthamiana* leaves affects subcellular localization of their interactors eIF(iso)4E and TuMV CP and NIb, *A. tumefaciens* harboring 102-NIb, 102-CP, and 102-eIF(iso)4E were infiltrated alone, or with 103-HSP70-1, 103-HSP70-2, 103-HSP70-8, 104-HSP70-11, or 104-HSP70-12, each at OD600 of 0.3. A plant expression vector that allows for the expression of the nucleus marker NLS-mCherry was also co-infiltrated. Subcellular localization of fluorescence fusion proteins was visualized by confocal microscopy at 48 hpi. NIb fusion protein (blue fluorescence signals) was evident in the nucleus and cytoplasm (Fig. 16A, top panel), consistent with previously published results (Li et al, 2018a). CP was present mostly in the cytoplasm, with small amount of fluorescence around the nucleus (Fig. 16B), as previously reported (Dai et al, 2020). *A. thaliana* eIF(iso)4E was distributed to mainly to the cytoplasm and to a lesser extent to the nucleus (Fig. 16C, top panel), in agreement with previous findings that it is mainly located on the cytoplasmic membrane fraction and the interaction of eIF(iso)4E with VPg occurs in the nucleus (Beauchemin et al, 2007). Co-expression with HSP70s did not seem to alter the subcellular distribution of NIb, CP, and eIF(iso)4E (Fig. 16). Yellow or green fluorescence tagged HSP70s partially overlapped with blue fluorescence tagged NIb, CP, and eIF(iso)4E, further indicating that they might be in close proximity.

	CFP	GFP/YFP	mCherry	Merge
102-CP + mCherry-NLS				
103-HSP70-1 + 102-CP + mCherry-NLS				
103-HSP70-2 + 102-CP + mCherry-NLS				
103-HSP70-8 + 102-CP + mCherry-NLS				
104-HSP70-11 + 102-CP + mCherry-NLS				
104-HSP70-12 + 102-CP + mCherry-NLS				

B

	CFP	GFP/YFP	mCherry	Merge
102-eIF(iso)4E + mCherry-NLS				
103-HSP70-1 + 102-eIF(iso)4E + mCherry-NLS				
103-HSP70-2 + 102-eIF(iso)4E + mCherry-NLS				
103-HSP70-8 + 102-eIF(iso)4E + mCherry-NLS				
104-HSP70-11 + 102-eIF(iso)4E + mCherry-NLS				
104-HSP70-12 + 102-eIF(iso)4E + mCherry-NLS				

Figure 16. HSP70s do not change the subcellular localization of its interaction partners

(A) Co-expression of GFP or YFP-tagged HSP70s with CFP tagged NIb *in planta*.

(B) Co-expression of GFP or YFP-tagged HSP70s with CFP tagged CP *in planta*.

(C) Co-expression of GFP or YFP-tagged HSP70s with CFP tagged eIF(iso)4E *in planta*.

Cell nuclei were labeled with mCherry, photos were taken at 48 hpi using confocal microscope. Bar=30 μm.

3.6.2 HSP70s alter the protein level of transiently co-expressed NIb

To examine the effect of transient expression of HSP70s on the protein level of NIb, *A. tumefaciens* harboring 101-NIb was co-agroinfiltrated with pBA-HSP70-1, pBA-HSP70-2, pBA-HSP70-8, pBA-HSP70-11, or pBA-HSP70-12. pBA empty vector and 101-NIb were co-infiltrated into one half *of an N. benthamiana* leaf (as a control) and 101-NIb and pBA-HSP70s were co-infiltrated on the other half of the leaf. P19 was also co-infiltrated as an RNA silencing suppressor. Samples collected 3 dpi were subjected to immunoblotting with anti-GFP antibodies. Transient expression of HSP70-1, HSP70-2, and HSP70-8 significantly reduced the protein level of co-expressed NIb (Fig. 17A left panel; Fig. S7 left panel), while transient expression of HSP70-11 and HSP70-12 increased the protein level of co-expressed NIb (Fig. 17A right panel; Fig. S7 right panel). RT-qPCR was performed to assess if co-expression of HSP70s affects NIb mRNA level. No significant difference was found between NIb mRNA level from the sample co-infiltrated with HSP70s and that from the sample co-infiltrated with the empty vector (Fig. 17B). These results suggest that the presence of HSP70s alters NIb accumulation possibly through affecting its turnover.

3.6.3 Co-expression of HSP70-1, HSP70-2, and HSP70-8 facilitates NIb degradation in a ubiquitin-proteasome pathway dependent manner

To examine the possibility that HSP70s promote NIb degradation through the ubiquitin-proteasome pathway, NIb ubiquitination in *N. benthamiana* was examined. *A. tumefaciens* harboring 101-NIb was expressed in *N. benthamiana* by agroinfiltration and *A. tumefaciens* containing 104 empty vector was also infiltrated as a control. Leaf samples were collected at 3 dpi for protein extraction and immunoprecipitation by incubating with anti-GFP affinity beads. The affinity beads were washed 5 times and subjected to immunoblotting using anti-GFP (Fig. 18A right panel) and anti-ubiquitin antibodies (Fig. 18A left panel). It was found that NIb could be ubiquitinated via the ubiquitin-proteasome pathway for degradation. In agreement with this result, when the ubiquitin-proteasome pathway inhibitor MG-132 was infiltrated at 50 µM 16 h prior to sample collection, NIb protein levels increased (Fig. 18B; Fig. S8 right panel). To examine if HSP70s-mediated NIb degradation is dependent on the ubiquitin-proteasome pathway, HSP70-1, HSP70-2, or HSP70-8 was co-expressed with 101-NIb in *N. benthamiana* leaves and co-infiltration of pBA empty vector and 101-NIb served as a control. P19 was also co-infiltrated to suppress RNA silencing. Leaf samples were collected at 3 dpi and MG-132 was infiltrated 16 h

prior to sample collection. The samples were subjected to immunoblotting with anti-GFP antibodies. The amount of NIb from the sample co-infiltrated with HSP70s was similar to that from the sample co-infiltrated with the empty pBA vector (Fig. 18C; Fig. S8 right panel). Without MG-132 treatment, co-expression of HSP70-1, HSP70-2 or HSP70-8 enhanced NIb degradation (Fig. 17A left panel). Clearly, MG-132 treatment inhibited HSP70-1, HSP70-2 or HSP70-8-mediated NIb degradation. Taken together these data suggest that HSP70-1, HSP70-2, and HSP70-8-mediated NIb degradation is through the ubiquitin-proteasome pathway.
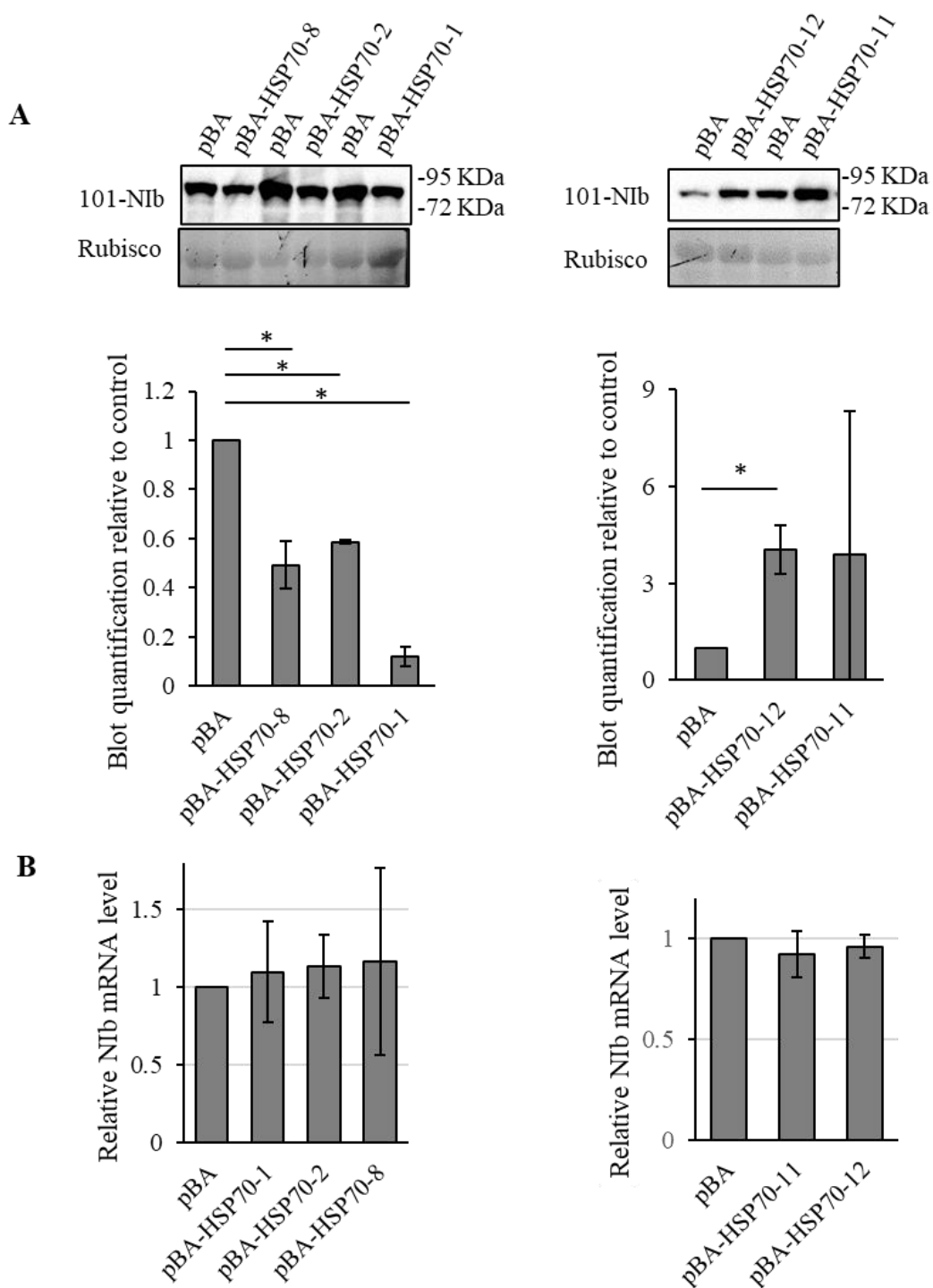
Figure 17. Co-expression of HSP70-1, HSP70-2, HSP70-8, HSP70-11 and HSP70-12 alters NIb protein accumulation

(A) Immunoblotting analysis of GFP-tagged NIb protein level in *N. benthamiana* leaves co-infiltrated with pBA-HSP70s or pBA empty vector. Rubisco large subunit is shown as a loading control. The blots were quantified with ImageJ from three experiments using rubisco band as internal control and pBA control band intensity was set to 1. * $P < 0.05$, student's t test, two-tailed, unpaired.

(B) RT-qCR analysis of GFP-tagged NIb protein mRNA expression level in *N. benthamiana* leaves co-infiltrated with pBA-HSP70s or pBA empty vector. The NIb mRNA level in control sample infiltrated with pBA empty vector in place of pBA-HSP70s was set to 1. All mRNA levels were normalized against Actin transcripts in the same sample, n=3.
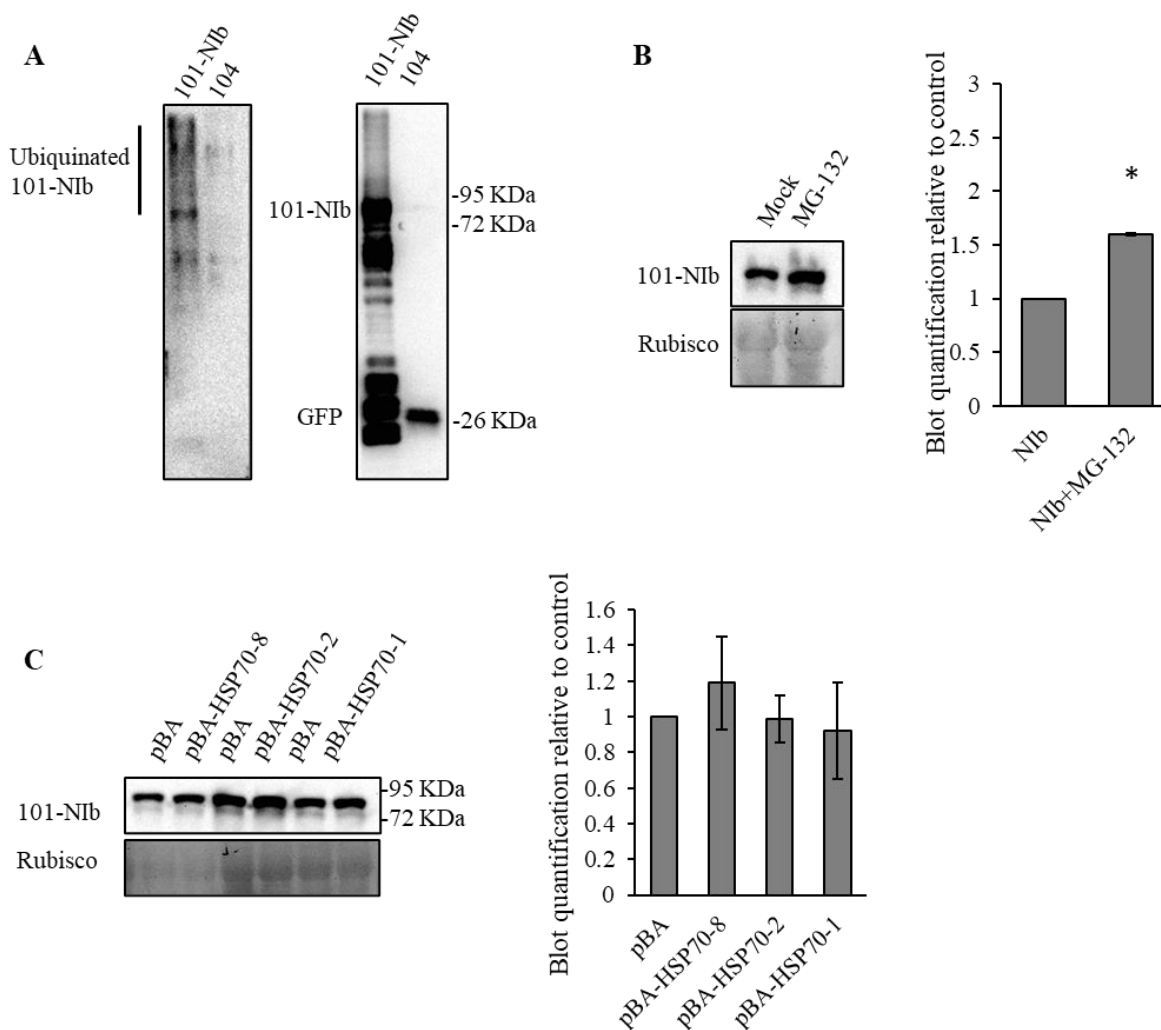
Figure 18. Co-expression of HSP70-1, HSP70-2, and HSP70-8 promotes NIb degradation in a ubiquitin-proteasome pathway-dependent manner

(A) Immunoblotting analysis of the ubiquitination of 101-NIb and 104 empty vectors expressed in *N. benthamiana* leaves and pulled down by anti-GFP affinity beads. Left panel, immunoblotting with ubiquitin antibody. Right panel, immunoblotting with GFP antibody.

(B) Immunoblotting analysis of YFP-tagged NIb protein level expressed in *N. benthamiana* leaves with MG-132 added 16 h prior to sample collection. Rubisco large subunit is shown as a loading control. The blots were quantified by ImageJ from three experiments using rubisco band as internal control and NIb control band intensity set to 1. * $P<0.05$, student's t test, two-tailed, unpaired.

(C) Immunoblotting analysis of GFP-tagged NIb protein level in *N. benthamiana* leaves co-infiltrated with pBA-HSP70s or pBA empty vector with MG-132 added 16 h prior to sample collection. Rubisco large subunit is shown as a loading control. The blots were quantified with ImageJ from three experiments using rubisco band as internal control and pBA control band intensity set to 1.

3.6.4 HSP70s alter the protein level of transiently co-expressed CP and eIF(iso)4E

To examine if co-expression of HSP70s also affect the protein stability of other interaction partners, namely, TuMV CP and host eIF(iso)4E, I conducted a similar experiment as described above for NIb. Immunoblotting results indicated that transient co-expression of HSP70-1, HSP70-2, and HSP70-8 also remarkably reduced the protein levels of CP and eIF(iso)4E (Fig. 19A; Fig. S9), whereas transient co-expression of HSP70-11 and HSP70-12 largely enhanced CP and eIF(iso)4E accumulation (Fig. 19B; Fig. S9). These results are very similar to what I found on NIb. I also ruled out the possibility that HSP70s alter the expression levels of co-expressed NIb, CP, and eIF(iso)4E through their YFP tags. The protein level of YFP was examined in *N. benthamiana* leaves transiently co-expressing empty 104 vector with pBA empty vector or with pBA vectors expressing HSP70s following the same procedure. The expression level of YFP was not affected by transient expression of HSP70s (Fig. S10). Apparently, HSP70-1, HP70-2 and HSP70-8 mediate degradation of their interaction partners, e.g., NIb, CP and eIF(iso)4E whereas HSP70-11 and HSP70-12 enhance the stability of these interactors.
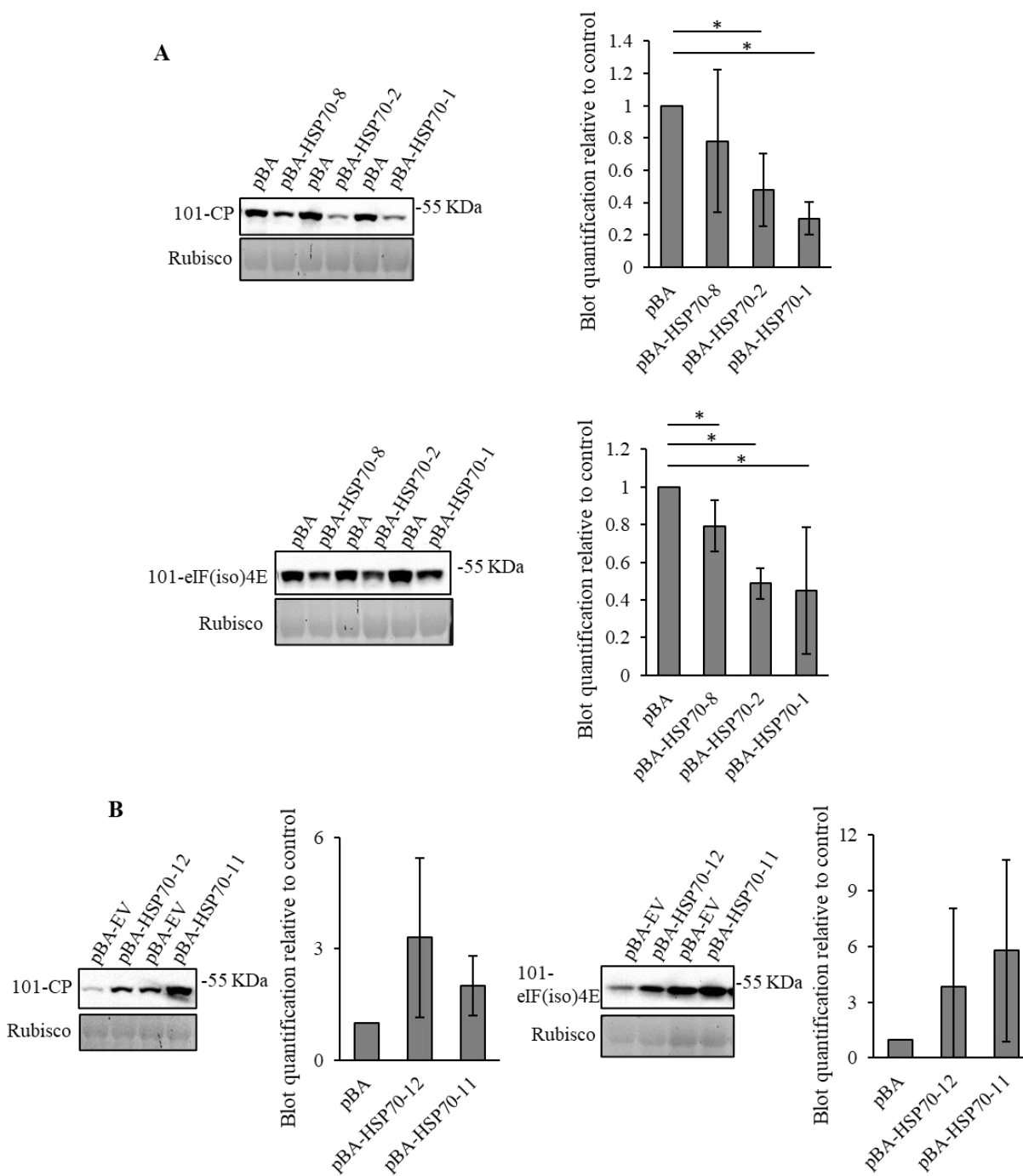
Figure 19. Co-expression of HSP70-1, HSP70-2, HSP70-8, HSP70-11 and HSP70-12 affects CP and eIF(iso)4E turnover

(A) Immunoblotting analysis of YFP-tagged CP and eIF(iso)4E protein level in *N. benthamiana* leaves co-infiltrated with pBA-HSP70-1, pBA-HSP70-2, pBA-HSP70-8 or pBA empty vector. Rubisco large subunit is shown as a loading control. The blots were quantified with ImageJ from three experiments using rubisco as an internal control, CP and eIF(iso)4E level in pBA control were set to 1. * $P<0.05$, student's t test, two-tailed, unpaired.

(B) Immunoblotting analysis of YFP-tagged CP and eIF(iso)4E protein level in *N. benthamiana* leaves co-infiltrated with pBA-HSP70-11 and pBA-HSP70-12 or pBA empty vector. Rubisco large subunit is shown as a loading control. The blots were quantified with ImageJ from three experiments using rubisco as an internal control, CP and eIF(iso)4E level in pBA control were set to 1.

3.6.5 Transient expression of HSP70-11 and HSP70-12 promotes TuMV infection is dependent on their ER localization

The fact that HSP70-11 and HSP70-12 are tightly associated with the ER network in the cytoplasm, promote TuMV infection and enhance the stability of their interacting proteins makes me wonder whether the proviral function of HSP70-11 and HSP70-12 require their ER targeting. To answer this question, expression vectors of HSP70s were re-constructed. The ER retention signal HDEL was added to the C-terminus of HSP70-1, HSP70-2, and HSP70-8, and the HDEL sequence at the C-terminus of HSP70-11 and HSP70-12 was deleted. *A. tumefaciens* harboring yellow fluorescence tagged HSP70s with altered localization signals was infiltrated into *N. benthamiana* with the ER marker mCherry-HDEL. Addition of the ER retention signal did not change subcellular localization of the cytoplasm HSP70s, as the C-terminal HDEL tagged HSP70-1, HSP70-2, and HSP70-8 emitted blurry shaped yellow fluorescence, rather than a sharp, clear-defined web-like structure highlighted by mCherry-HDEL, HSP70-11 or HSP70-12 (Fig. 14; Fig. 20A three upper panels). Deletion of HDEL from HSP70-11 and HSP70-12 apparently largely affected their ER association shown by the fuzzy shape of yellow fluorescence (Fig. 20A two lower panels).

To investigate the effect of transient expression of these altered HSP70 proteins on TuMV infection in *N. benthamiana* inoculated leaves, the coding sequences for HSP70s with altered localization signals were inserted into the pBA expression vector, and their expression in *N. benthamiana* were verified by immunoblotting (Fig. 20B). *A. tumefaciens* harboring pCBTuMV-GFP/mCherry (at OD600 of 0.1) was co-infiltrated into *N. benthamiana* with either *A. tumefaciens* harboring one of pBA-HSP70 vectors or the pBA empty vector (as a control). Immunoblotting with anti-TuMV CP antibodies was performed to detect CP in leaf samples collected at 3 dpi. In the *N. benthamiana* leaf transiently expressing HSP70-1-HDEL, HSP70-2-HDEL, HSP70-8-HDEL, HDEL-less HSP70-11 or HDEL-less HSP70-12, TuMV local infection was significantly reduced as shown by reduced CP protein levels compared with the control infiltrated with the pBA empty vector (Fig. 20C, Fig. 20D; Fig. S11). Removal of the HDEL from HSP70-11 and HSP70-12 reversed their proviral function, suggesting their role in promoting TuMV infection is dependent on their ER localization.

A

	YFP	mCherry	Merge
104-HSP70-1-HDEL + mCherry-HDEL			
104-HSP70-2-HDEL + mCherry-HDEL			
104-HSP70-8-HDEL + mCherry-HDEL			
104-HSP70-11-ΔHDEL + mCherry-HDEL			
104-HSP70-12-ΔHDEL + mCherry-HDEL			
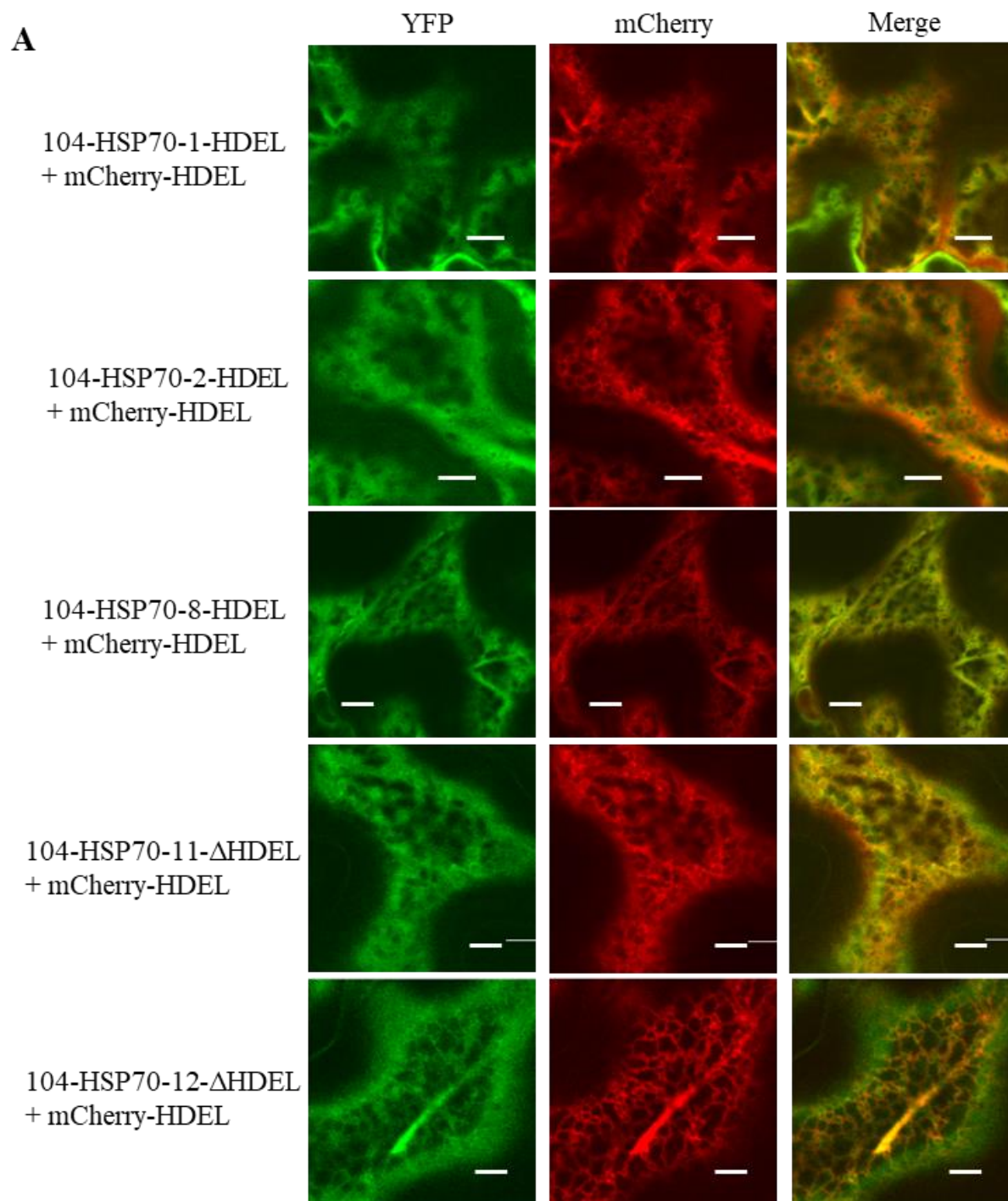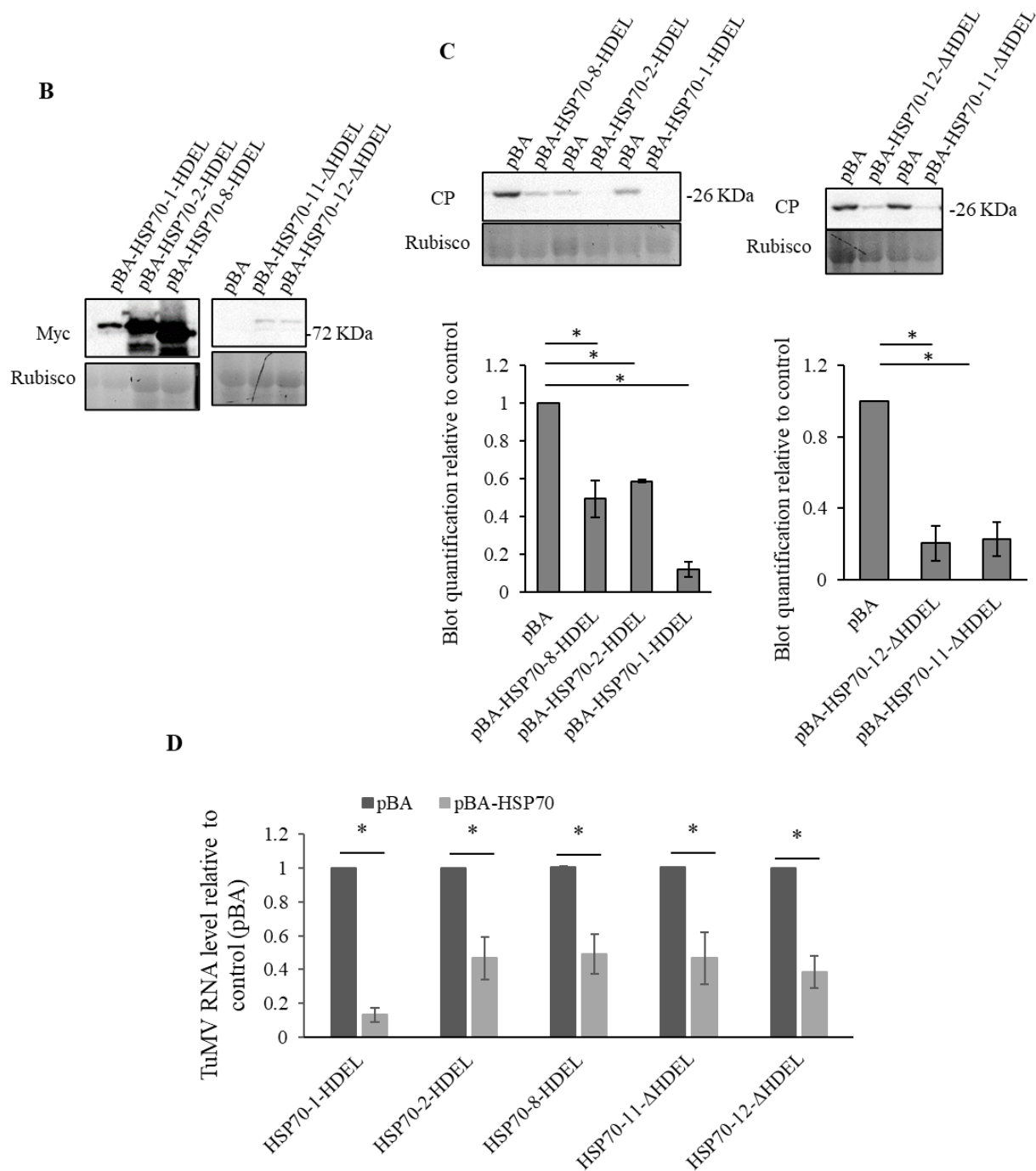
Figure 20. The proviral function of HSP70-11 and HSP70-12 is dependent on their ER localization

(A) Co-expression of fluorescence-tagged HSP70s with altered localization signals and mCherry labelled ER *in planta*. Photos were taken 2 dpi under a confocal microscope. Bar=5 μm.

(B) Immunoblotting analysis of transiently expressed HSP70-1-HDEL, HSP70-2-HDEL, and HSP70-8-HDEL as well as HSP70-11-ΔHDEL and HSP70-12-ΔHDEL in *N. benthamiana* plants. Rubisco large subunit is shown as a loading control.

(C) Immunoblotting analysis of TuMV CP in *N. benthamiana* leaves infiltrated with pBA-HSP70s or pBA empty vector. Rubisco large subunit is shown as a loading control. The blots were quantified with ImageJ from three experiments using rubisco as an internal control, and CP in the pBA control was set to 1. * $P<0.05$, student's t test, two-tailed, unpaired.

(D) Fold change of TuMV RNA accumulation in *N. benthamiana* transiently expressing HSP70s. *A. tumefaciens* harboring pBA empty vector infiltrated in place of HSP70 expression vectors on the same leaf was used as a control with TuMV RNA level set to 1. All TuMV RNA levels were normalized against actin transcripts in the same sample. Data were collected from three independent experiments. Error bars represent standard deviation (n=3), ** $P<0.05$, student's t test, two-tailed, unpaired.

4 Discussion

4.1 HSP70s localize to TuMV VRC and interact with TuMV NIb

HSP70 is one of the host components commonly found in the VRCs of several positive single stranded RNA viruses to promote their replication, namely, CMV (Alam & Rochon, 2016; Serva & Nagy, 2006), TBSV (Pogany & Nagy, 2015; Pogany et al, 2008; Wang et al, 2009a) and RCNMV (Mine et al, 2012; Mine et al, 2010) of the genus *Tombusvirus*; BaMV of the genus *Potexvirus* (Huang et al, 2017); CWMV of the genus *furovirus* (Yang et al, 2017). More detailed studies indicate HSP70s facilitate the VRC assembly, as in the case of TBSV and BaMV. Moreover, HSP70s have been found to associate with the replication protein of other viruses such as a negative single stranded RNA virus, RSV of the genus *Tenuivirus* (Jiang et al, 2014) and BBSV (Wang et al, 2018). In a previous study, Dufresne et al (2008) identified *A. thaliana* Hsc70-3 (HSP70-3) as an interactor of TuMV NIb. In TuMV-infected plants, Hsc70-3 is redistributed to nuclear and membranous fractions and is a component of the membrane-enriched protein complexes co-immunoprecipitated using NIb-specific antibodies. Hsc70-3 is also localized to TuMV 6K2-induced vesicles. It is not clear if other members of the HSP70 family act the same way as Hsc70-3 in response to TuMV infection. For Hsc70-3 itself, it remains to be determined whether Hsc70-3 promotes the replication of TuMV and what role(s) Hsc70-3 plays in the TuMV VRC. In another study, *A. thaliana* HSP70-15-deficient plant was found to be more tolerant to infection by TuMV (Jungkunz et al, 2011), indicating that HSP70-15 might be a host factor facilitating TuMV infection. HSP70-15 belongs to the Hsp110/SSE sub-family of HSP70s with HSP70 signatures (Lin et al, 2001). I did not include the four *A. thaliana* Hsp110/SSE orthologs in TuMV infection assay as none of them was identified as eIF(iso)4E complex component in our initial screen.

In this thesis, the interaction between TuMV replicase NIb with selected *A. thaliana* HSP70s was explored, and five HSP70s including HSP70-1, HSP70-2, HSP70-8, HSP70-11 and HSP70-12 were identified to be the interactors of NIb (Fig. 12). NIb is not the only viral client of these HSP70s as the interaction between TuMV CP and these HSP70s was also detected (Fig. 12). The finding is not unexpected since HSP70s have been found to associate with CP of other viruses as well. For example, in the case of CNV, HSP70 associates with virus CP to increase CP solubility, facilitates CP chloroplast targeting, and accelerates virion disassembly and assembly (Alam &

Rochon, 2016; 2017). In BBSV, HSP70 promotes viral replication by alleviating CP's inhibition on replication, and CP in turn impairs the interaction between the replication protein and HSP70 (Wang et al, 2018). In the potyvirus PVA, HSP70 associates with CP and increases the degradation of CP to shift the balance towards favoring virus replication rather than virus particle assembly (Hafrén et al, 2010; Lõhmus et al, 2017). In the single-stranded DNA virus TYLCV, a *begomovirus*, HSP70 promotes the formation of nuclear viral DNA-CP aggregate and facilitates virus infection (Gorovits & Czosnek, 2017; Gorovits et al, 2013). Apart from interacting with viral proteins, the five selected HSP70s in my project also bound to the host factor eIF(iso)4E (Fig. 13) in consistency with the result from our initial screen of eIF(iso)4E complex components that cytoplasmic HSP70s and ER HSP70s can be associated with eIF(iso)4E. The interactions of HSP70s confirmed in this thesis are summarized in table 3.

As noted, I used BiFC, Y2H, split ubiquitin membrane Y2H and Co-IP for protein-protein interaction assays. In my initial screening for viral proteins that interact with HSP70s using the BiFC assay, I found that most of the TuMV proteins showed positive signals with HSP70s, though the interaction signal intensity varied. Unexpectedly, when I conducted Y2H to confirm these interactions, the only positive interaction was between HSP70s and NIb. As +ssRNA virus replication is associated with cellular membranes, I switched to the split ubiquitin Y2H system for detection of membrane protein interactions to screen for the interaction between HSP70 and TuMV proteins. Unfortunately, HSP70s autoactivated the reporter genes in the system both as a prey and as a bait (Fig. S4). Another technical issue was that HSP70-11 and HSP70-12 were not expressed in our BiFC system probably due to rapid protein turnover. Co-IP is laborious, and it is not an ideal technology for screening protein interactions. Therefore, I could not rule out the possibility that these HSP70s interact with other TuMV proteins, and that other HSP70 family members interact with TuMV proteins and eIF(iso)4E. HSP70s are protein chaperones that are able to bind to short liner stretches of hydrophobic residues, and for this reason they are believed to have promiscuous interaction with a wide range of clients (Lin et al, 2001; Sung et al, 2001a). It is very likely that HSP70s interact with a number of other viral or host factors, with different affinities and interaction outcomes, in a spatial and temporal manner, to affect TuMV infection.

In this study, the localization of fluorescent protein tagged HSP70s in *N. benthamiana* cell was examined by confocal microscopy. Consistent with previous reports (Leng et al, 2017; Lin et al,

2001), HSP70-1 and HSP70-2 were distributed throughout the cytoplasm and nucleus. HSP70-8 was first identified as a chloroplast localized protein (Lin et al, 2001), but it was proven later that it targets the cytoplasm and nucleus instead (Inoue et al, 2008). My result supported the finding that HSP70-8 is not exclusively located to the chloroplast, its distribution in the membranous structures in the cytoplasm and nucleus was similar to HSP70-1 and HSP70-2 (Fig. 14A). HSP70-11 and HSP70-12 carry an HDEL ER-targeting signal. In my observation, they were mainly present in the cytoplasm and in the perinuclear region, likely on the ER membrane network (Fig. 14B). Small amount of fluorescence could also be detected inside the nucleus. Indeed, when zoomed to the ER, HSP70-11 and HSP70-12 could be seen as a web-shape structure that overlapped very well with the mCherry-HDEL-labeled ER network (Fig. 14D). Though HSP70-1, HSP70-2, and HSP70-8 also seemed to overlap with the ER, the shape highlighted by these HSP70s was fuzzier and did not perfectly overlap with the ER labelled by mCherry-HDEL (Fig. 14C). All the five HSP70s examined were co-localized with 6K2 induced vesicles in infected cells (Fig. 15), suggesting that they are potential components of TuMV VRC. These data support the speculation by Dufresne et al, (2008) that Hsc70-3 might not be the only HSP70 protein that could be found in VRC.

Table 3. Summary of HSP70 interactions and detection methods

Methods	NIb			CP			eIF(iso)4E		
	Y2H	BiFC	Co-IP	Y2H	BiFC	Co-IP	Y2H	BiFC	Co-IP
HSP70-1	√	√	√	N	√	-	N	√	-
HSP70-2	√	√	√	N	√	-	N	√	-
HSP70-8	√	√	√	N	√	-	N	√	-
HSP70-11	√	\	-	N	\	√	N	\	√
HSP70-12	√	\	-	N	\	√	N	\	√

"√" positive result; "\" not detected due to technical issue; "-" not performed; "N" negative result.

4.2 HSP70s' effect on TuMV infection may be associated with their broad-spectrum chaperone activity

4.2.1 HSP70-1, HSP70-2, and HSP70-8 have ambiguous roles in TuMV infection

In this project, the effects of HSP70s on TuMV infection was examined in several systems. TuMV infection was evaluated in HSP70 knockout/knockdown *A. thaliana* lines as well as HSP70 overexpression *A. thaliana* lines. TuMV replication was evaluated in protoplasts isolated from HSP70 knockout/knockdown *A. thaliana* mesophyll cells. TuMV cell-to-cell movement was evaluated in *N. benthamiana* plants transiently expressing HSP70s. And finally, TuMV local infection was evaluated in *N. benthamiana* plants transiently expressing HSP70s.

Initial TuMV infection assay with HSP70-1 and HSP70-2 single knockout *A. thaliana* mutants showed no difference with wild-type plants (Fig. S1). It was speculated that these two HSP70s might have redundant function in TuMV infection due to their similar amino acid sequences (Lin et al, 2001). As HSP70-1 is one of HSP70s identified from the affinity-purified eIF(iso)4E complex, it was worthy to generate HSP70-1 and HSP70-2 double knockout mutant to examine if TuMV infection is affected in the double knockout *A. thaliana* plants. To my surprise, TuMV infection was accelerated in this double mutant, which did not support my hypothesis that HSP70-1 and HSP70-2 are host factors for TuMV infection (Fig. 7A & 7D). However, HSP70-1 and HSP70-2 might support TuMV multiplication in protoplasts, as the TuMV genome replication level was reduced in protoplasts isolated from HSP70-1 and HSP70-2 double knockout plants (Fig. 9B left panel). Confusing data were also obtained from TuMV infection assays with stable transgenic *A. thaliana* lines overexpressing HSP70-1 or HSP70-2 and with *N. benthamiana* plants transiently expressing HSP70-1 or HSP70-2. Transient expression of HSP70-1 or HSP70-2 reduced TuMV local infection in *N. benthamiana* (Fig. 11B left panel) whereas stable overexpression of HSP70-1 or HSP70-2 in *A. thaliana* did not affect TuMV infection (Fig. 8D). These results further disprove my hypothesis that HSP70-1 and HSP70-2 are host factors facilitating TuMV infection. The role of HSP70-1 and HSP70-2 in viral infection needs further investigation.

In my initial TuMV infection assay, TuMV infection was reduced in the HSP70-8 knockout *A. thaliana* line, compared to wild type plants (Fig. 7B & 7F). Consistently, TuMV genome replication was also inhibited in protoplasts isolated from the knockout line (Fig. 9 middle panel).

These results supported that HSP70-8 is a proviral factor. However, TuMV local infection in *N. benthamiana* transiently expressing HSP70-8 was reduced (Fig. 11B left panel) and stable overexpression of HSP70-8 did not promote TuMV infection. So, it is premature to conclude that HSP70-8 is an essential host factor facilitating TuMV infection.

As summarized in Table 1, HSP70 is recognized as host factor that promotes infection by a number of plant viruses. This has been demonstrated by the observation that virus infection is reduced after HSP70s being knocked out, silenced, or inhibited (by quercetin) (Alam & Rochon, 2016; Chen et al, 2008; Gorovits & Czosnek, 2017; Gorovits et al, 2013; Hafrén et al, 2010; Huang et al, 2017; Jiang et al, 2014; Jungkunz et al, 2011; Krenz et al, 2010; Lõhmus et al, 2017; Mine et al, 2012; Wang et al, 2009a; Wang et al, 2018; Yang et al, 2017), as well as that virus infection is upregulated by overexpressing HSP70s or by heat treatment (Alam & Rochon, 2016; Chen et al, 2008; Jiang et al, 2014; Wang et al, 2018; Yang et al, 2017).

On the other hand, as reviewed by Hýsková et al. (2021), heat treatment may impair virus multiplication and translocation in plants (Kwon et al, 2012) and high temperature is often correlated with attenuated symptoms as well as low virus titer in infected plants (Szittya et al, 2003). Moreover, thermotherapy to eradicate virus has been practiced with success under different schemes or by combination of cryotherapy with chemotherapy depending on the virus and its host (Hýsková et al, 2021). One of the possible underlying mechanisms might be that high temperature promotes RNA silencing in the host plant (Szittya et al, 2003). Actually, for plants, the induction of HSP70 is one of the strategies to respond to biotic stresses, as HSP70s may contribute to plant resistance by assisting the production and maturation of membrane PPRs, the production and secretion of defence-related proteins, as well as the pathogen-induced hypersensitive response (reviewed in Park & Seo, 2015). HSP70 also cooperates with HSP90 to stabilize resistance proteins (Noël et al, 2007). However, heat treatment can induce a wide spectrum of resistance proteins. These proteins may also exert antiviral roles. So, it is impossible to attribute the anti-virus effect of heat treatment to HSP70 alone. Moreover, the outcome of thermotherapy depends on the temperature and duration of the heat treatment, as well as the specific plant and virus combination being examined (Aguilar-Camacho *et al.* 2016; Achachi *et al.* 2014; Kwon *et al.* 2012; Tan *et al.* 2010). In some cases, heat treatment even has positive effects on virus infection (Alam & Rochon, 2016; Chen et al, 2008; Jiang et al, 2014), and heat stress might downregulate the hypersensitive

response in hosts to viruses (Kiraly et al, 2008; Wang et al, 2009b). Therefore, the roles of HSP70s in virus infection may vary dependent on specific virus-plant combinations.

4.2.2 HSP70-11 are HSP70-12 are proviral host factors in TuMV infection and their proviral function depends on ER-localization

In this thesis work, several lines of evidence support the hypothesis that HSP70-11 and HSP70-12 are host factors facilitating TuMV infection. Since TuMV infection was not affected in HSP70-11 and HSP70-12 single knockdown lines, I speculated that HSP70-11 and HSP70-12 might be complementary to each other and have overlapping functions. This speculation is supported by the fact that HSP70-11 and HSP70-12 share 99% of amino acid sequence similarity (Lin et al, 2001). A HSP70-11 and HSP70-12 double knockdown line was obtained by crossing and selfing to evaluate TuMV infection. TuMV infection was attenuated in the HSP70-11 and HSP70-12 double knockdown *A. thaliana* plants (Fig. 7C & 7F), and the replication of TuMV genome was reduced in protoplasts isolated from the HSP70-11 and HSP70-12 knockdown plants (Fig. 9 right panel). In *N. benthamiana* leaves transiently expressing HSP70-11 and HSP70-12, local infection of TuMV was enhanced (Fig. 11B right panel). Unexpectedly, TuMV infection in HSP70-12 stable overexpression *A. thaliana* lines was not changed (Fig. 8D & 8E). It is possible that the expression level of HSP70-12 and HSP70-11 together (due to their functional redundancy in TuMV infection) is saturated in wild-type *A. thaliana* for TuMV infection but not in *N. benthamiana*. Further investigation is needed to clarify this assumption.

The role of ER-located HSP70s as host factors facilitating TuMV infection seems dependent on their ER localization. Deletion of the ER targeting signal HEDL from HSP70-11 and HSP70-12 made them lose their ER localization, shown by the fuzzy shape instead of a clear-cut web shape of the fluorescence tagged HSP70s in *N. benthamiana* cells when focused to ER (Fig. 20A two lower panels). HSP70-11 and HSP70-12 mutants without the ER localization signal no longer promoted TuMV local infection in *N. benthamiana* when transiently expressed (Fig. 20B right panel). Instead, they functioned like HSP70-1, HSP70-2, and HSP70-8 to inhibit TuMV local infection. More work is needed to determine the relationship between ER localization as well as other HSP70 functional domains and the role of HSP70s in TuMV infection, because addition of the HDEL ER-targeting signal to HSP70-1, HSP70-2, and HSP70-8 did not reverse their anti-viral activity in *N. benthamiana*.

4.2.3 HSP70s-mediated client protein turnover

In this study, we found that transient expression of HSP70-1, HSP70-2, and HSP70-8 negatively regulated NIb accumulation (Fig. 17A left panel) whereas co-expression of HSP70-11 and HSP70-12 positively affected NIb protein level. RT-qPCR analysis of NIb mRNA levels showed that expression of these HSP70s did not alter NIb mRNA level (Fig. 17A & 17B). Therefore up- or downregulation of NIb protein by HSP70-1 is likely through regulation of NIb stability. Since NIb might be ubiquitinated and thus undergo degradation via the ubiquitin-proteosome pathway (Cheng et al, 2017), and HSP70s are chaperones that may target their client to degradation pathways (Rosenzweig et al, 2019; Usman et al, 2017), I wondered whether HSP70-1, HSP70-2 and HSP70-8 may promote NIb degradation in a ubiquitin-proteosome dependent manner. After confirming NIb was indeed ubiquitinated by immunoblotting with anti-ubiquitin antibodies (Fig. 18A), I conducted a drug inhibitor test using the ubiquitin-proteosome pathway inhibitor MG-132. Treatment with MG-132 did prevent NIb degradation (Fig. 18C). Therefore, it is concluded that HSP70-1, HSP70-2 and HSP70-8 accelerated NIb degradation via the ubiquitin-proteosome pathway.

As mentioned above, co-expression of HSP70-11 and HSP70-12 protected NIb from degradation (Fig. 17A & 17B). As protein chaperones, HSP70s recognize misfolded proteins, either to restore their normal conformation, or target them to degradation if it fails (Mayer et al, 2001; Rosenzweig et al, 2019; Usman et al, 2017). Here, it is possible that HSP70-11 and HSP70-12 recognize NIb and restore its conformation, which protects NIb from degradation.

The implication of viral protein degradation should be further explored. Regular western blotting detects denatured proteins containing epitopes recognized by given antibodies regardless they are folded correctly or not in cells. So, we do not know the amount of functional NIb is affected or not by HSP70s chaperones. In a recent study, our lab reported that TuMV infection activates the autophagy pathway and Beclin1 (ATG6), an essential component of autophagy, specifically interacts with NIb and directs its degradation (Li et al., 2018). It would be interesting to determine if HSP70-11 and HSP70-12 have the ability to outcompete Beclin1 for NIb and thus enhance NIb accumulation. HSP70-1, HSP70-2, and HSP70-8 may also regulate NIb degradation through the autophagy pathway, as HSP70s in animals have been found to mediate autophagy (Fernández-Fernández et al, 2017). In a study from our lab that was published a few years ago, Cheng et al.

discovered the importance of sumoylation, a form of posttranslational modification by small ubiquitin-like modifiers in TuMV infection. In this case, TuMV NIb is sumoylated, and this sumoylation retargets NIb from the nucleus to the cytoplasm (where TuMV and other +ssRNA viruses replicate) to enhance virus replication. In addition, NIb sumoylation also suppresses the host immunity response (Cheng et al; 2017). It remains to be explored whether HSP70s might play a part in the posttranslational modifications of NIb.

In addition to NIb, I also examined whether HSP70s affected the protein level of two other interaction partners, TuMV CP and host eIF(iso)4E. I found that HSP70s affected the protein level of CP and eIF(iso)4E in the same way as they did for NIb (Fig. 19). Contrary to NIb, downregulation CP might have a positive effect on TuMV infection, especially at the stage of replication. HSP70 has been shown to regulate the replication of PVA through mediating CP degradation (Hafrén et al, 2010; Lõhmus et al, 2017). Since CP subunits coat the virus genome to form virion favoring virus movement and transmission, reducing CP level may facilitate genome replication. HSP70s have been also found to promote BBSV replication by lifting CP's inhibition on replication (Wang et al, 2018). In other cases, HSP70 association with CP is proviral through facilitating the virus particle assembly and disassembly as well as targeting CP to its destination (Alam & Rochon, 2016; 2017; Gorovits & Czosnek, 2017; Gorovits et al, 2013). In my *N. benthamiana* transient expression test, samples were collected at 3 dpi, which was too early for active virus movement to happen. Therefore, it's possible, as in the case of HSP70-8, to obtain contradictory results from the TuMV systematically infecting *A. thaliana* model. It is still difficult to explain the contradictory results from protoplast assay of TuMV genome replication, which indicates that HSP70s promote TuMV replication. It is plausible to assume that HSP70s interact with a great number of viral and host protein that might be involve in the TuMV infection cycle, and the overall effect of HSP70s might be determined by the balance of these different actions.

My experiment on the effect of transient expression of HSP70s on the cell-to-cell movement of TuMV did not discern obvious differences in viral intercellular spread (cells emitting GFP signals only) from primarily infected cells showing dual fluorescence of RFP and GFP between treatment groups expressing HSP70s and the control group expressing an empty vector (Fig. 10). However, it is premature to conclude that HSP70s do not affect cell-to-cell movement. One technical limitation is that it is extremely difficult to use HSP70s knockout *A. thaliana* mutants to assess

viral cell-to-cell movement. Moreover, potyviral viral genome translation and replication are coupled processes, which is a rate-limiting step before movement. My experiment system cannot single out cell-to-cell movement alone. Therefore, I could not exclude the possibility that HSP70s might have certain influence on TuMV cell-to-cell movement through regulating TuMV CP or even CI proteins.

4.2.4 ER-localized HSP70s facilitate TuMV infection and might be a direct effector in UPR stress promoting TuMV infection

The current understanding of the relationship between viral infection, UPR, and ER-localized HSP70s is summarized in Fig. 21. The involvement of UPR in viral infection is also ambiguous. Several studies suggest that IRE1/bZIP60 as well as the bZIP28 pathway is associated with restricting potyvirus infection (Gaguancela et al, 2016; Gayral et al, 2020) and some others report that viral infection induces ER stress related unfolded protein response (UPR) via the IRE1/bZIP60s pathway, and this pathway is crucial for viral infection (Zhang et al, 2015; Li et al, 2020). It is known that UPR upregulates the expression of ER-localized HSP70s, which in turn negatively regulates UPR stress (Alcântara et al, 2020; Herath et al, 2020; Srivastava et al, 2018), and consistent results were obtained in this project (Fig. 5D, Fig. 5E, Fig. S12). ER-localized HSP70s may affect TuMV infection through alleviating UPR stress. I tend to speculate that ER-localized HSP70s might be one of the direct players in the process of UPR promoting TuMV infection, since ER-localized HSP70s, as protein chaperone, interact with TuMV proteins and the essential host factor eIF(iso)4E. Expressing HSP70-11 and HSP70-12 in *N. benthamiana* downregulated the expression of UPR markers (Fig. S12), whereas expressing HSP70-12 in TuMV-infected *N. benthamiana* upregulated the expression of UPR marker genes (Fig. S13). This indicates that HSP70-12 promoted, instead of alleviated UPR stress, in TuMV-infected cells, contrary to the fact that HSP70-12 should be a negative regulator of UPR stress. Therefore, the upregulation of UPR marker genes might be a result of increased TuMV infection, further confirming that ER-HSP70s may act as a direct regulator of TuMV infection rather than regulating TuMV infection through UPR stress. Strangely, expressing HSP70-11 in TuMV-infected *N. benthamiana* did not upregulate UPR stress (Fig. S13), probably because HSP70-11 did not upregulate TuMV infection as much as HSP70-12 (Fig. 11B right panel) and thus the UPR stress alleviating effect of HSP70-11 balanced out its effect in enhancing TuMV infection. A previous study (Zhang et al, 2015) evaluated TuMV infection in HSP70-11 single knockout plants to

examine the effect of an UPR-induced protein on TuMV infection. The authors found that TuMV infection was not affected in this mutant. I obtained similar results in HSP70-11 and HSP70-12 single knockdown lines (Fig. S1). In contrast, I observed a reduction in TuMV infection in HSP70-11 and HSP70-12 double knockdown lines. This infection discrepancy is probably due to the complementary functions of HSP70-11 and HSP70-12.
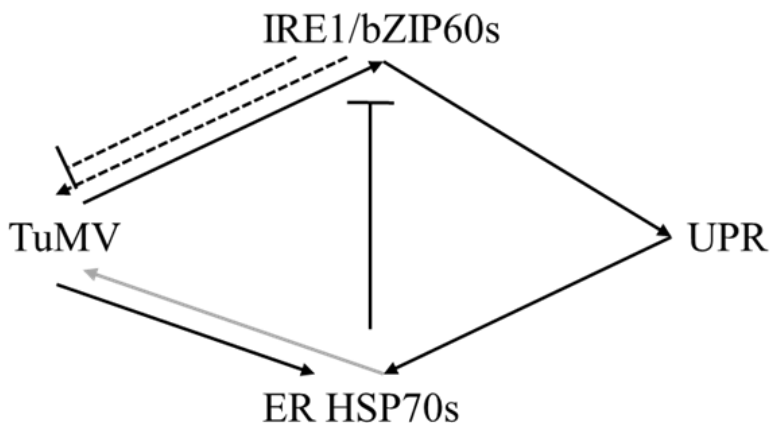

Figure 21. ER-located HSP70s might be the direct effector in the process of UPR promoting TuMV infection

"->" indicates having promotive effect, "-|" indicates having inhibitory effect, dashed line indicates the existence of ambiguous conclusions, grey line indicates the conclusion made from this project.

4.3 Future directions

This thesis project was designed to unveil the interactions between the host HSP70 proteins and the invading TuMV, especially in the context of HSP70s as eIF(iso)4E-associated proteins. Although this study identified HSP70-11 and HSP70-12 are novel host factors of TuMV infection and discovered the role of HSP70s in regulating turnover of their clients including both viral and cellular proteins, it raised more questions than answered.

Firstly, the most interesting question is whether ER location determining HSP70s role in TuMV infection. Deleting the HDEL signal abolished the proviral effect of transiently expressed HSP70-11 and HSP70-12 on TuMV local infection in *N. benthamiana*. However, adding the HEDL signal to cytoplasmic HSP70s including HSP70-1, HSP70-2, and HSP70-8 did not successfully bring them to the ER. It is unknown whether if I manage to make these HSP70s locate to the ER and resulting ER-localized HSP70 mutants would perform the same function as those native ER localized HSP70s (e.g., HSP70-11 and HSP70-12). Furthermore, it would be interesting to exchange the NBD, SBD, and the C-terminal variable domain (CVD) between cytoplasmic HSP70s and ER HSP70s to see which domain(s) determine the opposite effects on TuMV infection. For this purpose, three constructs may be designed for future assays (Fig. 22). The first construct deletes 16 amino acids from the end of C-terminus of HSP70-1 containing the alleged cytoplasm targeting sequences (Lin et al, 2001) and adds the HEDL ER-targeting signal. The second construct deletes the entire CVD of HSP70-1 after amino acid 614 and adds HSP70-12 CVD from amino acid 640. The third construct only keeps the NBD from HSP70-1, before amino acid 390 and replaces the remaining protein with HSP70-12 SBD and CVD, from amino acid 415 to the end. The fourth and fifth construct are based on construct 2 and 3, respectively, but also swap the N-terminal variable domain (NVD) from HSP70-12 from amino acid 1 to 37 with NVD of HSP70-1 from amino acid 1 to 9. Localization of those constructs will be examined and TuMV local infection in *N. benthamiana* expressing these constructs will also be evaluated.

Secondly, the interaction network between HSP70s and all TuMV proteins remains to be constructed. Due to technical limitations this project examined the interactions of TuMV NIb and CP with HSP70s and was unable to exam the possible interactions between other 9 viral proteins and HSP70s. A complete interaction network between HSP70s and all the 11 TuMV proteins

would shed new insights into molecular interactions between HSP70s and TuMV. For proteins whose interaction with HSP70s confirmed in this research, namely NIb, CP, and host eIF(iso)4E, their expression profile such as localization, aggregation, and interaction under the influence of HSP70s should be studied with greater detail.

Thirdly, it is essential to find out the mechanism of TuMV infection promoted by ER-located HSP70s. Though I have found in this project that some HSP70s can increase the protein level of TuMV proteins NIb and CP, as well as the important host factor eIF(iso)4E by inhibiting protein degradation, it is still unknown if ER HSP70s facilitate TuMV infection in other ways. For example, it would be interesting to know if HSP70s can upregulate plant's native eIF(iso)4E, and, as a result, increase the interaction between eIF(iso)4E and VPg to accelerate translation of virus genome. The possibility that HSP70s promote TuMV infection through alleviating UPR cannot be ruled out since the effect of UPR on TuMV infection is also ambiguous.

Lastly, how the conclusions from this project may facilitate the development of genetic virus resistance in crops. Stable *A. thaliana* overexpression lines of HSP70-1 and HSP70-2 were not less susceptible to TuMV infection. Knocking out HSP70-8 or HSP70-11 and HSP70-12 in *A. thaliana* reduced TuMV infection in these plants. Although these mutants did not show obvious phenotypic difference from wild-type plants, it is not clear if there are any trade-offs with undesirable traits such as reduced tolerance/resistance to abiotic stress in these mutants. Therefore, a detailed understanding of the roles of each HSP70s in the infection cycle of TuMV as well as the functional domain essential to carry out their roles is necessary to allow fine-tuned editing of HSP70s for engineering durable resistance to potyviruses.
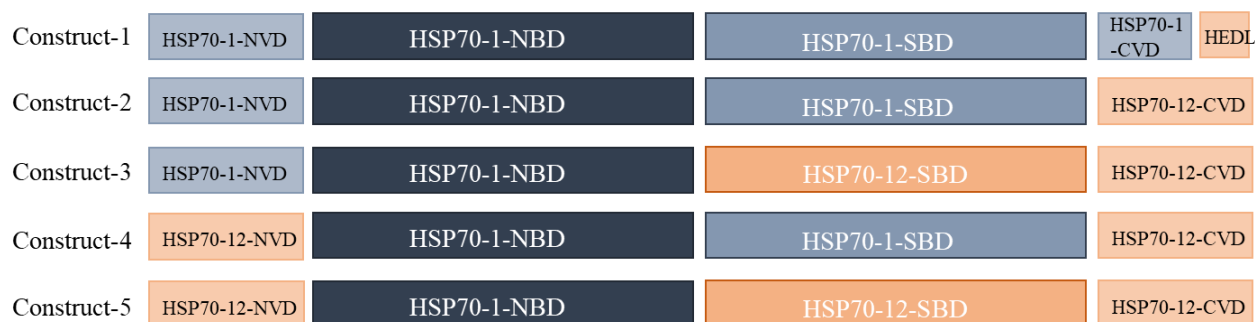

Figure 22. HSP70-1 and HSP70-12 exchange domain constructs for future assays

Reference

Abdul-Razzak, A., Guiraud, T., Peypelut, M., Walter, J., Houvenaghel, M.C., Candresse, T., LE Gall, O. & German-Retana, S. (2009). Involvement of the cylindrical inclusion (CI) protein in the overcoming of an eIF4E-mediated resistance against Lettuce mosaic potyvirus. Mol Plant Pathol **10(1)**, 109-113.

Achachi, A., Ait Barka, E., Ibriz, M. (2014). Recent advances in Citrus psorosis virus. Virus disease **25(3)**, 261-76.

Afrin, T., Diwan, D., Sahawneh, K. & Pajerowska-Mukhtar, K. (2019). Multilevel regulation of endoplasmic reticulum stress responses in plants: where old roads and new paths meet. J Exp Bot **71(5)**, 1659-1667.

Aguilar-Camacho, M., Mora-Herrera, M.E., López-Delgado, H.A. (2016). Potato virus X (PVX) elimination as short and long term effects of hydrogen peroxide and salicylic acid is differentially mediated by oxidative stress in synergism with thermotherapy. Amer J Potato Res **93(4)**, 360-367.

Akerfelt, M., Morimoto, R.I. & Sistonen, L. (2010). Heat shock factors: integrators of cell stress, development and lifespan. Nat Rev Mol Cell Biol **11(8)**, 545-55.

Ala-Poikela, M., Goytia, E., Haikonen, T., Rajamäki, M.L. & Valkonen, J.P. (2011). Helper component proteinase of the genus potyvirus is an interaction partner of translation initiation factors eIF(iso)4E and eIF4E and contains a 4E binding motif. J Virol **85(13)**, 6784-6794.

Alam, S.B. & Rochon, D.A. (2016). Cucumber necrosis virus recruits cellular heat shock protein 70 homologs at several stages of infection. J Virol **90(7)**, 3302-3317.

Alam, S.B. & Rochon, D.A. (2017). Evidence that Hsc70 is associated with Cucumber necrosis virus particles and plays a role in particle disassembly. J Virol **91(2)**, e01555-16.

Albar, L., Bangratz-Reyser, M., Hébrard, E., Ndjiondjop, M.N., Jones, M. & Ghesquière, A. (2006). Mutations in the eIF(iso)4G translation initiation factor confer high resistance of rice to Rice yellow mottle virus. Plant J **47(3)**, 417-426.

Alcântara, A., Seitner, D., Navarrete, F. & Djamei, A. (2020). A high-throughput screening method to identify proteins involved in unfolded protein response of the endoplasmic reticulum in plants. Plant Methods **16(1)**, 4.

Ali, A., Bharadwaj, S., O'Carroll, R. & Ovsenek, N. (1998). HSP90 Interacts with and regulates the activity of Heat shock factor 1 in *Xenopus Oocytes*. Mol Cell Biol **18(9)**, 4949-4960.

Alvim, F.C., Carolino, S.M., Cascardo, J.C., Nunes, C.C., Martinez, C.A., Otoni, W.C. & Fontes, E.P. (2001). Enhanced accumulation of BiP in transgenic plants confers tolerance to water stress. Plant Physiol **126(3)**. 1042-1054.

Alzhanova, D.V., Napuli, A.J., Creamer, R. & Dolja, V.V. (2001). Cell-to-cell movement and assembly of a plant closterovirus: roles for the capsid proteins and Hsp70 homolog. EMBO J **20(24)**, 6997-7007.

Anaraki, Z.E., Tafreshi, S.A.H. & Shariati, M. (2018). Transient silencing of heat shock proteins showed remarkable roles for HSP70 during adaptation to stress in plants. Environ Exp Bot **155**, 142-157.

Andrade, M., Abe, Y., Nakahara, K.S. & Uyeda, I. (2009). The cyv-2 resistance to Clover yellow vein virus in pea is controlled by the eukaryotic initiation factor 4E. J Gen Plant Pathol **75(3)**, 241-249.

Anindya, R. & Savithri, H.S. (2004). Potyviral NIa proteinase, a proteinase with novel deoxyribonuclease activity. J Biol Chem **279(31)**, 32159-32169.

Aoki, K., Kragler, F., Xoconostle-Cázares, B. & Lucas, W.J. (2002). A subclass of plant heat shock cognate 70 chaperones carries a motif that facilitates trafficking through plasmodesmata. Proc Natl Acad Sci U S A **99(25)**, 16342-16347.

Aparicio, F., Thomas, C.L., Lederer, C., Niu, Y., Wang, D. & Maule, A.J. (2005). Virus induction of Heat shock protein 70 reflects a general response to protein accumulation in the plant cytosol. Plant Physiol **138(1)**, 529-536.

Aranda, M.A., Escaler, M., Wang, D. & Maule, A.J. (1996). Induction of HSP70 and polyubiquitin expression associated with plant virus replication. Proc Natl Acad Sci U S A **93(26)**, 15289-15293.

Atarashi, H., Jayasinghe, W.H., Kwon, J., Kim, H., Taninaka, Y., Igarashi, M., Ito, K., Yamada, T., Masuta, C. & Nakahara, K. S. (2020). Artificially edited alleles of the Eukaryotic translation initiation factor 4E1 gene differentially reduce susceptibility to Cucumber mosaic virus and Potato virus Y in tomato. Front Microbiol **11**, 564310

Au, H.H. & Jan, E. (2014). Novel viral translation strategies. Wiley Interdiscip Rev RNA **5(6)**, 779-801.

Bastet, A., Robaglia, C. & Gallois, J.L. (2017). eIF4E resistance: natural variation should guide gene editing. Trends Plant Sci **22(5)**, 411-419.

Beauchemin, C., Boutet, N. & Laliberté, J.F. (2007). Visualization of the interaction between the precursors of VPg, the viral protein linked to the genome of Turnip mosaic virus, and the translation Eukaryotic initiation factor iso 4E in planta. J Virol **81(2)**, 775-782.

Beauchemin, C. & Laliberté, J.F. (2007). The Poly(A) binding protein is internalized in virus-induced vesicles or redistributed to the nucleolus during Turnip mosaic virus infection. J Virol **81(20)**, 10905-10913.

Bertolotti, A., Zhang, Y., Hendershot, L.M., Harding, H.P. & Ron, D. (2000). Dynamic interaction of BiP and ER stress transducers in the unfolded-protein response. Nat Cell Biol **2(6)**, 326-332.

Blanc, S., López-Moya, J.J., Wang, R., García-Lampasona, S., Thornbury, D.W. & Pirone, T.P. (1997). A specific interaction between Coat protein and Helper component correlates with aphid transmission of a potyvirus. Virology **231(1)**, 141-147.

Bokszczanin, K.L., Solanaceae Pollen Thermotolerance Initial Training Network (SPOT-ITN) Consortium, Fragkostefanakis, S. (2013). Perspectives on deciphering mechanisms underlying plant heat stress response and thermotolerance. Front Plant Sci **4**, 315.

Borden, K.L.B. & Volpon, L. (2020). The diversity, plasticity, and adaptability of cap-dependent translation initiation and the associated machinery. RNA Biol **17(9)**, 1239-1251.

Borgstrøm, B. & Johansen, I.E. (2001). Mutations in Pea seedborne mosaic virus Genome-linked protein VPg alter pathotype-specific virulence in *Pisum sativum*. Mol Plant Microbe Interact **14(6)**, 707-714.

Bush, M.S., Hutchins, A.P., Jones, A.M., Naldrett, M.J., Jarmolowski, A., Lloyd, C.W. & Doonan, J.H. (2009). Selective recruitment of proteins to 5′ cap complexes during the growth cycle in Arabidopsis. Plant J **59(3)**, 400-412.

Calderwood, S.K., Xie, Y., Wang, X., Khaleque, M.A., Chou, S.D., Murshid, A., Prince, T. & Zhang, Y. (2010). Signal transduction pathways leading to heat shock transcription. Sign Transduct Insights **2**, 13-24.

Callot, C. & Gallois, J.L. (2014). Pyramiding resistances based on translation initiation factors in Arabidopsis is impaired by male gametophyte lethality. Plant Signal Behav **9(2)**, e27940.

Cavatorta, J., Perez, K.W., Gray, S.M., Van Eck, J., Yeam, I. & Jahn, M. (2011). Engineering virus resistance using a modified potato gene. Plant Biotechnol J **9(9)**, 1014-1021.

Chandrasekaran, J., Brumin, M., Wolf, D., Leibman, D., Klap, C., Pearlsman, M., Sherman, A., Arazi, T. & Gal-On, A. (2016). Development of broad virus resistance in non-transgenic cucumber using CRISPR/Cas9 technology. Mol Plant Pathol **17(7)**, 1140-1153.

Charon, J., Theil, S., Nicaise, V. & Michon, T. (2016). Protein intrinsic disorder within the Potyvirus genus: from proteome-wide analysis to functional annotation. Mol Biosyst **12(2)**, 634-652.

Charron, C., Nicolaï, M., Gallois, J.L., Robaglia, C., Moury, B., Palloix, A. & Caranta, C. (2008). Natural variation and functional analyses provide evidence for co-evolution between plant eIF4E and potyviral VPg. Plant J **54(1)**, 56-68.

Chen, Y. & Brandizzi, F. (2013). IRE1: ER stress sensor and cell fate executor. Trends Cell Biol **23(11)**, 547-555.

Chen, Z., Zhou, T., Wu, X., Hong, Y., Fan, Z. & Li, H. (2008). Influence of cytoplasmic heat shock protein 70 on viral infection of *Nicotiana benthamiana*. Mol Plant Pathol **9(6)**, 809-817.

Cheng, X., Li, F., Cai, J., Chen, W., Zhao, N., Sun, Y., Guo, Y., Yang, X. & Wu, X. (2015). Artificial TALE as a convenient protein platform for engineering broad-spectrum resistance to Begomoviruses. Viruses **7(8)**, 4772-4782.

Cheng, X., Xiong, R., Li, Y., Li, F., Zhou, X. & Wang, A. (2017). Sumoylation of Turnip mosaic virus RNA polymerase promotes viral infection by counteracting the host NPR1-mediated immune response. Plant Cell **29(3)**, 508-525.

Cho, E.K. & Choi, Y.J. (2009). A nuclear-localized HSP70 confers thermoprotective activity and drought-stress tolerance on plants. Biotechnol Lett **31(4)**, 597-606.

Choi, S.H., Nakahara, K.S., Andrade, M. & Uyeda, I. (2012). Characterization of the recessive resistance gene cyv1 of *Pisum sativum* against Clover yellow vein virus. J Gen Plant Pathol **78(4)**, 269-276.

Chung, B. Y.W., Miller, W.A., Atkins, J.F. & Firth, A.E. (2008). An overlapping essential gene in the Potyviridae. Proc Natl Acad Sci U S A **105(15)**, 5897-5902.

Clavel, M., Michaeli, S. & Genschik, P. (2017). Autophagy: a double-edged sword to fight plant viruses. Trends Plant Sci **22(8)**, 646-648.

Cohen, N., Sharma, M., Kentsis, A., Perez, J.M., Strudwick, S. & Borden, K.L. (2001). PML RING suppresses oncogenic transformation by reducing the affinity of eIF4E for mRNA. EMBO J **20(16)**, 4547-4559.

Comai, L., Young, K., Till, B. J., Reynolds, S. H., Greene, E. A., Codomo, C. A., Enns, L. C., Johnson, J. E., Burtner, C., Odden, A. R. & Henikoff, S. (2004). Efficient discovery of DNA polymorphisms in natural populations by Ecotilling. Plant J **37(5)**, 778-786.

Combe, J.P., Petracek, M.E., van Eldik, G., Meulewaeter, F. & Twell, D. (2005). Translation initiation factors eIF4E and eIFiso4E are required for polysome formation and regulate plant growth in tobacco. Plant Mol Biol **57(5)**, 749-760.

Cong, L., Ran, F.A., Cox, D., Lin, S., Barretto, R., Habib, N., Hsu, P.D., Wu, X., Jiang, W., Marraffini, L.A. & Zhang, F. (2013). Multiplex Genome Engineering Using CRISPR/Cas Systems. Science **339(6121)**, 819-823.

Contreras-Paredes, C.A., Silva-Rosales, L., Daròs, J.A., Alejandri-Ramírez, N.D. & Dinkova, T.D. (2013). The absence of Eukaryotic initiation factor eIF(iso)4E affects the systemic spread of a Tobacco etch virus isolate in *Arabidopsis thaliana*. Mol Plant Microbe Interact **26(4)**, 461-470.

Cotton, S., Grangeon, R., Thivierge, K., Mathieu, I., Ide, C., Wei, T., Wang, A. & Laliberté, J.F. (2009). Turnip mosaic virus RNA replication complex vesicles are mobile, align with microfilaments, and are each derived from a single viral genome. J Virol **83(20)**, 10460-10471.

Coutinho de Oliveira, L., Volpon, L., Osborne, M. J. & Borden, K. L. B. (2019a). Chemical shift assignment of the viral protein genome-linked (VPg) from potato virus Y. Biomol NMR Assign **13(1)**, 9-13**.**

Coutinho de Oliveira, L., Volpon, L., Rahardjo, A.K., Osborne, M.J., Culjkovic-Kraljacic, B., Trahan, C., Oeffinger, M., Kwok, B.H. & Borden, K.L.B. (2019b). Structural studies of the eIF4E–VPg complex reveal a direct competition for capped RNA: Implications for translation, Proc Natl Acad Sci U S A **116(48)**, 24056-24065.

Cuesta, R., Yuste-Calvo, C., Gil-Cartón, D., Sánchez, F., Ponz, F. & Valle, M. (2019). Structure of Turnip mosaic virus and its viral-like particles. Sci Rep **9(1)**, 15396.

Cui, H. & Wang, A. (2016). Plum pox virus 6K1 protein is required for viral replication and targets the viral replication complex at the early stage of infection. J Virol **90(10)**, 5119-5131.

Cui, H. & Wang, A. (2019). The biological impact of the hypervariable N-terminal region of potyviral genomes. Annu Rev Virol **6(1)**, 255-274.

Cui, X., Wei, T., Chowda-Reddy, R.V., Sun, G. & Wang, A. (2010). The Tobacco etch virus P3 protein forms mobile inclusions via the early secretory pathway and traffics along actin microfilaments. Virology **397(1)**, 56-63.

Cui, X., Yaghmaiean, H., Wu, G., Wu, X., Chen, X., Thorn, G. & Wang, A. (2017). The C-terminal region of the Turnip mosaic virus P3 protein is essential for viral infection via targeting P3 to the viral replication complex. Virology **510**, 147-155.

Culjkovic-Kraljacic, B., Baguet, A., Volpon, L., Amri, A. & Borden, K.L. (2012). The oncogene eIF4E reprograms the nuclear pore complex to promote mRNA export and oncogenic transformation. Cell Rep **2(2)**, 207-215.

Culjkovic-Kraljacic, B., Skrabanek, L., Revuelta, M. V., Gasiorek, J., Cowling, V.H., Cerchietti, L. & Borden, K.L.B. (2020). The Eukaryotic translation initiation factor eIF4E elevates steady-state m7G capping of coding and noncoding transcripts. Proc Natl Acad Sci U S A **117(43)**, 26773-26783.

Culjkovic, B. & Borden, K.L. (2009). Understanding and targeting the Eukaryotic translation initiation factor eIF4E in head and neck cancer. J Oncol **2009**, 981679.

Culver, J.N. (2002). Tobacco mosaic virus assembly and disassembly: determinants in pathogenicity and resistance. Annu Rev Phytopathol **40(1)**, 287-308.

Dai, Z. (2018). Characterization of the coat protein of Turnip mosaic virus and its Arabidopsis interactors in the virus infection process. The University of Western Ontario (Canada).

Dai, Z., He, R., Bernards, M.A. & Wang, A. (2020). The cis-expression of the coat protein of Turnip mosaic virus is essential for viral intercellular movement in plants. Mol Plant Pathol **21(9)**, 1194-1211.

Dai, Z. & Wang, A. (2022). Isolation and transfection of plant mesophyll protoplasts for virology research. Methods Mol Biol **2400**, 43-53.

Davis, M.R., Delaleau, M. & Borden, K.L.B. (2019). Nuclear eIF4E stimulates 3′-end cleavage of target RNAs. Cell Rep **27(5)**, 1397-1408.

de Sousa Abreu, R., Penalva, L.O., Marcotte, E.M. & Vogel, C. (2009). Global signatures of protein and mRNA expression levels. Mol Biosyst **5(12)**, 1512-1526.

del Toro, F.J., Mencía, E., Aguilar, E., Tenllado, F. & Canto, T. (2018). HCPro-mediated transmission by aphids of purified virions does not require its silencing suppression function and correlates with its ability to coat cell microtubules in loss-of-function mutant studies. Virology **525**, 10-18.

Deng, P., Wu, Z. & Wang, A. (2015). The multifunctional protein CI of potyviruses plays interlinked and distinct roles in viral genome replication and intercellular movement. Virol J **12(1)**, 141.

Deng, Y., Humbert, S., Liu, J.X., Srivastava, R., Rothstein, S.J. & Howell, S.H. (2011). Heat induces the splicing by IRE1 of a mRNA encoding a transcription factor involved in the unfolded protein response in Arabidopsis. Proc Natl Acad Sci U S A **108(17)**, 7247-7252.

Ding, X.Z., Tsokos, G.C. & Kiang, J.G. (1998). Overexpression of HSP-70 inhibits the phosphorylation of HSF1 by activating protein phosphatase and inhibiting protein kinase C activity. FASEB J **12(6)**, 451-459.

Dinkova, T.D., Márquez-Velázquez, N.A., Aguilar, R., Lázaro-Mixteco, P.E. & Sánchez de Jiménez, E. (2011). Tight translational control by the initiation factors eIF4E and eIF(iso)4E is required for maize seed germination. Seed Sci Res **21(2)**, 85-93.

Dinkova, T.D., Martinez-Castilla, L. & Cruz-Espíndola, M.A. (2016). The diversification of eIF4E family members in plants and their role in the plant-virus interaction. Evolution of the Protein Synthesis Machinery and Its Regulation, 187-205.

Dong, O.X. & Ronald, P.C. (2019). Genetic engineering for disease resistance in plants: recent Progress and future perspectives. Plant Physiol **180(1)**, 26-38.

Dong, X., Yi, H., Lee, J., Nou, I.S., Han, C.T. & Hur, Y. (2015). Global gene-expression analysis to identify differentially expressed genes critical for the heat stress response in *Brassica rapa*. PLoS One **10(6)**, e0130451.

Dragovic, Z., Broadley, S.A., Shomura, Y., Bracher, A. & Hartl, F.U. (2006). Molecular chaperones of the Hsp110 family act as nucleotide exchange factors of Hsp70s. EMBO J **25(11)**, 2519-2528.

Duan, H., Richael, C. & Rommens, C.M. (2012). Overexpression of the wild potato eIF4E-1 variant Eva1 elicits Potato virus Y resistance in plants silenced for native eIF4E-1. Transgenic Res **21(5)**, 929-938.

Dudley, P., Wood, C.K., Pratt, J.R. & Moore, A.L. (1997). Developmental regulation of the plant mitochondrial matrix located HSP70 chaperone and its role in protein import. FEBS Lett **417(3)**, 321-324.

Dufresne, P.J., Thivierge, K., Cotton, S., Beauchemin, C., Ide, C., Ubalijoro, E., Laliberté, J.F. & Fortin, M.G. (2008). Heat shock 70 protein interaction with Turnip mosaic virus RNA-dependent RNA polymerase within virus-induced membrane vesicles. Virology **374(1)**, 217-227.

Duprat, A., Caranta, C., Revers, F., Menand, B., Browning, K.S. & Robaglia, C. (2002). The Arabidopsis eukaryotic initiation factor (iso)4E is dispensable for plant growth but required for susceptibility to potyviruses. Plant J **32(6)**, 927-934.

Edwards, K., Johnstone, C. & Thompson, C.A. (1991). A simple and rapid method for the preparation of plant genomic DNA for PCR analysis. Nucleic Acids Res **19(6)**, 1349.

Eiamtanasate, S., Juricek, M. & Yap, Y.K. (2007). C-terminal hydrophobic region leads PRSV P3 protein to endoplasmic reticulum. Virus Genes **35(3)**, 611-617.

Eskelin, K., Hafrén, A., Rantalainen, K.I. & Mäkinen, K. (2011). Potyviral VPg enhances viral RNA translation and inhibits reporter mRNA translation in planta. J Virol **85(17)**, 9210-9221.

Estevan, J., Maréna, A., Callot, C., Lacombe, S., Moretti, A., Caranta, C. & Gallois, J.L. (2014). Specific requirement for translation initiation factor 4E or its isoform drives plant host susceptibility to Tobacco etch virus. BMC Plant Biol **14(1)**, 67.

Faus, I., Zabalza, A., Santiago, J., Nebauer, S.G., Royuela, M., Serrano, R. & Gadea, J. (2015). Protein kinase GCN2 mediates responses to glyphosate in Arabidopsis. BMC Plant Biol **15(1)**, 14.

Feoktistova, K., Tuvshintogs, E., Do, A. & Fraser, C.S. (2013). Human eIF4E promotes mRNA restructuring by stimulating eIF4A helicase activity. Proc Natl Acad Sci U S A **110(33)**, 13339-13344.

Fernández, A., Guo, H.S., Sáenz, P., Simón-Buela, L., de Cedrón, M.G. & García, J.A. (1997). The motif V of Plum pox potyvirus CI RNA helicase is involved in NTP hydrolysis and is essential for virus RNA replication. Nucleic Acids Res **25(22)**, 4474-4480.

Fernández-Fernández, M.R., Gragera, M., Ochoa-Ibarrola, L., Quintana-Gallardo, L., Valpuesta, J.M. (2017). Hsp70 - a master regulator in protein degradation. FEBS Lett **591(17)**, 2648-2660.

Fondong, V.N., Nagalakshmi, U. & Dinesh-Kumar, S.P. (2016). Novel functional genomics approaches: a promising future in the combat against plant viruses. Phytopathology **106(10)**, 1231-1239.

Gadhave, K.R., Gautam, S., Rasmussen, D.A. & Srinivasan, R. (2020). Aphid transmission of potyvirus: the largest plant-infecting RNA virus genus. Viruses **12(7)**, 773.

Gaguancela, O.A., Zúñiga, L.P., Arias, A.V., Halterman, D., Flores, F.J., Johansen, I.E., Wang, A., Yamaji, Y. & Verchot, J. (2016). The IRE1/bZIP60 pathway and Bax inhibitor 1 suppress systemic accumulation of Potyviruses and Potexviruses in Arabidopsis and *Nicotiana benthamiana* Plants. Mol Plant Microbe Interact **29(10)**, 750-766.

Gallie, D.R. (2001). Cap-independent translation conferred by the 5′ leader of Tobacco etch virus is Eukaryotic initiation factor 4G dependent. J Virol **75(24)**, 12141-12152.

Gallo, A., Valli, A., Calvo, M. & García, J.A. (2018). A functional link between RNA replication and virion assembly in the potyvirus Plum pox virus. J Virol **92(9)**, e02179-17.

Gallois, J.L., Charron, C., Sánchez, F., Pagny, G., Houvenaghel, M.C., Moretti, A., Ponz, F., Revers, F., Caranta, C. & German-Retana, S. (2010). Single amino acid changes in the Turnip mosaic virus viral genome-linked protein (VPg) confer virulence towards *Arabidopsis thaliana* mutants knocked out for eukaryotic initiation factors eIF(iso)4E and eIF(iso)4G. J Gen Virol **91(1)**, 288-293.

Gao, H., Brandizzi, F., Benning, C. & Larkin, R.M. (2008). A membrane-tethered transcription factor defines a branch of the heat stress response in *Arabidopsis thaliana*. Proc Natl Acad Sci U S A **105(42)**, 16398-16403.

Gao, L., Luo, J., Ding, X., Wang, T., Hu, T., Song, P., Zhai, R., Zhang, H., Zhang, K., Li, K. & Zhi, H. (2020). Soybean RNA interference lines silenced for eIF4E show broad potyvirus resistance. Mol Plant Pathol **21(3)**, 303-317.

Gao, Z., Eyers, S., Thomas, C., Ellis, N. & Maule, A. (2004a). Identification of markers tightly linked to *sbm* recessive genes for resistance to Pea seed-borne mosaic virus. Theor Appl Genet **109(3)**, 488-494.

Gao, Z., Johansen, E., Eyers, S., Thomas, C.L., Noel Ellis, T.H. & Maule, A.J. (2004b). The potyvirus recessive resistance gene, *sbm1*, identifies a novel role for translation initiation factor eIF4E in cell-to-cell trafficking. Plant J **40(3)**, 376-385.

Gauffier, C., Lebaron, C., Moretti, A., Constant, C., Moquet, F., Bonnet, G., Caranta, C. & Gallois, J.L. (2016). A TILLING approach to generate broad-spectrum resistance to potyviruses in tomato is hampered by eIF4E gene redundancy. Plant J **85(6)**, 717-729.

Gayral, M., Arias Gaguancela, O., Vasquez, E., Herath, V., Flores, F.J., Dickman, M.B. & Verchot, J. (2020). Multiple ER-to-nucleus stress signaling pathways are activated during Plantago asiatica mosaic virus and Turnip mosaic virus infection in *Arabidopsis thaliana*. Plant J **103(3)**, 1233-1245.

Geng, C., Cong, Q.Q., Li, X.D., Mou, A.L., Gao, R., Liu, J.L. & Tian, Y.P. (2014). Developmentally regulated plasma membrane protein of *Nicotiana benthamiana* contributes to Potyvirus movement and transports to plasmodesmata via the early secretory pathway and the actomyosin system. Plant Physiol **167(2)**, 394-410.

German-Retana, S., Walter, J., Doublet, B., Roudet-Tavert, G., Nicaise, V., Lecampion, C., Houvenaghel, M.C., Robaglia, C., Michon, T. & Le Gall, O. (2008). Mutational analysis of plant Cap-binding protein eIF4E reveals key amino acids involved in biochemical functions and potyvirus infection. J Virol **82(15)**, 7601-7612.

Ghram, M., Morris, G., Culjkovic-Kraljacic, B., Mars, J.C., Gendron, P., Skrabanek, L., Revuelta, M.V., Cerchietti, L., Guzman, M.L. & Borden, K.L. (2022). The eukaryotic translation initiation factor eIF4E reprogrammes the splicing machinery and drives alternative splicing. bioRxiv 2021-12.

Gong, Y.N., Tang, R.Q., Zhang, Y., Peng, J., Xian, O., Zhang, Z.H., Zhang, S.B., Zhang, D.Y., Liu, H., Luo, X.W. & Liu, Y. (2020). The NIa-protease protein encoded by the Pepper mottle virus is a pathogenicity determinant and releases DNA methylation of *Nicotiana benthamiana*. Front Microbiol **11**, 102.

González, R., Wu, B., Li, X., Martínez, F. & Elena, S.F. (2019). Mutagenesis scanning uncovers evolutionary constraints on Tobacco etch potyvirus membrane-associated 6K2 protein. genome biology and evolution. Genome Biol Evol **11(4)**, 1207-1222.

Gorovits, R. & Czosnek, H. (2017). The involvement of heat shock proteins in the establishment of Tomato yellow leaf curl virus infection. Front Plant Sci **8**, 355.

Gorovits, R., Liu, Y. & Czosnek, H. (2016). The involvement of HSP70 and HSP90 in Tomato yellow leaf curl virus infection in tomato plants and insect vectors. Heat Shock Proteins and Plants 189-207.

Gorovits, R., Moshe, A., Ghanim, M. & Czosnek, H. (2013). Recruitment of the host plant Heat shock protein 70 by Tomato yellow leaf curl virus coat protein is required for virus infection. PLoS One **8(7)**, e70280.

Goswami, A., Banerjee, R. & Raha, S. (2010). Mechanisms of plant adaptation/memory in rice seedlings under arsenic and heat stress: expression of heat-shock protein gene HSP70. AoB Plants **2010**, plq023.

Grangeon, R., Agbeci, M., Chen, J., Grondin, G., Zheng, H. & Laliberté, J.F. (2012). Impact on the endoplasmic reticulum and golgi apparatus of Turnip mosaic virus infection. J Virol **86(17)**, 9255-9265.

Grüner, S., Peter, D., Weber, R., Wohlbold, L., Chung, M.Y., Weichenrieder, O., Valkov, E., Igreja, C. & Izaurralde, E. (2016). The structures of eIF4E-eIF4G complexes reveal an extended interface to regulate translation initiation. Mol Cell **64(3)**, 467-479.

Guo, B., Lin, J. & Ye, K. (2011). Structure of the autocatalytic cysteine protease domain of potyvirus Helper-component proteinase. J Biol Chem **286(24)**, 21937-21943.

Guo, M., Zhai, Y.F., Lu, J.P., Chai, L., Chai, W.G., Gong, Z.H. & Lu, M.H. (2014). Characterization of CaHsp70-1, a pepper Heat-shock protein gene in response to heat stress and some regulation exogenous substances in *Capsicum annuum L.* Int J Mol Sci **15(11)**, 19741-19759.

Guo, Y., Guettouche, T., Fenna, M., Boellmann, F., Pratt, W.B., Toft, D.O., Smith, D.F. & Voellmy, R. (2001). Evidence for a mechanism of repression of Heat shock factor 1 transcriptional activity by a multichaperone complex. J Biol Chem **276(49)**, 45791-45799.

Gupta, R.S. & Golding, G.B. (1993). Evolution of HSP70 gene and its implications regarding relationships between archaebacteria, eubacteria, and eukaryotes. J Mol Evol **37(6)**, 573-582.

Gutierrez Sanchez, P.A., Babujee, L., Jaramillo Mesa, H., Arcibal, E., Gannon, M., Halterman, D., Jahn, M., Jiang, J. & Rakotondrafara, A.M. (2020). Overexpression of a modified eIF4E regulates potato virus Y resistance at the transcriptional level in potato. BMC Genomics **21(1)**, 18.

Hafrén, A., Hofius, D., Rönnholm, G., Sonnewald, U. & MÄkinen, K. (2010). HSP70 and its cochaperone CPIP promote potyvirus infection in *Nicotiana benthamiana* by regulating viral coat protein functions. Plant Cell **22(2)**, 523-535.

Hagiwara-Komoda, Y., Choi, S.H., Sato, M., Atsumi, G., Abe, J., Fukuda, J., Honjo, M.N., Nagano, A.J., Komoda, K., Nakahara, K.S., Uyeda, I. & Naito, S. (2016). Truncated yet functional viral protein produced via RNA polymerase slippage implies underestimated coding capacity of RNA viruses. Sci Rep **6(1)**, 21411.

Hahn, A., Bublak, D., Schleiff, E. & Scharf, K.D. (2011). Crosstalk between Hsp90 and Hsp70 chaperones and heat stress transcription factors in tomato. Plant Cell **23(2)**, 741-755.

Haldeman-Cahill, R., Daròs, J.A. & Carrington, J.C. (1998). Secondary structures in the capsid protein coding sequence and 3′ nontranslated region involved in amplification of the Tobacco etch virus genome. J Virol **72(5)**, 4072-4079.

Hartl, F.U., Bracher, A. & Hayer-Hartl, M. (2011). Molecular chaperones in protein folding and proteostasis. Nature **475(7356)**, 324-332.

Hashimoto, M., Neriya, Y., Yamaji, Y. & Namba, S. (2016). Recessive resistance to plant viruses: potential resistance genes beyond translation initiation factors. Front Microbiol **7**, 1695.

Hasiów-Jaroszewska, B., Fares, M.A. & Elena, S.F. (2014). Molecular evolution of viral multifunctional proteins: the case of potyvirus HC-Pro. J Mol Evol **78(1)**, 75-86.

Haynes, C.M. & Ron, D. (2010). The mitochondrial UPR – protecting organelle protein homeostasis. J Cell Sci **123(22)**, 3849-3855.

He, R., Li, Y., Bernards, M. A. & Wang, A. (2023). Manipulation of the cellular membrane-cytoskeleton network for RNA virus replication and movement in plants. Viruses **15(3)**, 744.

He, Z., Xie, R., Wang, Y., Zou, H., Zhu, J. & Yu, G. (2008). Cloning and characterization of a heat shock protein 70 gene, MsHSP70-1, in *Medicago sativa*. Acta Biochim Biophys Sin **40(3)**, 209-216.

Hébrard, E., Poulicard, N., Gérard, C., Traoré, O., Wu, H.C., Albar, L., Fargette, D., Bessin, Y. & Vignols, F. (2010). Direct interaction between the Rice yellow mottle virus (RYMV) VPg and the central domain of the Rice eIF(iso)4G1 factor correlates with rice susceptibility and RYMV virulence. Mol Plant Microbe Interact **23(11)**, 1506-1513.

Henriquez-Valencia, C., Moreno, A.A., Sandoval-Ibañez, O., Mitina, I., Blanco-Herrera, F., Cifuentes-Esquivel, N. & Orellana, A. (2015). bZIP17 and bZIP60 regulate the expression of BiP3 and other salt stress responsive genes in an UPR-independent manner in *Arabidopsis thaliana*. J Cell Biochem **116(8)**, 1638-1645.

Herath, V., Gayral, M., Miller, R.K. & Verchot, J. (2020). BIP and the unfolded protein response are important for Potyvirus and Potexvirus infection. Plant Signal Behav **15(11)**, 1807723.

Hernández, G. & Vazquez-Pianzola, P. (2005). Functional diversity of the eukaryotic translation initiation factors belonging to eIF4 families. Mech Dev **122(7)**, 865-876.

Hetz, C. (2012). The unfolded protein response: controlling cell fate decisions under ER stress and beyond. Nat Rev Mol Cell Biol **13(2)**, 89-102.

Hinnebusch, A.G. (2014). The scanning mechanism of eukaryotic translation initiation. Annu Rev Biochem **83(1)**, 779-812.

Huang, T.S., Wei, T., Laliberte, J.F. & Wang, A. (2009). A host RNA helicase-like protein, AtRH8, interacts with the potyviral genome-linked protein, VPg, associates with the virus accumulation complex, and is essential for infection. Plant Physiol **152(1)**, 255-266.

Huang, Y.W., Hu, C.C., Tsai, C.H., Lin, N.S. & Hsu, Y.H. (2017). Chloroplast Hsp70 isoform is required for age-dependent tissue preference of Bamboo mosaic virus in mature *Nicotiana benthamiana* leaves. Mol Plant Microbe Interact **30(8)**, 631-645.

Hwang, J., Li, J., Liu, W.Y., An, S.J., Cho, H., Her, N. H., Yeam, I., Kim, D. & Kang, B.C. (2009). Double mutations in eIF4E and eIFiso4E confer recessive resistance to Chilli veinal mottle virus in pepper. Mol Cells **27(3)**, 329-336.

Hýsková, V., Bělonožníková, K., Čeřovská, N. & Ryšlavá, H. (2021). HSP70 plays an ambiguous role during viral infections in plants. Biol Plantarum **65**, 68-79.

Inoue, H., Nonami, H., Akita, M. (2008). Alternative processing of Arabidopsis Hsp70 precursors during protein import into chloroplasts. Biosci Biotech Bioch **72(11)**, 2926-2935.

Ivanov, K.I., Puustinen, P., Gabrenaite, R., Vihinen, H., Rönnstrand, L., Valmu, L., Kalkkinen, N. & Mäkinen, K. (2003). Phosphorylation of the Potyvirus Capsid Protein by Protein Kinase CK2 and Its Relevance for Virus Infection. Plant Cell **15(9)**, 2124-2139.

Iwata, Y. & Koizumi, N. (2012). Plant transducers of the endoplasmic reticulum unfolded protein response. Trends Plant Sci **17(12)**, 720-727.

Jacob, P., Hirt, H. & Bendahmane, A. (2017). The heat-shock protein/chaperone network and multiple stress resistance. Plant Biotechnol J **15(4)**, 405-414.

Jelenska, J., van Hal, J.A. & Greenberg, J.T. (2010). *Pseudomonas syringae* hijacks plant stress chaperone machinery for virulence. Proc Natl Acad Sci U S A **107(29)**, 13177-13182.

Jenner, C.E., Nellist, C.F., Barker, G.C. & Walsh, J.A. (2010). Turnip mosaic virus (TuMV) is able to use alleles of both eIF4E and eIF(iso)4E from multiple loci of the diploid *Brassica rapa*. Mol Plant Microbe Interact **23(11)**, 1498-1505.

Jenner, C.E., Wang, X., Tomimura, K., Ohshima, K., Ponz, F. & Walsh, J.A. (2003). The dual role of the Potyvirus P3 protein of Turnip mosaic virus as a symptom and avirulence determinant in Brassicas. Mol Plant Microbe Interact **16(9)**, 777-784.

Jeong, S. J., Park, S., Nguyen, L.T., Hwang, J., Lee, E.Y., Giong, H.K., Lee, J.S., Yoon, I., Lee, J.H., Kim, J.H., Kim, H.K., Kim, D., Yang, W.S., Kim, S.Y., Lee, C.Y., Yu, K., Sonenberg, N., Kim, M.H. & Kim, S. (2019). A threonyl-tRNA synthetase-mediated translation initiation machinery. Nat Commun **10(1)**, 1357.

Jiang, J. & Laliberté, J.F. (2011). The genome-linked protein VPg of plant viruses—a protein with many partners. Curr Opin Virol **1(5)**, 347-354.

Jiang, J., Patarroyo, C., Cabanillas, D., Zheng, H. & Laliberté, J.F. (2015). The vesicle-forming 6K2 protein of Turnip mosaic virus interacts with the COPII coatomer Sec24a for viral systemic infection. J Virol **89(13)**, 6695-6710.

Jiang, S., Lu, Y., Li, K., Lin, L., Zheng, H., Yan, F. & Chen, J. (2014). Heat shock protein 70 is necessary for Rice stripe virus infection in plants. Mol Plant Pathol **15(9)**, 907-917.

Joshi, B., Lee, K., Maeder, D.L. & Jagus, R. (2005). Phylogenetic analysis of eIF4E-family members. BMC Evol Biol **5(1)**, 48.

Jung, K.H., Gho, H.J., Nguyen, M.X., Kim, S.R. & An, G. (2013). Genome-wide expression analysis of HSP70 family genes in rice and identification of a cytosolic HSP70 gene highly induced under heat stress. Funct Integr Genomics **13(3)**, 391-402.

Jungkunz, I., Link, K., Vogel, F., Voll, L. M., Sonnewald, S. & Sonnewald, U. (2011). AtHsp70-15-deficient Arabidopsis plants are characterized by reduced growth, a constitutive cytosolic protein response and enhanced resistance to TuMV. Plant J **66(6)**, 983-995.

Kallamadi, P.R., Dandu, K., Kirti, P.B., Rao, C.M., Thakur, S.S. & Mulpuri, S. (2018). An insight into powdery mildew–infected, susceptible, resistant, and immune sunflower genotypes. Proteomics **18(16)**, 1700418.

Kanchiswamy, C.N., Malnoy, M., Velasco, R., Kim, J.S. & Viola, R. (2015). Non-GMO genetically edited crop plants. Trends Biotechnol **33(9)**, 489-491.

Kang, B.C., Yeam, I., Frantz, J.D., Murphy, J.F. & Jahn, M.M. (2005). The pvr1 locus in Capsicum encodes a translation initiation factor eIF4E that interacts with Tobacco etch virus VPg. Plant J **42(3)**, 392-405.

Kang, B.C., Yeam, I., Li, H., Perez, K. W. & Jahn, M.M. (2007). Ectopic expression of a recessive resistance gene generates dominant potyvirus resistance in plants. Plant Biotechnol J **5(4)**, 526-536.

Kanyuka, K., Druka, A., Caldwell, D.G., Tymon, A., Mccallum, N., Waugh, R. & Adams, M.J. (2005). Evidence that the recessive bymovirus resistance locus rym4 in barley corresponds to the eukaryotic translation initiation factor 4E gene. Mol Plant Pathol **6(4)**, 449-458.

Kanyuka, K., McGrann, G., Alhudaib, K., Hariri, D. & Adams, M.J. (2004). Biological and sequence analysis of a novel European isolate of Barley mild mosaic virus that overcomes the barley *rym5* resistance gene. Arch Virol **149(8)**, 1469-1480.

Kanzaki, H., Saitoh, H., Ito, A., Fujisawa, S., Kamoun, S., Katou, S., Yoshioka, H. & Terauchi, R. (2003). Cytosolic HSP90 and HSP70 are essential components of INF1-mediated hypersensitive response and non-host resistance to *Pseudomonas cichorii* in *Nicotiana benthamiana*. Mol Plant Pathol **4(5)**, 383-391.

Karlin, S. & Brocchieri, L. (1998). Heat shock protein 70 family: multiple sequence comparisons, function, and evolution. J Mol Evol **47(5)**, 565-577.

Kasschau, K.D. & Carrington, J.C. (1998). A counterdefensive strategy of plant viruses: suppression of posttranscriptional gene silencing. Cell **95(4)**, 461-470.

Kawaguchi, R. & Bailey-Serres, J. (2002). Regulation of translational initiation in plants. Curr Opin Plant Biol **5(5)**, 460-465.

Kežar, A., Kavčič, L., Polák, M., Nováček, J., Gutiérrez-Aguirre, I., Žnidarič, M.T., Coll, A., Stare, K., Gruden, K., Ravnikar, M., Pahovnik, D., Žagar, E., Merzel, F., Anderluh, G. & Podobnik, M. (2019). Structural basis for the multitasking nature of the potato virus Y coat protein. Sci Adv **5(7)**, eaaw3808.

Khan, M.A., Miyoshi, H., Gallie, D.R. & Goss, D.J. (2008). Potyvirus genome-linked protein, VPg, directly affects wheat germ *in vitro* translation: interactions with translation initiation factors eIF4F and eIFiso4F. J Biol Chem **283(3)**, 1340-1349.

Kim, J., Kang, W.H., Hwang, J., Yang, H.B., Dosun, K., Oh, C.S. & Kang, B.C. (2014). Transgenic *Brassica rapa* plants over-expressing eIF(iso)4E variants show broad-spectrum Turnip mosaic virus (TuMV) resistance. Mol Plant Pathol **15(6)**, 615-626.

Kim, J., Kang, W.H., Yang, H.B., Park, S., Jang, C.S. Yu, H.J. & Kang, B.C. (2013). Identification of a broad-spectrum recessive gene in *Brassica rapa* and molecular analysis of the eIF4E gene family to develop molecular markers. Mol Breeding **32(2)**, 385-398.

Kim, N.H. & Hwang, B.K. (2014). Pepper Heat shock protein 70a interacts with the Type III effector AvrBsT and triggers plant cell death and immunity. Plant Physiol **167(2)**, 307-322.

Kim, S.R. & An, G. (2013). Rice chloroplast-localized heat shock protein 70, OsHsp70CP1, is essential for chloroplast development under high-temperature conditions. J Plant Physiol **170(9)**, 854-863.

Király, L., Hafez, Y.M., Fodor, J., Király, Z. (2008). Suppression of tobacco mosaic virus-induced hypersensitive-type necrotization in tobacco at high temperature is associated with downregulation of NADPH oxidase and superoxide and stimulation of dehydroascorbate reductase. J gen Virol **89(3)**, 799-808.

Klein, P.G., Klein, R.R., Rodriguez-Cerezo, E., Hunt, A.G. & Shaw, J.G. (1994). Mutational analysis of the Tobacco vein mottling virus genome. Virology **204(2)**, 759-769.

Kleizen, B. & Braakman, I. (2004). Protein folding and quality control in the endoplasmic reticulum. Curr Opin Cell Biol **16(4)**, 343-349.

Knuhtsen, H., Hiebert, E. & Purcifull, D.E. (1974). Partial purification and some properties of tobacco etch virus induced intranuclear inclusions. Virology **61(1)**, 200-209.

Kørner, C.J., Du, X., Vollmer, M.E. & Pajerowska-Mukhtar, K.M. (2015). Endoplasmic reticulum stress signaling in plant immunity—at the crossroad of life and death. Int J Mol Sci **16(11)**, 26582-26598.

Kotak, S., Larkindale, J., Lee, U., von Koskull-Döring, P., Vierling, E. & Scharf, K.D. (2007). Complexity of the heat stress response in plants. Curr Opin Plant Biol **10(3)**, 310-316.

Krenz, B., Windeisen, V., Wege, C., Jeske, H. & Kleinow, T. (2010). A plastid-targeted heat shock cognate 70kDa protein interacts with the Abutilon mosaic virus movement protein. Virology **401(1)**, 6-17.

Kropiwnicka, A., Kuchta, K., Lukaszewicz, M., Kowalska, J., Jemielity, J., Ginalski, K., Darzynkiewicz, E. & Zuberek, J. (2015). Five eIF4E isoforms from *Arabidopsis thaliana* are characterized by distinct features of cap analogs binding. Biochem Biophys Res Commun **456(1)**, 47-52.

Kubienova, L., Sedlářová, M., Vítečková-Wünschová, A., Piterkova, J., Luhova, L., Mieslerova, B., Lebeda, A., Navratil, M. & Petřivalský, M. (2013). Effect of extreme temperatures on powdery mildew development and Hsp70 induction in tomato and wild Solanum spp. Plant Protect Sci **49(Special Issue)**, S41-S54.

Kühne, T., Shi, N., Proeseler, G., Adams, M.J. & Kanyuka, K. (2003). The ability of a bymovirus to overcome the rym4-mediated resistance in barley correlates with a codon change in the VPg coding region on RNA1. J Gen Virol **84(10)**, 2853-2859.

Kuroiwa, K., Thenault, C., Nogué, F., Perrot, L., Mazier, M. & Gallois, J.L. (2022). CRISPR-based knock-out of eIF4E2 in a cherry tomato background successfully recapitulates resistance to pepper veinal mottle virus. Plant Sci **316**, 111160.

Kurowska, M., Daszkowska-Golec, A., Gruszka, D., Marzec, M., Szurman, M., Szarejko, I. & Maluszynski, M. (2011). **TILLING** - a shortcut in functional genomics. J Appl Genet **52(4),** 371-390.

Kwon, Y., Kabir, M.A., Wang, H.W., Karuppanapandian, T., Moon, J.C., Ryu, K.H., Lee, G.P., Kim, W. (2012). Elimination of pepper mild mottle virus from infected tobacco (*Nicotiana benthamiana L.*) plants by callus culture and the sieving technique. In Vitro cell dev Biol Plant **48(6)**, 595-599.

Kyle, M.M. & Palloix, A. (1997). Proposed revision of nomenclature for potyvirus resistance genes in Capsicum. Euphytica **97(2)**, 183-188.

Lageix, S., Lanet, E., Pouch-Pélissier, M.N., Espagnol, M.C., Robaglia, C., Deragon, J.M. & Pélissier, T. (2008). Arabidopsis eIF2α kinase GCN2 is essential for growth in stress conditions and is activated by wounding. BMC Plant Biol **8(1)**, 134.

Laliberté, J.F. & Sanfaçon, H. (2010). Cellular remodeling during plant virus infection. Annu Rev Phytopathol **48(1)**, 69-91.

Lee, A.S., Kranzusch, P.J., Doudna, J. A. & Cate, J.H. (2016). eIF3d is an mRNA cap-binding protein that is required for specialized translation initiation. Nature **536(7614)**, 96-99.

Lee, J.H., An, J.T., Siddique, M.I., Han, K., Choi, S., Kwon, J.K. & Kang, B.C. (2017). Identification and molecular genetic mapping of Chili veinal mottle virus (ChiVMV) resistance genes in pepper (*Capsicum annuum*). Mol Breeding **37(10)**, 121.

Lee, J.H., Muhsin, M., Atienza, G.A., Kwak, D.Y., Kim, S.M., De Leon, T.B., Angeles, E.R., Coloquio, E., Kondoh, H., Satoh, K., Cabunagan, R.C., Cabauatan, P.Q., Kikuchi, S., Leung, H. & Choi, I.R. (2010). Single nucleotide polymorphisms in a gene for translation initiation factor (eIF4G) of rice (*Oryza sativa*) associated with resistance to Rice tungro spherical virus. Mol Plant Microbe Interact **23(1)**, 29-38.

Lee, S., Lee, D.W., Lee, Y., Mayer, U., Stierhof, Y.D., Lee, S., Jürgens, G. & Hwang, I. (2009). Heat shock protein cognate 70-4 and an E3 ubiquitin ligase, CHIP, mediate plastid-destined precursor degradation through the ubiquitin-26S proteasome system in Arabidopsis. Plant Cell **21(12)**, 3984-4001.

Lellis, A.D., Kasschau, K.D., Whitham, S.A. & Carrington, J.C. (2002). Loss-of-susceptibility mutants of *Arabidopsis thaliana* reveal an essential role for eIF(iso)4E during potyvirus infection. Curr Biol **12(12)**, 1046-1051.

Leng, L., Liang, Q., Jiang, J., Zhang, C., Hao, Y., Wang, X. & Su, W. (2017). A subclass of HSP70s regulate development and abiotic stress responses in *Arabidopsis thaliana*. J Plant Res **130(2)**, 349-363.

Léonard, S., Plante, D., Wittmann, S., Daigneault, N., Fortin, M.G. & Laliberté, J.F. (2000). Complex formation between Potyvirus VPg and Translation eukaryotic initiation factor 4E correlates with virus infectivity. J Virol **74(17)**, 7730-7737.

Li, C., Xu, Y., Fu, S., Liu, Y., Li, Z., Zhang, T., Wu, J. & Zhou, X. (2021). The unfolded protein response plays dual roles in Rice stripe virus infection through fine-tuning the movement protein accumulation. PLoS Pathog **17(3)**, e1009370.

Li, C., Zhang, T., Liu, Y., Li, Z., Wang, Y., Fu, S., Xu, Y., Zhou, T., Wu, J. & Zhou, X. (2022). Rice stripe virus activates the bZIP17/28 branch of the unfolded protein response signalling pathway to promote viral infection. Mol Plant Pathol **23(3)**, 447-458.

Li, F., Zhang, C., Li, Y., Wu, G., Hou, X., Zhou, X. & Wang, A. (2018a). Beclin1 restricts RNA virus infection in plants through suppression and degradation of the viral polymerase. Nat Commun **9(1)**, 1268.

Li, F., Zhang, C., Tang, Z., Zhang, L., Dai, Z., Lyu, S., Li, Y., Hou, X., Bernards, M. & Wang, A. (2020). A plant RNA virus activates selective autophagy in a UPR-dependent manner to promote virus infection New Phytol **228(2)**, 622-639.

Li, F.F., Sun, H.J., Jiao, Y.B., Wang, F.L., Yang, J.G. & Shen, L.L. (2018b). Viral infection-induced endoplasmic reticulum stress and a membrane-associated transcription factor NbNAC089 are involved in resistance to virus in *Nicotiana benthamiana*. Plant Pathol **67(1)**, 233-243.

Li, G., Lv, H., Zhang, S., Zhang, S., Li, F., Zhang, H., Qian, W., Fang, Z. & Sun, R. (2019). TuMV management for brassica crops through host resistance: retrospect and prospects. Plant Pathol **68(6)**, 1035-1044.

Li, H., Kondo, H., Kühne, T. & Shirako, Y. (2016). Barley yellow mosaic virus VPg is the determinant protein for breaking eIF4E-mediated recessive resistance in barley plants. Front Plant Sci **7**, 1449.

Li, H. & Shirako, Y. (2015). Association of VPg and eIF4E in the host tropism at the cellular level of Barley yellow mosaic virus and Wheat yellow mosaic virus in the genus Bymovirus. Virology **476**, 159-167.

Li, N., Zhang, S.J., Zhao, Q., Long, Y., Guo, H., Jia, H.F., Yang, Y.X., Zhang, H.Y., Ye, X.F. & Zhang, S.T. (2018c). Overexpression of Tobacco GCN2 stimulates multiple physiological changes associated with stress tolerance. Front Plant Sci **9**, 725.

Lin, B.L., Wang, J.S., Liu, H.C., Chen, R.W., Meyer, Y., Barakat, A. & Delseny, M. (2001). Genomic analysis of the Hsp70 superfamily in *Arabidopsis thaliana*. Cell Stress Chaperones **6(3)**, 201-208.

Lindquist, S. (1986). The heat-shock response. Annu Rev Biochem **45**, 39-72.

Ling, K.S., Harris, K.R., Meyer, J.D.F., Levi, A., Guner, N., Wehner, T.C., Bendahmane, A. & Havey, M.J. (2009). Non-synonymous single nucleotide polymorphisms in the watermelon eIF4E gene are closely associated with resistance to Zucchini yellow mosaic virus. Theor Appl Genet **120(1)**, 191-200.

Liu, J.X. & Howell, S.H. (2010). bZIP28 and NF-Y transcription factors are activated by ER stress and assemble into a transcriptional complex to regulate stress response genes in Arabidopsis. Plant Cell **22(3)**, 782-796.

Liu, J.X., Srivastava, R., Che, P. & Howell, S.H. (2007). Salt stress responses in Arabidopsis utilize a signal transduction pathway related to endoplasmic reticulum stress signaling. Plant J **51(5)**, 897-909.

Liu, S., Wang, J., Cong, B., Huang, X., Chen, K. & Zhang, P. (2014). Characterization and expression analysis of a mitochondrial heat-shock protein 70 gene from the Antarctic moss *Pohlia nutans*. Polar Biol **37(8)**, 1145-1155.

Liu, W., Jankowska-Anyszka, M., Piecyk, K., Dickson, L., Wallace, A., Niedzwiecka, A., Stepinski, J., Stolarski, R., Darzynkiewicz, E., Kieft, J., Zhao, R., Jones, D.N. & Davis, R.E. (2011). Structural basis for nematode eIF4E binding an m 2,2,7 G-Cap and its implications for translation initiation. Nucleic Acids Res **39(20)**, 8820-8832.

Liu, X., Afrin, T. & Pajerowska-Mukhtar, K.M. (2019). Arabidopsis GCN2 kinase contributes to ABA homeostasis and stomatal immunity. Commun Biol **2(1)**, 302.

Liu, X., Kørner, C.J., Hajdu, D., Guo, T., Ramonell, K.M., Argueso, C.T. & Pajerowska-Mukhtar, K.M. (2015). *Arabidopsis thaliana* atGCN2 kinase is involved in disease resistance against pathogens with diverse life styles. J Phytopathol **4(2)**, 93-104.

Lõhmus, A., Hafrén, A. & Mäkinen, K. (2017). Coat protein regulation by CK2, CPIP, HSP70, and CHIP is required for Potato virus A replication and coat protein accumulation. J Virol **91(3)**, e01316-16.

Lõhmus, A., Varjosalo, M. & Mäkinen, K. (2016). Protein composition of 6K2-induced membrane structures formed during Potato virus A infection. Mol Plant Pathol **17(6)**, 943-958.

Lu, Q., Tang, X., Tian, G., Wang, F., Liu, K., Nguyen, V., Kohalmi, S. E., Keller, W.A., Tsang, E.W., Harada, J.J., Rothstein, S.J. & Cui, Y. (2010). Arabidopsis homolog of the yeast TREX-2 mRNA export complex: components and anchoring nucleoporin. Plant J **61(2)**, 259-270.

Lu, R.C., Tan, M.S., Wang, H., Xie, A.M., Yu, J.T. & Tan, L. (2014). Heat shock protein 70 in Alzheimer's disease. Biomed Res Int **2014**, 435203.

Luan, H., Shine, M.B., Cui, X., Chen, X., Ma, N., Kachroo, P., Zhi, H. & Kachroo, A. (2016). The potyviral P3 protein targets Eukaryotic elongation factor 1A to promote the unfolded protein response and viral pathogenesis. Plant Physiol **172(1)**, 221-234.

Lund, P.A. (2001). Molecular chaperones in the cell. 37

Makarova, S.S., Khromov, A.V., Spechenkova, N.A., Taliansky, M.E. & Kalinina, N.O. (2018). Application of the CRISPR/Cas system for generation of pathogen-resistant plants. Biochemistry (Mosc) **83(12)**, 1552-1562.

Mali, P., Yang, L., Esvelt, K.M., Aach, J., Guell, M., DiCarlo, J.E., Norville, J.E. & Church, G.M. (2013). RNA-guided human genome engineering via Cas9. Science **339(6121)**, 823-826.

Mann, K.S. & Sanfaçon, H. (2019). Expanding repertoire of plant positive-strand RNA virus proteases. Viruses **11(1)**, 66.

Mars, J.C., Ghram, M., Culjkovic-Kraljacic, B. & Borden, K.L. (2021). The Cap-binding complex CBC and the eukaryotic translation factor eIF4E: co-conspirators in Cap-dependent RNA maturation and translation. Cancers (Basel) **13(24)**, 6185.

Martin, F., Barends, S., Jaeger, S., Schaeffer, L., Prongidi-Fix, L. & Eriani, G. (2011). Cap-assisted internal initiation of translation of Histone H4. Mol Cell **41(2)**, 197-209.

Martínez-Silva, A.V., Aguirre-Martínez, C., Flores-Tinoco, C.E., Alejandri-Ramírez, N.D. & Dinkova, T.D. (2012). Translation initiation factor AteIF(iso)4E is involved in selective mRNA translation in *Arabidopsis thaliana* seedlings. PLoS One **7(2)**, e31606.

Martínez-Turiño, S. & García, J.A. (2020). Chapter Five - Potyviral coat protein and genomic RNA: A striking partnership leading virion assembly and more. Adv Virus Res **108**, 165-211.

Martínez-Turiño, S., Pérez, J.D.J., Hervás, M., Navajas, R., Ciordia, S., Udeshi, N.D., Shabanowitz, J., Hunt, D.F. & García, J.A. (2018). Phosphorylation coexists with O-GlcNAcylation in a plant virus protein and influences viral infection. Mol Plant Pathol **19(6)**, 1427-1443.

Maruyama, D., Endo, T. & Nishikawa, S. (2010). BiP-mediated polar nuclei fusion is essential for the regulation of endosperm nuclei proliferation in *Arabidopsis thaliana*. Proc Natl Acad Sci U S A **107(4)**, 1684-1689.

Maruyama, D., Sugiyama, T., Endo, T. & Nishikawa, S. (2014). Multiple BiP genes of *Arabidopsis thaliana* are required for male gametogenesis and pollen competitiveness. Plant Cell Physiol **55(4)**, 801-810.

Mathioudakis, M.M., Veiga, R., Ghita, M., Tsikou, D., Medina, V., Canto, T., Makris, A.M. & Livieratos, I.C. (2012). Pepino mosaic virus capsid protein interacts with a tomato heat shock protein cognate 70. Virus Res **163(1)**, 28-39.

Maule, A.J., Caranta, C. & Boulton, M.I. (2007). Sources of natural resistance to plant viruses: status and prospects. Mol Plant Pathol **8(2)**, 223-231.

Mayberry, L.K., Allen, M.L., Dennis, M.D. & Browning, K.S. (2009). Evidence for variation in the Optimal Translation Initiation Complex: Plant eIF4B, eIF4F, and eIF(iso)4F differentially promote translation of mRNAs. Plant Physiol **150(4)**, 1844-1854.

Mayer, M.P. (2010). Gymnastics of Molecular Chaperones. Mol Cell **39(3)**, 321-331.

Mayer, M.P., Brehmer, D., Gässler, C.S. & Bukau, B. (2001). Hsp70 chaperone machines. Adv in Protein Chem **59**, 1-44.

Mazier, M., Flamain, F., Nicolaï, M., Sarnette, V. & Caranta, C. (2011). Knock-down of both eIF4E1 and eIF4E2 genes confers broad-spectrum resistance against Potyviruses in tomato. PLoS One **6(12)**, e29595.

McCallum, C.M., Comai, L., Greene, E.A. & Henikoff, S. (2000). Targeting induced local lesions IN genomes (TILLING) for plant functional genomics. Plant Physiol **123(2)**, 439-442.

Meiri, D., Tazat, K., Cohen-Peer, R., Farchi-Pisanty, O., Aviezer-Hagai, K., Avni, A. & Breiman, A. (2010). Involvement of Arabidopsis ROF2 (FKBP65) in thermotolerance. Plant Mol Biol **72(1)**, 191-203.

Michel, V., Julio, E., Candresse, T., Cotucheau, J., Decorps, C., Volpatti, R., Moury, B., Glais, L., Jacquot, E., de Borne, F.D., Decroocq, V., Gallois, J.L. & German-Retana, S. (2019). A complex eIF4E locus impacts the durability of *va* resistance to Potato virus Y in tobacco. Mol Plant Pathol **20(8)**, 1051-1066.

Michon, T., Estevez, Y., Walter, J., German-Retana, S. & Le Gall, O. (2006). The potyviral virus genome-linked protein VPg forms a ternary complex with the eukaryotic initiation factors eIF4E and eIF4G and reduces eIF4E affinity for a mRNA cap analogue. FEBS J **273(6)**, 1312-1322.

Mine, A., Hyodo, K., Tajima, Y., Kusumanegara, K., Taniguchi, T., Kaido, M., Mise, K., Taniguchi, H. & Okuno, T. (2012). Differential roles of Hsp70 and Hsp90 in the assembly of the replicase complex of a positive-strand RNA plant virus. J Virol **86(22)**, 12091-12104.

Mine, A., Takeda, A., Taniguchi, T., Taniguchi, H., Kaido, M., Mise, K. & Okuno, T. (2010). Identification and characterization of the 480-Kilodalton template-specific RNA-dependent RNA polymerase complex of Red Clover Necrotic Mosaic virus. J Virol **84(12)**, 6070-6081.

Mingot, A., Valli, A., Rodamilans, B., León, D.S., Baulcombe, D.C., García, J.A. & López-Moya, J.J. (2016). The P1N-PISPO trans-frame gene of Sweet potato feathery mottle Potyvirus is produced during virus infection and functions as an RNA silencing suppressor. J Virol **90(7)**, 3543-3557.

Miras, M., Truniger, V., Silva, C., Verdaguer, N., Aranda, M.A. & Querol-Audí, J. (2017). Structure of eIF4E in complex with an eIF4G peptide supports a universal bipartite binding mode for protein translation. Plant Physiol **174(3)**, 1476-1491.

Miroshnichenko, D., Timerbaev, V., Okuneva, A., Klementyeva, A., Sidorova, T., Pushin, A. & Dolgov, S. (2020). Enhancement of resistance to PVY in intragenic marker-free potato plants by RNAi-mediated silencing of eIF4E translation initiation factors. Plant Cell, Tissue and Organ Culture (PCTOC) **140(3)**, 691-705.

Mittler, R., Finka, A. & Goloubinoff, P. (2012). How do plants feel the heat? Trends Biochem Sci **37(3)**, 118-125.

Monaghan, J. & Li, X. (2010). The HEAT repeat protein ILITYHIA is required for plant immunity. Plant Cell Physiol **51(5)**, 742-753.

Monzingo, A.F., Dhaliwal, S., Dutt-Chaudhuri, A., Lyon, A., Sadow, J.H., Hoffman, D.W., Robertus, J.D. & Browning, K.S. (2007). The structure of Eukaryotic translation initiation factor-4E from wheat reveals a novel disulfide bond. Plant Physiol **143(4)**, 1504-1518.

Moury, B., Lebaron, C., Szadkowski, M., Ben Khalifa, M., Girardot, G., Bolou Bi, B.A., Koné, D., Nitiema, L.W., Fakhfakh, H. & Gallois, J.L. (2020). Knock-out mutation

of eukaryotic initiation factor 4E2 (eIF4E2) confers resistance to Pepper veinal mottle virus in tomato. Virology **539**, 11-17.

Moury, B., Morel, C., Johansen, E., Guilbaud, L., Souche, S., Ayme, V., Caranta, C., Palloix, A. & Jacquemond, M. (2004). Mutations in Potato virus Y genome-linked protein determine virulence toward recessive resistances in *Capsicum annuum* and *Lycopersicon hirsutum*. Mol Plant Microbe Interact **17(3)**, 322-329.

Nagashima, Y., Mishiba, K., Suzuki, E., Shimada, Y., Iwata, Y. & Koizumi, N. (2011). Arabidopsis IRE1 catalyses unconventional splicing of bZIP60 mRNA to produce the active transcription factor. Sci Rep **1(1)**, 29.

Nair, A.U., Bhukya, D.P.N., Sunkar, R., Chavali, S. & Allu, A.D. (2022). Molecular basis of priming-induced acquired tolerance to multiple abiotic stresses in plants. J Exp Bot **73(11)**, 3355-3371.

Nakahara, K.S., Shimada, R., Choi, S.H., Yamamoto, H., Shao, J. & Uyeda, I. (2010). Involvement of the P1 cistron in overcoming eIF4E-mediated recessive resistance against Clover yellow vein virus in pea. Mol Plant Microbe Interact **23(11)**, 1460-1469.

Nellist, C.F., Ohshima, K., Ponz, F. & Walsh, J.A. (2022). Turnip mosaic virus, a virus for all seasons. Ann Appl Biol **180(3)**, 312-327.

Nellist, C.F., Qian, W., Jenner, C.E., Moore, J.D., Zhang, S., Wang, X., Briggs, W.H., Barker, G. C., Sun, R. & Walsh, J.A. (2014). Multiple copies of eukaryotic translation initiation factors in Brassica rapa facilitate redundancy, enabling diversification through variation in splicing and broad-spectrum virus resistance. Plant J **77(2)**, 261-268.

Nicaise, V., Gallois, J.L., Chafiai, F., Allen, L.M., Schurdi-Levraud, V., Browning, K.S., Candresse, T., Caranta, C., Le Gall, O. & German-Retana, S. (2007). Coordinated and selective recruitment of eIF4E and eIF4G factors for potyvirus infection in *Arabidopsis thaliana*. FEBS Lett **581(5)**, 1041-1046.

Nicaise, V. r., German-Retana, S., Sanjuán, R., Dubrana, M.P., Mazier, M., Maisonneuve, B., Candresse, T., Caranta, C. & LeGall, O. (2003). The Eukaryotic translation initiation factor 4E controls lettuce susceptibility to the potyvirus Lettuce mosaic virus. Plant Physiol **132(3)**, 1272-1282.

Nieto, C., Morales, M., Orjeda, G., Clepet, C., Monfort, A., Sturbois, B., Puigdomènech, P., Pitrat, M., Caboche, M., Dogimont, C., Garcia-Mas, J., Aranda, M.A. & Bendahmane, A. (2006). An eIF4E allele confers resistance to an uncapped and non-polyadenylated RNA virus in melon. Plant J **48(3)**, 452-462.

Nieto, C., Piron, F., Dalmais, M., Marco, C.F., Moriones, E., Gómez-Guillamón, M.L., Truniger, V., Gómez, P., Garcia-Mas, J., Aranda, M.A. & Bendahmane, A. (2007). EcoTILLING for the identification of allelic variants of melon eIF4E, a factor that controls virus susceptibility. BMC Plant Biol **7(1)**, 34.

Nigam, D., LaTourrette, K., Souza, P.F.N. & Garcia-Ruiz, H. (2019). Genome-wide variation in Potyviruses. Front Plant Sci **10**, 1439.

Niraula, P.M. & Fondong, V.N. (2021). Development and adoption of genetically engineered plants for virus resistance: advances, opportunities and challenges. Plants (Basel) **10(11)** 2339.

Noël, L.D., Cagna, G., Stuttmann, J., Wirthmüller, L., Betsuyaku, S., Witte, C.P., Bhat, R., Pochon, N., Colby, T. & Parker, J.E. (2007). Interaction between SGT1 and cytosolic/nuclear HSC70 chaperones regulates Arabidopsis immune responses. Plant Cell **19(12)**, 4061-4076.

Ohta, M., Wakasa, Y., Takahashi, H., Hayashi, S., Kudo, K. & Takaiwa, F. (2013). Analysis of rice ER-resident J-proteins reveals diversity and functional differentiation of the ER-resident Hsp70 system in plants. J Exp Bot **64(18)**, 5429-5441.

Olspert, A., Chung, B. Y.W., Atkins, J.F., Carr, J.P. & Firth, A.E. (2015). Transcriptional slippage in the positive-sense RNA virus family *Potyviridae*. EMBO reports **16(8)**, 995-1004.

Ordiz, M.I., Magnenat, L., Barbas, C.F. & Beachy, R.N. (2010). Negative regulation of the RTBV promoter by designed zinc finger proteins. Plant Mol Biol **72(6)**, 621-630.

Osborne, M.J. & Borden, K.L. (2015). The eukaryotic translation initiation factor eIF4E in the nucleus: taking the road less traveled. Immunol Rev **263(1)**, 210-223.

Park, C.J. & Park, J.M. (2019). Endoplasmic reticulum plays a critical role in integrating signals generated by both biotic and abiotic stress in plants. Front Plant Sci **10**, 399.

Park, C.J. & Seo, Y.S. (2015). Heat shock proteins: a review of the molecular chaperones for plant immunity. Plant Pathol J **31(4)**, 323.

Park, S.H., Li, F., Renaud, J., Shen, W., Li, Y., Guo, L., Cui, H., Sumarah, M. & Wang, A. (2017). NbEXPA1, an α-expansin, is plasmodesmata-specific and a novel host factor for potyviral infection. Plant J **92(5)**, 846-861.

Pasin, F., Simón-Mateo, C. & García, J.A. (2014). The hypervariable amino-terminus of P1 protease modulates potyviral replication and host defense responses. PLoS Pathog **10(3)**, e1003985.

Pastor-Cantizano, N., Ko, D.K., Angelos, E., Pu, Y. & Brandizzi, F. (2020). Functional diversification of ER stress responses in Arabidopsis. Trends Biochem Sci **45(2)**, 123-136.

Patrick, R.M. & Browning, K.S. (2012). The eIF4F and eIFiso4F complexes of plants: an evolutionary perspective. Comp Funct Genomics **2012**, 287814.

Patrick, R.M., Mayberry, L.K., Choy, G., Woodard, L.E., Liu, J.S., White, A., Mullen, R.A., Tanavin, T.M., Latz, C.A. & Browning, K.S. (2014). Two Arabidopsis loci encode novel Eukaryotic initiation factor 4E isoforms that are functionally distinct from the conserved plant Eukaryotic initiation factor 4E. Plant Physiol **164(4)**, 1820-1830.

Pavan, S., Jacobsen, E., Visser, R.G. & Bai, Y. (2010). Loss of susceptibility as a novel breeding strategy for durable and broad-spectrum resistance. Mol Breed **25(1)**, 1-12.

Peremyslov, V.V., Hagiwara, Y. & Dolja, V.V. (1999). HSP70 homolog functions in cell-to-cell movement of a plant virus. Proc Natl Acad Sci U S A **96(26)**, 14771-14776.

Perovic, D., Krämer, I., Habekuss, A., Perner, K., Pickering, R., Proeseler, G., Kanyuka, K. & Ordon, F. (2014). Genetic analyses of BaMMV/BaYMV resistance in barley accession HOR4224 result in the identification of an allele of the translation initiation factor 4e (Hv-eIF4E) exclusively effective against Barley mild mosaic virus (BaMMV). Theor Appl Genet **127(5)**, 1061-1071.

Pirkkala, L., Nykänen, P. & Sistonen, L. (2001). Roles of the heat shock transcription factors in regulation of the heat shock response and beyond. FASEB J **15(7)**, 1118-1131.

Piron, F., Nicolaï, M., Minoïa, S., Piednoir, E., Moretti, A., Salgues, A., Zamir, D., Caranta, C. & Bendahmane, A. (2010). An induced mutation in tomato eIF4E leads to immunity to two Potyviruses. PLoS One **5(6)**, e11313.

Piterková, J., Luhová, L., Mieslerová, B., Lebeda, A. & Petřivalský, M. (2013). Nitric oxide and reactive oxygen species regulate the accumulation of heat shock proteins in tomato leaves in response to heat shock and pathogen infection. Plant Sci **207**, 57-65.

Plante, D., Viel, C., Léonard, S., Tampo, H., Laliberté, J.F. & Fortin, M.G. (2004). Turnip mosaic virus VPg does not disrupt the translation initiation complex but interferes with cap binding. Physiol and Mol Plant Pathol **64(4)**, 219-226.

Pogany, J. & Nagy, P.D. (2015). Activation of Tomato bushy stunt virus RNA-dependent RNA polymerase by cellular Heat shock protein 70 is enhanced by phospholipids *in vitro*. J Virol **89(10)**, 5714-5723.

Pogany, J., Stork, J., Li, Z. & Nagy, P.D. (2008). *In vitro* assembly of the Tomato bushy stunt virus replicase requires the host Heat shock protein 70. Proc Natl Acad Sci U S A **105(50)**, 19956-19961.

Prokhnevsky, A.I., Peremyslov, V.V. & Dolja, V.V. (2005). Actin cytoskeleton is involved in targeting of a viral Hsp70 homolog to the cell periphery. J Virol **79(22)**, 14421-14428.

Prokhnevsky, A.I., Peremyslov, V.V., Napuli, A.J. & Dolja, V.V. (2002). Interaction between long-distance transport factor and Hsp70-related movement protein of Beet yellows virus. J Virol **76(21)**, 11003-11011.

Puustinen, P. & Mäkinen, K. (2004). Uridylylation of the Potyvirus VPg by viral replicase NIb correlates with the nucleotide binding capacity of VPg. J Biol Chem **279(37)**, 38103-38110.

Pyott, D. E., Sheehan, E. & Molnar, A. (2016). Engineering of CRISPR/Cas9-mediated potyvirus resistance in transgene-free Arabidopsis plants. Mol Plant Pathol **17(8)**, 1276-1288.

Qin, F., Shinozaki, K. & Yamaguchi-Shinozaki, K. (2011). Achievements and challenges in understanding plant abiotic stress responses and tolerance. Plant Cell Physiol **52(9)**, 1569-1582.

Rajamäki, M.L. & Valkonen, J.P. (2009). Control of nuclear and nucleolar localization of nuclear inclusion protein a of Picorna-like potato virus A in Nicotiana species. Plant Cell **21(8)**, 2485-2502.

Rana, R.M., Iqbal, A., Wattoo, F.M., Khan, M.A. & Zhang, H. (2018). HSP70 mediated stress modulation in plants. Heat Shock Proteins and Stress 281-290.

Rantalainen, K.I., Eskelin, K., Tompa, P. & Mäkinen, K. (2011). Structural flexibility allows the functional diversity of Potyvirus genome-linked protein VPg. J Virol **85(5)**, 2449-2457.

Ray, D., Ghosh, A., Mustafi, S.B. & Raha, S. (2016). Plant stress response: Hsp70 in the spotlight. Heat Shock Proteins and Plants 123-147.

Ré, M.D., Gonzalez, C., Escobar, M.R., Sossi, M.L., Valle, E.M. & Boggio, S.B. (2017). Small heat shock proteins and the postharvest chilling tolerance of tomato fruit. Physiol Plant **159(2)**, 148-160.

Revers, F. & García, J.A. (2015). Chapter three - molecular biology of Potyviruses. Advances in Virus Research 101-199.

Riechmann, J.L., Cervera, M.T. & García, J.A. (1995). Processing of the Plum pox virus polyprotein at the P3−6K1 junction is not required for virus viability. J Gen Virol **76(4)**, 951-956.

Robaglia, C. & Caranta, C. (2006). Translation initiation factors: a weak link in plant RNA virus infection. Trends Plant Sci **11(1)**, 40-45.

Rodamilans, B., Valli, A., Mingot, A., León, D.S., Baulcombe, D., López-Moya, J.J. & García, J.A. (2015). RNA Polymerase Slippage as a Mechanism for the Production of

Frameshift Gene Products in Plant Viruses of the Potyviridae Family. J Virol **89(13)**, 6965-6967.

Rodamilans, B., Valli, A., Mingot, A., San León, D., López-Moya, J.J. & García, J.A. (2018). An atypical RNA silencing suppression strategy provides a snapshot of the evolution of sweet potato-infecting potyviruses. Sci Rep **8(1)**, 15937.

Rodríguez-hernández, A.M., Gosalvez, B., Sempere, R.N., Burgos, L., Aranda, M.A. & Truniger, V. (2012). Melon RNA interference (RNAi) lines silenced for Cm-eIF4E show broad virus resistance. Mol Plant Pathol **13(7)**, 755-763.

Rodriguez, C.M., Freire, M.A., Camilleri, C. & Robaglia, C. (1998). The *Arabidopsis thaliana* cDNAs coding for eIF4E and eIF(iso)4E are not functionally equivalent for yeast complementation and are differentially expressed during plant development. Plant J **13(4)**, 465-473.

Rosenzweig, R., Nillegoda, N.B., Mayer, M.P. & Bukau, B. (2019). The Hsp70 chaperone network. Nat Rev Mol Cell Biol **20(11)**, 665-680.

Roudet-Tavert, G., Michon, T., Walter, J., Delaunay, T., Redondo, E. & Le Gall, O. (2007). Central domain of a potyvirus VPg is involved in the interaction with the host translation initiation factor eIF4E and the viral protein HcPro. J Gen Virol **88(3)**, 1029-1033.

Rowarth, N.M., Dauphinee, A.N., Denbigh, G.L. & Gunawardena, A.H. (2019). Hsp70 plays a role in programmed cell death during the remodelling of leaves of the lace plant (*Aponogeton madagascariensis*). J Exp Bot **71(3)**, 907-918.

Rubio, B., Cosson, P., Caballero, M., Revers, F., Bergelson, J., Roux, F. & Schurdi-Levraud, V. (2019). Genome-wide association study reveals new loci involved in *Arabidopsis thaliana* and Turnip mosaic virus (TuMV) interactions in the field. New Phytol **221(4)**, 2026-2038.

Ruffel, S., Gallois, J.L., Moury, B., Robaglia, C., Palloix, A. & Caranta, C. (2006). Simultaneous mutations in translation initiation factors eIF4E and eIF(iso)4E are required to prevent Pepper veinal mottle virus infection of pepper. J Gen Virol **87(7)**, 2089-2098.

Ruffel, S., Gallois, J.L., Lesage, M.L. & Caranta, C. (2005). The recessive potyvirus resistance gene pot-1 is the tomato orthologue of the pepper pvr2-eIF4E gene. Mol Genet Genomics **274(4)**, 346-353.

Rupp, J.S., Cruz, L., Trick, H.N. & Fellers, J.P. (2019). RNAi-mediated silencing of endogenous wheat genes EIF (Iso) 4E-2 and EIF4G induce resistance to multiple RNA viruses in transgenic wheat. Crop Sci **59(6)**, 2642-2651.

Rusholme, R.L., Higgins, E.E., Walsh, J.A. & Lydiate, D.J. (2007). Genetic control of broad-spectrum resistance to Turnip mosaic virus in *Brassica rapa* (Chinese cabbage). J Gen Virol **88(11)**, 3177-3186.

Salazar-Díaz, K., Aquino-Luna, M., Hernández-Lucero, E., Nieto-Rivera, B., Pulido-Torres, M. A., Jorge-Pérez, J.H., Gavilanes-Ruiz, M. & Dinkova, T.D. (2021). *Arabidopsis thaliana* eIF4E1 and eIF(iso)4E participate in cold response and promote translation of some stress-related mRNAs. Front Plant Sci **12**, 698585.

Sánchez, F., Wang, X., Jenner, C.E., Walsh, J.A. & Ponz, F. (2003). Strains of Turnip mosaic potyvirus as defined by the molecular analysis of the coat protein gene of the virus. Virus Res **94(1)**, 33-43.

Sanfaçon, H. (2015). Plant translation factors and virus resistance. Viruses **7(7)**, 3392-3419.

Sarkar, N.K., Kundnani, P. & Grover, A. (2013). Functional analysis of Hsp70 superfamily proteins of rice (*Oryza sativa*). Cell Stress and Chaperones **18(4)**, 427-437.

Sato, M., Nakahara, K., Yoshii, M., Ishikawa, M. & Uyeda, I. (2005). Selective involvement of members of the eukaryotic initiation factor 4E family in the infection of *Arabidopsis thaliana* by potyviruses. FEBS Lett **579(5)**, 1167-1171.

Saxena, P. & Lomonossoff, G.P. (2014). Virus infection cycle events coupled to RNA replication. Annu Rev Phytopathol **52(1)**, 197-212.

Schaad, M.C., Jensen, P.E. & Carrington, J.C. (1997). Formation of plant RNA virus replication complexes on membranes: role of an endoplasmic reticulum-targeted viral protein. EMBO J **16(13)**, 4049-4059.

Schmitt-Keichinger, C. (2019). Manipulating cellular factors to combat viruses: a case study from the plant eukaryotic translation initiation factors eIF4. Front Microbiol **10**, 17.

Sera, T. (2005). Inhibition of virus DNA replication by artificial zinc finger proteins. J Virol **79(4)**, 2614-2619.

Serva, S. & Nagy, P.D. (2006). Proteomics analysis of the Tombusvirus replicase: Hsp70 molecular chaperone is associated with the replicase and enhances viral RNA replication. J Virol **80(5)**, 2162-2169.

Shan, H., Pasin, F., Tzanetakis, I.E., Simón-Mateo, C., García, J.A. & Rodamilans, B. (2018). Truncation of a P1 leader proteinase facilitates potyvirus replication in a non-permissive host. Mol Plant Pathol **19(6)**, 1504-1510.

Sharma, D. & Masison, D.C. (2009). Hsp70 structure, function, regulation and influence on yeast prions. Protein Pept Lett **16(6)**, 571-581.

Shen, W., Shi, Y., Dai, Z. & Wang, A. (2020). The RNA-dependent RNA polymerase NIb of Potyviruses plays multifunctional, contrasting roles during Viral infection. Viruses **12(1)**, 77.

Shi, L., Jiang, C., He, Q., Habekuß, A., Ordon, F., Luan, H., Shen, H., Liu, J., Feng, Z., Zhang, J. & Yang, P. (2019). Bulked segregant RNA-sequencing (BSR-seq) identified a novel rare allele of eIF4E effective against multiple isolates of BaYMV/BaMMV. Theor Appl Genet **132(6)**, 1777-1788.

Shi, L.X. & Theg, S.M. (2010). A stromal Heat shock protein 70 system functions in protein import into chloroplasts in the moss *Physcomitrella patens*. Plant Cell **22(1)**, 205-220.

Shopan, J., Lv, X., Hu, Z., Zhang, M. & Yang, J. (2020). Eukaryotic translation initiation factors shape RNA viruses resistance in plants. Hortic Plant J **6(2)**, 81-88.

Shopan, J., Mou, H., Zhang, L., Zhang, C., Ma, W., Walsh, J.A., Hu, Z., Yang, J. & Zhang, M. (2017). Eukaryotic translation initiation factor 2B-beta (eIF2Bβ), a new class of plant virus resistance gene. Plant J **90(5)**, 929-940.

Simon, A.E. & Miller, W.A. (2013). 3′ Cap-independent translation enhancers of plant viruses. Annu Rev Microbiol **67(1)**, 21-42.

Singh, M.B., Lohani, N. & Bhalla, P.L. (2021). The role of endoplasmic reticulum stress response in pollen development and heat stress tolerance. Front Plant Sci **12**, 661062.

Singh, R.K., Gupta, V. & Prasad, M. (2019). Plant molecular chaperones: structural organization and their roles in abiotic stress tolerance. Molecular Plant Abiotic Stress 221-239.

Singh, R.K., Jaishankar, J., Muthamilarasan, M., Shweta, S., Dangi, A. & Prasad, M. (2016). Genome-wide analysis of heat shock proteins in C4 model, foxtail millet

identifies potential candidates for crop improvement under abiotic stress. Sci Rep **6(1)**, 32641.

Sorel, M., Garcia, J.A. & German-Retana, S. (2014). The Potyviridae cylindrical inclusion helicase: a key multipartner and multifunctional protein. Mol Plant Microbe Interact **27(3)**, 215-226.

Spetz, C. & Valkonen, J.P. (2004). Potyviral 6K2 protein long-distance movement and symptom-induction functions are independent and host-specific. Mol Plant Microbe Interact **17(5)**, 502-510.

Srivastava, R., Deng, Y., Shah, S., Rao, A.G. & Howell, S.H. (2013). Binding protein is a master regulator of the endoplasmic reticulum stress sensor/transducer bZIP28 in Arabidopsis. Plant Cell **25(4)**, 1416-1429.

Srivastava, R., Li, Z., Russo, G., Tang, J., Bi, R., Muppirala, U., Chudalayandi, S., Severin, A., He, M., Vaitkevicius, S.I., Lawrence-Dill, C.J., Liu, P., Stapleton, A. E., Bassham, D.C., Brandizzi, F. & Howell, S.H. (2018). Response to persistent ER stress in plants: a multiphasic process that transitions cells from prosurvival activities to cell death. Plant Cell **30(6)**, 1220-1242.

Stein, N., Perovic, D., Kumlehn, J., Pellio, B., Stracke, S., Streng, S., Ordon, F. & Graner, A. (2005). The eukaryotic translation initiation factor 4E confers multiallelic recessive Bymovirus resistance in *Hordeum vulgare* (L.). Plant J **42(6)**, 912-922.

Su, P.H. & Li, H.M. (2008). Arabidopsis stromal 70-kD heat shock proteins are essential for plant development and important for thermotolerance of germinating seeds. Plant Physiol **146(3)**, 1231-1241.

Sung, D.Y., Kaplan, F. & Guy, C.L. (2001a). Plant Hsp70 molecular chaperones: protein structure, gene family, expression and function. Physiol Plantarum **113(4)**, 443-451.

Sung, D.Y., Vierling, E. & Guy, C.L. (2001b). Comprehensive expression profile analysis of the Arabidopsis Hsp70 gene family. Plant Physiol **126(2)**, 789-800.

Szittya, G., Silhavy, D., Molnar, A., Havelda, Z., Lovas, A., Lakatos, L., Banfalvi, Z., Burgyan, J. (2003). Low temperature inhibits RNA silencing-mediated defence by the control of siRNA generation. EMBO J **22(3)**, 633-640.

Takakura, Y., Udagawa, H., Shinjo, A. & Koga, K. (2018). Mutation of a *Nicotiana tabacum L.* eukaryotic translation-initiation factor gene reduces susceptibility to a resistance-breaking strain of Potato virus Y. Mol Plant Pathol **19(9)**, 2124-2133.

Tan, R., Wang, L., Hong, N., Wang, G. (2010). Enhanced efficiency of virus eradication following thermotherapy of shoot-tip cultures of pear. Plant Cell Tissue Organ Cult **101(2)**, 229-235.

Tang, Z., Bernards, M. & Wang, A. (2020). Chapter 48 - Identification and manipulation of host factors for the control of plant viruses. Applied Plant Virology 671-695.

Tang, Z., Bernards, M.A. & Wang, A. (2022). Simultaneous determination and subcellular localization of protein–protein interactions in plant cells using bimolecular fluorescence complementation assay. Methods Mol Biol **2400**, 75-85.

Tavert-Roudet, G., Abdul-Razzak, A., Doublet, B., Walter, J., Delaunay, T., German-Retana, S., Michon, T., Le Gall, O. & Candresse, T. (2012). The C terminus of Lettuce mosaic potyvirus cylindrical inclusion helicase interacts with the viral VPg and with lettuce Translation eukaryotic initiation factor 4E. J Gen Virol **93(1)**, 184-193.

Thivierge, K., Cotton, S., Dufresne, P.J., Mathieu, I., Beauchemin, C., Ide, C., Fortin, M.G. & Laliberté, J.F. (2008). Eukaryotic elongation factor 1A interacts with Turnip mosaic

virus RNA-dependent RNA polymerase and VPg-Pro in virus-induced vesicles. Virology **377(1)**, 216-225.

Timperio, A.M., Egidi, M.G. & Zolla, L. (2008). Proteomics applied on plant abiotic stresses: role of heat shock proteins (HSP). J Proteomics **71(4)**, 391-411.

Ueki, S. & Citovsky, V. (2011). To gate, or not to gate: regulatory mechanisms for intercellular protein transport and virus movement in plants. Mol Plant **4(5)**, 782-793.

Ul Haq, S., Khan, A., Ali, M., Khattak, A.M., Gai, W.X., Zhang, H.X., Wei, A.M. & Gong, Z.H. (2019). Heat shock proteins: dynamic biomolecules to counter plant biotic and abiotic stresses. Int J Mol Sci **20(21)**, 5321.

Ülker, B. & Weisshaar, B. (2011). Resources for reverse genetics approaches in *Arabidopsis thaliana*. Genetics and Genomics of the Brassicaceae 527-560.

Usman, M.G., Rafii, M.Y., Martini, M.Y., Yusuff, O.A., Ismail, M.R. & Miah, G. (2017). Molecular analysis of Hsp70 mechanisms in plants and their function in response to stress. Biotechnol Genet Eng Rev **33(1)**, 26-39.

Valente, M.A., Faria, J.A., Soares-Ramos, J.R., Reis, P.A., Pinheiro, G.L., Piovesan, N.D., Morais, A.T., Menezes, C.C., Cano, M.A.O., Fietto, L.G., Loureiro, M.E., Aragão, F.J. & Fontes, E.P. (2008). The ER luminal binding protein (BiP) mediates an increase in drought tolerance in soybean and delays drought-induced leaf senescence in soybean and tobacco. J Exp Bot **60(2)**, 533-546.

Valli, A.A., Gallo, A., Rodamilans, B., López-Moya, J.J. & García, J.A. (2018). The HCPro from the Potyviridae family: an enviable multitasking Helper Component that every virus would like to have. Mol Plant Pathol **19(3)**, 744-763.

Verchot, J. & Carrington, J.C. (1995). Evidence that the potyvirus P1 proteinase functions in trans as an accessory factor for genome amplification. J Virol **69(6)**, 3668-3674.

Verchot, J., Koonin, E.V. & Carrington, J.C. (1991). The 35-kDa protein from the N-terminus of the potyviral polyprotein functions as a third virus-encoded proteinase. Virology **185(2)**, 527-535.

Verchot, J. & Pajerowska-Mukhtar, K.M. (2021). UPR signaling at the nexus of plant viral, bacterial, and fungal defenses. Curr Opin Virol **47**, 9-17.

Vijayapalani, P., Maeshima, M., Nagasaki-Takekuchi, N. & Miller, W.A. (2012). Interaction of the trans-frame Potyvirus protein P3N-PIPO with host protein PCaP1 facilitates potyvirus movement. PLoS Pathog **8(4)**, e1002639.

Virdi, A.S., Singh, S. & Singh, P. (2015). Abiotic stress responses in plants: roles of calmodulin-regulated proteins. Front Plant Sci **6**, 6809.

Volkov, R.A., Panchuk, I.I., Mullineaux, P.M. & Schöffl, F. (2006). Heat stress-induced H_2O_2 is required for effective expression of heat shock genes in Arabidopsis. Plant Mol Biol **61(4)**, 733-746.

Voloudakis, A.E., Mukherjee, S.K. & Roy, A. (2021). Novel technologies for transgenic management for plant virus resistance. Genome Engineering for Crop Improvement 163-191.

Volpon, L., Osborne, M.J. & Borden, K.L.B. (2019). Biochemical and structural insights into the eukaryotic translation initiation factor eIF4E. Curr Protein Pept Sci **20(6)**, 525-535.

Wahyu Indra Duwi, F., Lee, S.Y. & Lee, K.O. (2013). The unfolded protein response in plants: A fundamental adaptive cellular response to internal and external stresses. J Proteomics **93**, 356-368.

Wakasa, Y., Yasuda, H., Oono, Y., Kawakatsu, T., Hirose, S., Takahashi, H., Hayashi, S., Yang, L. & Takaiwa, F. (2011). Expression of ER quality control-related genes in response to changes in BiP1 levels in developing rice endosperm. Plant J **65(5)**, 675-689.

Walsh, J.A. & Jenner, C.E. (2002). Turnip mosaic virus and the quest for durable resistance. Mol Plant Pathol **3(5)**, 289-300.

Walter, P. & Ron, D. (2011). The unfolded protein response: from stress pathway to homeostatic regulation. Science **334(6059)**, 1081-1086.

Wang, A. (2015). Dissecting the molecular network of virus-plant interactions: the complex roles of host factors. Annu Rev Phytopathol **53(1)**, 45-66.

Wang, A. (2021). Cell-to-cell movement of plant viruses via plasmodesmata: a current perspective on potyviruses. Curr Opin Virol **48**, 10-16.

Wang, A. & Krishnaswamy, S. (2012). Eukaryotic translation initiation factor 4E-mediated recessive resistance to plant viruses and its utility in crop improvement. Mol Plant Pathol **13(7)**, 795-803.

Wang, H., Niu, H., Zhai, Y. & Lu, M. (2017). Characterization of BiP genes from pepper (*Capsicum annuum L.*) and the role of CaBiP1 in response to endoplasmic reticulum and multiple abiotic stresses. Front Plant Sci **8**, 1122.

Wang, J., Pareja, K.A., Kaiser, C.A. & Sevier, C.S. (2014). Redox signaling via the molecular chaperone BiP protects cells against endoplasmic reticulum-derived oxidative stress. eLife **3**, e03496.

Wang, R.Y. & Nagy, P.D. (2008). Tomato bushy stunt virus co-opts the RNA-binding function of a host metabolic enzyme for viral genomic RNA synthesis. Cell Host Microbe **3(3)**, 178-187.

Wang, R.Y., Stork, J. & Nagy, P.D. (2009a). A key role for Heat shock protein 70 in the localization and insertion of Tombusvirus replication proteins to intracellular membranes. J Virol **83(7)**, 3276-3287.

Wang, Y., Bao, Z., Zhu, Y., Hua, J. (2009b). Analysis of temperature modulation of plant defense against biotrophic microbes. Mol Plant Microbe Interact **22(5)**, 498-506.

Wang, W., Vinocur, B., Shoseyov, O. & Altman, A. (2004). Role of plant heat-shock proteins and molecular chaperones in the abiotic stress response. Trends Plant Sci **9(5)**, 244-252.

Wang, X., Cao, X., Liu, M., Zhang, R., Zhang, X., Gao, Z., Zhao, X., Xu, K., Li, D. & Zhang, Y. (2018). Hsc70-2 is required for Beet black scorch virus infection through interaction with replication and capsid proteins. Sci Rep **8(1)**, 1-15.

Wang, X., Kohalmi, S.E., Svircev, A., Wang, A., Sanfaçon, H. & Tian, L. (2013). Silencing of the host factor eIF(iso)4E gene confers Plum pox virus resistance in plum. PLOS ONE **8(1)**, e50627.

Wang, X., Ullah, Z. & Grumet, R. (2000). Interaction between Zucchini yellow mosaic potyvirus RNA-dependent RNA polymerase and host Poly-(A) binding protein. Virology **275(2)**, 433-443.

Wang, Z., Parisien, M., Scheets, K. & Miller, W.A. (2011). The Cap-binding translation initiation factor, eIF4E, binds a pseudoknot in a viral Cap-independent translation element. Structure **19(6)**, 868-880.

Wei, T., Huang, T.S., McNeil, J., Laliberté, J.F., Hong, J., Nelson, R.S. & Wang, A. (2010a). Sequential recruitment of the endoplasmic reticulum and chloroplasts for plant potyvirus replication. J Virol **84(2)**, 799-809.

Wei, T. & Wang, A. (2008). Biogenesis of cytoplasmic membranous vesicles for plant potyvirus replication occurs at endoplasmic reticulum exit sites in a COPI- and COPII-dependent manner. J Virol **82(24)**, 12252-12264.

Wei, T., Zhang, C., Hong, J., Xiong, R., Kasschau, K.D., Zhou, X., Carrington, J.C. & Wang, A. (2010b). Formation of complexes at plasmodesmata for potyvirus intercellular movement is mediated by the viral protein P3N-PIPO. PLoS Pathog **6(6)**, e1000962.

Wei, T., Zhang, C., Hou, X., Sanfaçon, H. & Wang, A. (2013). The SNARE protein Syp71 is essential for Turnip mosaic virus infection by mediating fusion of virus-induced vesicles with chloroplasts. PLoS Pathog **9(5)**, e1003378.

Wek, R.C., Jiang, H.Y. & Anthony, T.G. (2006). Coping with stress: eIF2 kinases and translational control. Biochem Soc Trans **34(1)**, 7-11.

Wen, R.H. & Hajimorad, M.R. (2010). Mutational analysis of the putative pipo of soybean mosaic virus suggests disruption of PIPO protein impedes movement. Virology **400(1)**, 1-7.

White, K.A. (2015). The polymerase slips and PIPO exists. EMBO Rep **16(8)**, 885-886.

Whitham, S.A., Quan, S., Chang, H.S., Cooper, B., Estes, B., Zhu, T., Wang, X. & Hou, Y.M. (2003). Diverse RNA viruses elicit the expression of common sets of genes in susceptible *Arabidopsis thaliana* plants. Plant J **33(2)**, 271-283.

Williams, B., Verchot, J. & Dickman, M.B. (2014). When supply does not meet demand-ER stress and plant programmed cell death. Front Plant Sci **5**, 211.

Win, J., Kamoun, S. & Jones, A.M. (2011). Purification of effector–target protein complexes via transient expression in *Nicotiana benthamiana*. Methods Mol Biol **712**, 181-194.

Woo, J. W., Kim, J., Kwon, S.I., Corvalán, C., Cho, S. W., Kim, H., Kim, S.G., Kim, S.T., Choe, S. & Kim, J.S. (2015). DNA-free genome editing in plants with preassembled CRISPR-Cas9 ribonucleoproteins. Nat Biotechnol **33(11)**, 1162-1164.

Wu, G., Cui, X., Chen, H., Renaud, J.B., Yu, K., Chen, X. & Wang, A. (2018). Dynamin-like proteins of endocytosis in plants are coopted by potyviruses to enhance virus infection. J Virol **92(23)**, e01320-18.

Wu, G., Cui, X., Dai, Z., He, R., Li, Y., Yu, K., Bernards, M., Chen, X. & Wang, A. (2020). A plant RNA virus hijacks endocytic proteins to establish its infection in plants. Plant J **101(2)**, 384-400.

Xiong, R., Pajak, A., Wang, A., Yoshikawa, N., Marsolais, F. & Todd, C.D. (2019). Agrobacterium-mediated inoculation of asymptomatic Apple latent spherical virus as gene silencing vector in pea (*Pisum sativum L.*). Legume Sci **1(1)**, e14.

Yamamoto, H., Unbehaun, A. & Spahn, C.M.T. (2017). Ribosomal chamber music: toward an understanding of IRES mechanisms. Trends Biochem Sci **42(8)**, 655-668.

Yang, C., Guo, R., Jie, F., Nettleton, D., Peng, J., Carr, T., Yeakley, J.M., Fan, J.B. & Whitham, S.A. (2007). Spatial analysis of *Arabidopsis thaliana* gene expression in response to Turnip mosaic virus infection. Mol Plant Microbe Interact **20(4)**, 358-370.

Yang, J., Zhang, F., Cai, N.J., Wu, N., Chen, X., Li, J., Meng, X.F., Zhu, T.Q., Chen, J.P. & Zhang, H.M. (2017). A furoviral replicase recruits host HSP70 to membranes for viral RNA replication. Sci Rep **7(1)**, 1-15.

Yang, P., Perovic, D., Habekuß, A., Zhou, R., Graner, A., Ordon, F. & Stein, N. (2013). Gene-based high-density mapping of the gene rym7 conferring resistance to Barley mild mosaic virus (BaMMV). Mol Breeding **32(1)**, 27-37.

Yang, X., Li, Y. & Wang, A. (2021). Research advances in potyviruses: from the laboratory bench to the field. Annu Rev Phytopathol **59(1)**, 1-29.

Ye, C., Dickman, M.B., Whitham, S.A., Payton, M. & Verchot, J. (2011). The unfolded protein response is triggered by a plant viral movement protein. Plant Physiol **156(2)**, 741-755.

Yeam, I., Cavatorta, J.R., Ripoll, D.R., Kang, B.C. & Jahn, M.M. (2007). Functional dissection of naturally occurring amino acid substitutions in eIF4E that confers recessive potyvirus resistance in plants. Plant Cell **19(9)**, 2913-2928.

Yoon, Y.J., Venkatesh, J., Lee, J.H., Kim, J., Lee, H.E., Kim, D.S. & Kang, B.C. (2020). Genome editing of eIF4E1 in tomato confers resistance to Pepper mottle virus. Front Plant Sci **11**, 1098.

Yoshida, T., Ohama, N., Nakajima, J., Kidokoro, S., Mizoi, J., Nakashima, K., Maruyama, K., Kim, J.M., Seki, M., Todaka, D., Osakabe, Y., Sakuma, Y., Schöffl, F., Shinozaki, K. & Yamaguchi-Shinozaki, K. (2011). Arabidopsis HsfA1 transcription factors function as the main positive regulators in heat shock-responsive gene expression. Mol Genet Genomics **286(5)**, 321-332.

Yoshii, M., Nishikiori, M., Tomita, K., Yoshioka, N., Kozuka, R., Naito, S. & Ishikawa, M. (2004). The Arabidopsis cucumovirus multiplication 1 and 2 loci encode translation initiation factors 4E and 4G. J Virol **78(12)**, 6102-6111.

Yoshii, M., Yoshioka, N., Ishikawa, M. & Naito, S. (1998). Isolation of an *Arabidopsis thaliana* mutant in which accumulation of Cucumber mosaic virus coat protein is delayed. Plant J **13(2)**, 211-219.

Zamora, M., Méndez-López, E., Agirrezabala, X., Cuesta, R., Lavín, J.L., Sánchez-Pina, M.A., Aranda, M. A. & Valle, M. (2017). Potyvirus virion structure shows conserved protein fold and RNA binding site in ssRNA viruses. Sci Adv **3(9)**, eaao2182.

Zhang, L., Chen, H., Brandizzi, F., Verchot, J. & Wang, A. (2015). The UPR branch IRE1-bZIP60 in plants plays an essential role in viral infection and is complementary to the only UPR pathway in yeast. PLoS Genet **11(4)**, e1005164.

Zhang, L. & Wang, A. (2012). Virus-induced ER stress and the unfolded protein response. Front Plant Sci **3**. 293.

Zhang, L. & Wang, A. (2016). ER Stress, UPR and virus infections in plants. Current Research Topics in Plant Virology 173-195.

Zhang, X., Henriques, R., Lin, S.S., Niu, Q.W. & Chua, N.H. (2006). Agrobacterium-mediated transformation of *Arabidopsis thaliana* using the floral dip method. Nat Protoc **1(2)**, 641-646.

Zhao, L., Li, W., Wang, B., Gao, Y., Sui, X., Liu, Y., Chen, X., Yao, X., Jiao, F. & Song, Z. (2020a). Development of a PVY resistant flue-cured tobacco line via EMS mutagenesis of eIF4E. Agronomy **10(1)**, 36.

Zhao, Y., Yang, X., Zhou, G. & Zhang, T. (2020b). Engineering plant virus resistance: from RNA silencing to genome editing strategies. Plant Biotechnol J **18(2)**, 328-336.

Zhu, H., Hu, F., Wang, R., Zhou, X., Sze, S.H., Liou, Lisa W., Barefoot, A., Dickman, M. & Zhang, X. (2011). Arabidopsis Argonaute10 specifically sequesters miR166/165 to regulate shoot apical meristem development. Cell **145(2)**, 242-256.

Zou, J., Guo, Y., Guettouche, T., Smith, D.F. & Voellmy, R. (1998). Repression of Heat shock transcription factor HSF1 activation by HSP90 (HSP90 Complex) that forms a stress-sensitive complex with HSF1. Cell **94(4)**, 471-480.

Supplementary Tables

Table S1. Primer sequence for amplification of gene coding sequences for Gateway cloning

Primer name	Primer sequence
eIF(iso)4E-Gate-F	<u>GGGGACAAGTTTGTACAAAAAAGCAGGCTTC</u>ATGGCGACCGATGATGTGAACG
eIF(iso)4E-Gate-R	<u>GGGGACCACTTTGTACAAGAAAGCTGGGTC</u>GACAGTGAACCGGCTTCTTC
CP-Gate-F	<u>GGGGACAAGTTTGTACAAAAAAGCAGGCTTC</u>ATGGCAGGTGAAACGCTTGATGCA
CP-Gate-R	<u>GGGGACCACTTTGTACAAGAAAGCTGGGTC</u>CAACCCCTGAACGCCCAGTA
NIb-Gate-F	<u>GGGGACAAGTTTGTACAAAAAAGCAGGCTTC</u>ATGACCCAGCAGAATCGGTGGATG
NIb-Gate-R	<u>GGGGACCACTTTGTACAAGAAAGCTGGGTC</u>CTGGTGATAAACACAAGCCTCA
Hsp70-1-Gate-F	<u>GGGGACAAGTTTGTACAAAAAAGCAGGCTTC</u>ATGTCGGGTAAAGGAGAAGGACC
Hsp70-1-Gate-R	<u>GGGGACCACTTTGTACAAGAAAGCTGGGTC</u>GTCGACCTCCTCGATCTTAGGT
Hsp70-2-Gate-F	<u>GGGGACAAGTTTGTACAAAAAAGCAGGCTTC</u>ATGGCTGGTAAAGGAGAAGGTCC
Hsp70-2-Gate-R	<u>GGGGACCACTTTGTACAAGAAAGCTGGGTC</u>GTCGACTTCCTCGATCTTGGGA
HSP70-8-Gate-F	<u>GGGGACAAGTTTGTACAAAAAAGCAGGCTTC</u>ATGGCAGAAGCAGCATACACAG
HSP70-8-Gate-R	<u>GGGGACCACTTTGTACAAGAAAGCTGGGTC</u>CATCTTTCTCTGAAGAGTAATCAAATC
HSP70-11/12-Gate-F	<u>GGGGACAAGTTTGTACAAAAAAGCAGGCTTC</u>ATGGCTCGCTCGTTTGGAGC

HSP70-11/12-Gate-end-R	<u>GGGGACCACTTTGTACAAGAAAGCTGGGTC</u>**CTA**GAGCTCATCGTGAGACTCATCTTC
Hsp70-1-HDEL-Gate-R	<u>GGGGACCACTTTGTACAAGAAAGCTGGGTC</u>**CTA***AAGCTCATCATG*GTCGACCTCCTCGATCTTAGGT
Hsp70-2-HDEL-Gate-R	<u>GGGGACCACTTTGTACAAGAAAGCTGGGTC</u>**CTA***AAGCTCATCATG*GTCGACTTCCTCGATCTTGGGA
HSP70-8-HDEL-Gate-R	<u>GGGGACCACTTTGTACAAGAAAGCTGGGTC</u>**CTA***AAGCTCATCATG*CATCTTTCTCTGAAGAGTAATCAAATC
11/12-Gate-ΔHDEL-end-R	<u>GGGGACCACTTTGTACAAGAAAGCTGGGTC</u>**CTA**AGACTCATCTTCCTCCTCAGTC

Note: Underlined: attB sequences; Black: stop codon added to make sure HDEL ER localization signal at the C-terminal; italic: HDEL sequence added.

Table S2. Primer sequence for amplification of gene coding sequences with added restriction enzyme sites

Primer name	Primer sequence
PBTPPR-eIFiso4E-sfiI-F	GC<u>GGCC</u>ATTAC<u>GGCC</u>ATGGCGACCGATGATGTGAACG
PBT3-eIFiso4E-sfiI-R	GC<u>GGCC</u>GAGGC<u>GGCC</u>*TT*GACAGTGAACCGGCTTCTTC
PPR3N-eIFiso4E-sfiI-R	GC<u>GGCC</u>GAGGC<u>GGCC</u>G**TCA**GACAGTGAACCGGCTTCTTC
PBTPPR-CP-sfiI-F	GC<u>GGCC</u>ATTAC<u>GGCC</u>ATGGCAGGTGAAACGCTTGATGCA
PBT3-CP-sfiI-R	GC<u>GGCC</u>GAGGC<u>GGCC</u>*TT*CAACCCCTGAACGCCCAGTA
PPR3N-CP-sfiI-R	GC<u>GGCC</u>GAGGC<u>GGCC</u>G**TTA**CAACCCCTGAACGCCCAGTA
PBTPPR-NIB-sfiI-F	GC<u>GGCC</u>ATTAC<u>GGCC</u>ATGACCCAGCAGAATCGGTGGATG
PBT3-NIB-sfiI-R	GC<u>GGCC</u>GAGGC<u>GGCC</u>*TT*CTGGTGATAAACACAAGCCTCA
PPR3N-NIB-sfiI-R	GC<u>GGCC</u>GAGGC<u>GGCC</u>G**TTA**CTGGTGATAAACACAAGCCTCA
PBTPPR-Hsp70-1-sfiI-F	GC<u>GGCC</u>ATTAC<u>GGCC</u>ATGTCGGGTAAAGGAGAAGGACC
PBT3-Hsp70-1-sfiI-R	GC<u>GGCC</u>GAGGC<u>GGCC</u>*TT*GTCGACCTCCTCGATCTTAGGT
PPR3N-Hsp70-1-sfiI-R	GC<u>GGCC</u>GAGGC<u>GGCC</u>G**TTA**GTCGACCTCCTCGATCTTAGGT
PBTPPR-Hsp70-2-sfiI-F	GC<u>GGCC</u>ATTAC<u>GGCC</u>ATGGCTGGTAAAGGAGAAGGTCC
PBT3-Hsp70-2-sfiI-R	GC<u>GGCC</u>GAGGC<u>GGCC</u>*TT*GTCGACTTCCTCGATCTTGGGA
PPR3N-Hsp70-2-sfiI-R	GC<u>GGCC</u>GAGGC<u>GGCC</u>G**TTA**GTCGACTTCCTCGATCTTGGGA
PBTPPR-Hsp70-8-sfiI-F	GC<u>GGCC</u>ATTAC<u>GGCC</u>ATGGCAGAAGCAGCATACACAG
PBT3-Hsp70-8-sfiI-R	GC<u>GGCC</u>GAGGC<u>GGCC</u>*TT*CATCTTTCTCTGAAGAGTAATCAAATC
PPR3N-Hsp70-8-sfiI-R	GC<u>GGCC</u>GAGGC<u>GGCC</u>G**TTA**CATCTTTCTCTGAAGAGTAATCAAATC
PBTPPR-Hsp70-1112-sfiI-F	GC<u>GGCC</u>ATTAC<u>GGCC</u>ATGGCTCGCTCGTTTGGAGC
PBT3-Hsp70-11/12-sfiI-R	GC<u>GGCC</u>GAGGC<u>GGCC</u>*TT*GAGCTCATCGTGAGACTCATCTTC
PPR3N-11/12-sfiI-end-R	GC<u>GGCC</u>GAGGC<u>GGCC</u>G**CTA**GAGCTCATCGTGAGACTCATCTTC

Underlined: SfiI restriction site sequences; Black: stop codon; italic: extra sequence to maintain the coding frame.

Table S3. qPCR primers to quantify mRNA levels of HSP70s in *A. thaliana* lines

HSP70-1	qPCR-F	AGGGTCGTCTCTCCAAGGAT
(AT5G02500)	qPCR-R	TCCTCGATCTTCTTCTTGTCTGC
HSP70-2	qPCR-F	AGAAGAAGGTCGAGGCCAAG
(AT5G02490)	qPCR-R	AACTCGTCAGCTTCACCCAA
HSP70-3	qPCR-F	CGGAGGATGAGGAGCACAAG
(AT3G09440)	qPCR-R	ACTCTGCTAGCTGATTCGCTT
HSP70-4	qPCR-F	CGACGCCAATGGTATCCTGA
(AT3G12580)	qPCR-R	CGAGAGCGTTCTTTGCATCC
HSP70-6	qPCR-F	GCTTTTCTCAGAATGGGCACC
(AT4G24280)	qPCR-R	CACAACAGAAGGCGTTGTCC
HSP70-7	qPCR-F	CGCCCAAATTCACATCCTCG
(AT5G49910)	qPCR-R	CATACGAAGGAAGGCGGAGG
HSP70-8	qPCR-F	TCGCCCTTGGTATCGACATT
(AT2G32120)	qPCR-R	ATGTGCGAGCTGGTTGCTAA
HSP70-11	qPCR-F	GATGGTGAAGGAGGCAGAGG
(AT5G28540)	qPCR-R	CAAAGCCTCTTTCGTCGCTG
HSP70-12	qPCR-F	ACGAAAGAGGCCTTGGAGTG
(AT5G42020)	qPCR-R	GATTCTCCTCCTGCACCTGG
HSP70-13	qPCR-F	GGTTTTTCTGACTGCTTTGATGTC
(AT1G09080)	qPCR-R	AAATGCAACCCAAGATGGTGT
Actin8	qPCR-F	CTCAGGTATTGCAGACCGTATGAG
(AT1G49240)	qPCR-R	CTGGACCTGCTTCATCATACTCTG

Supplementary Figures
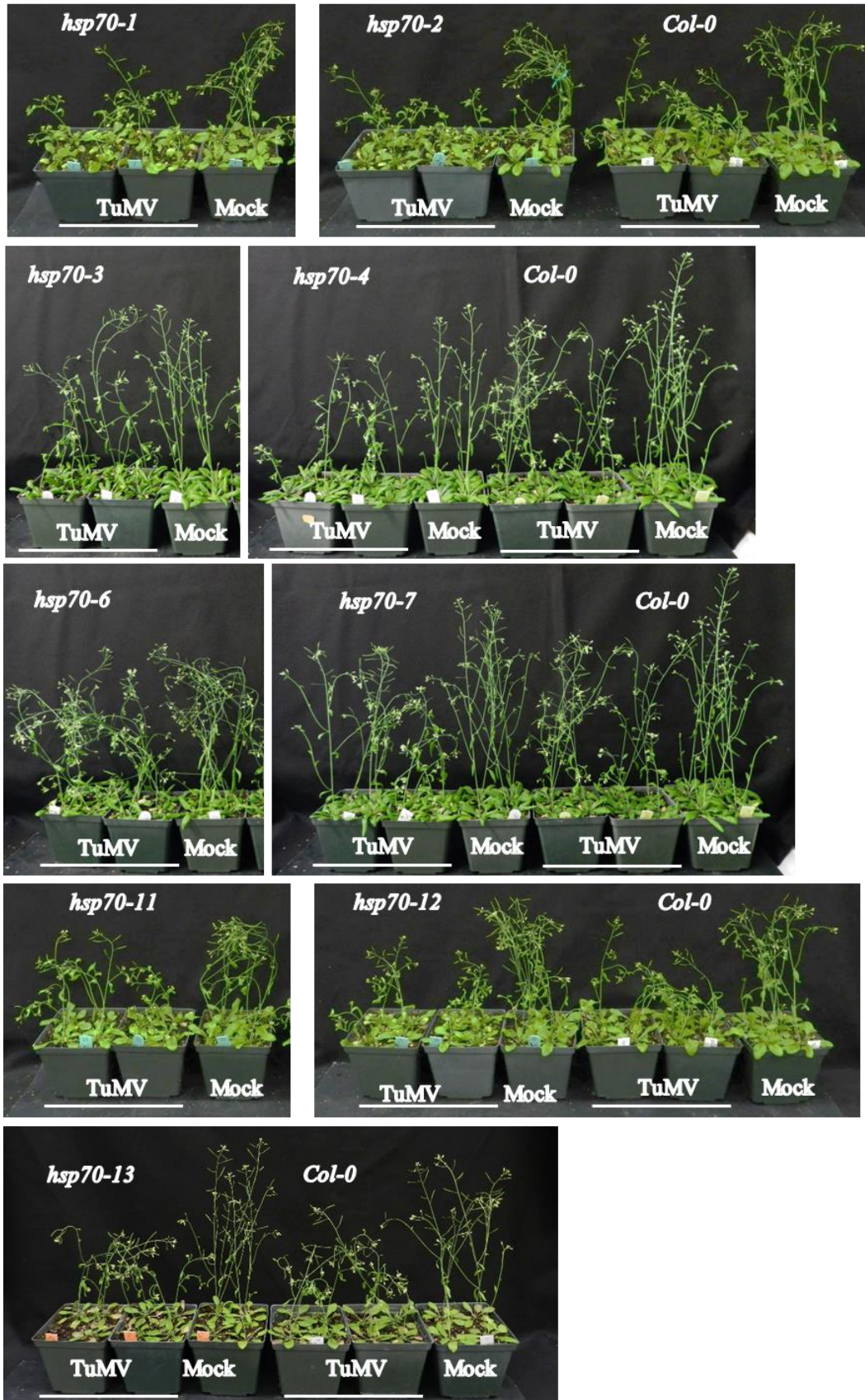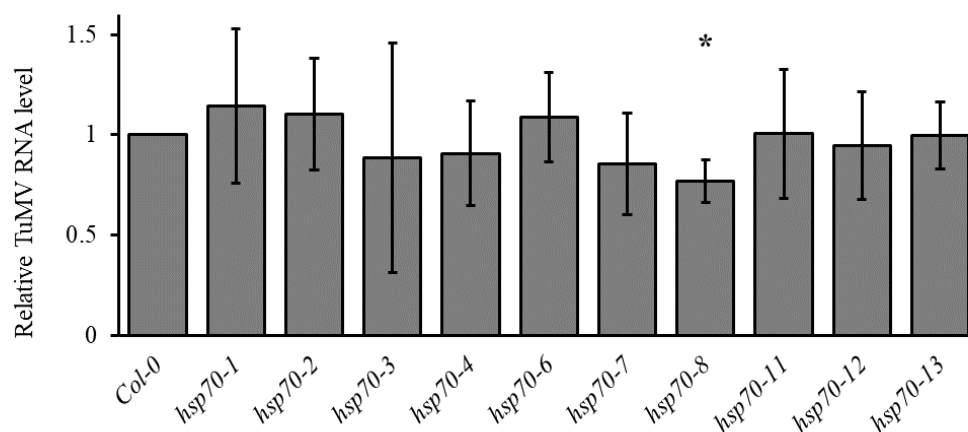
Figure S1: TuMV infection symptoms and TuMV RNA levels in some HSP70 single knockout/knockdown lines
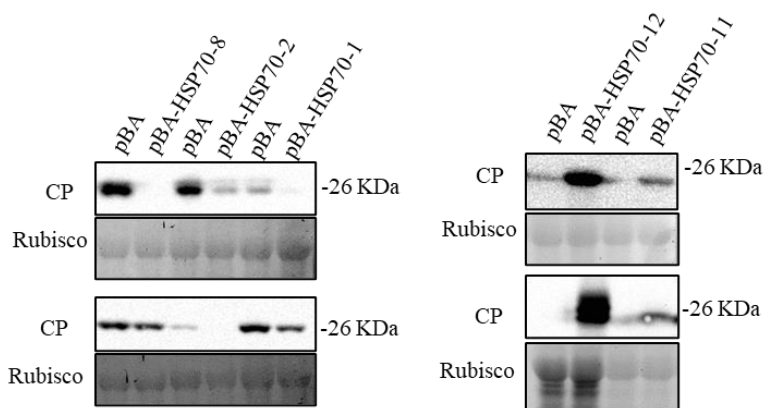
Figure S2: TuMV local infection is affected in *N. benthamiana* transiently expressing HSP70s
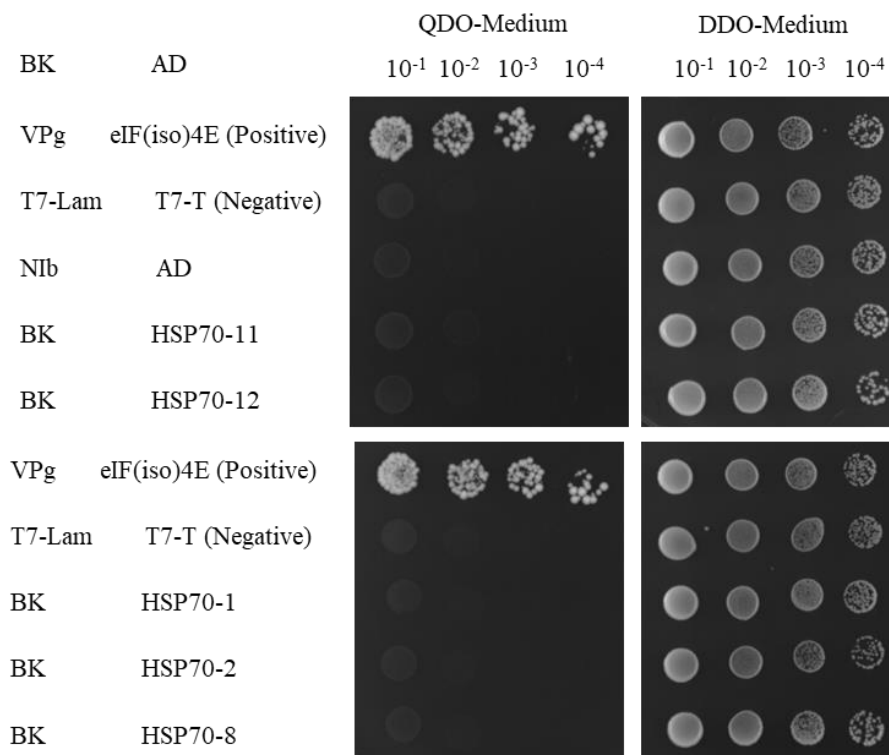
Figure S3: Absence of autoactivation of BK-NIb and AD-HSP70s in the Matchmaker Gold Yeast Two-Hybrid System
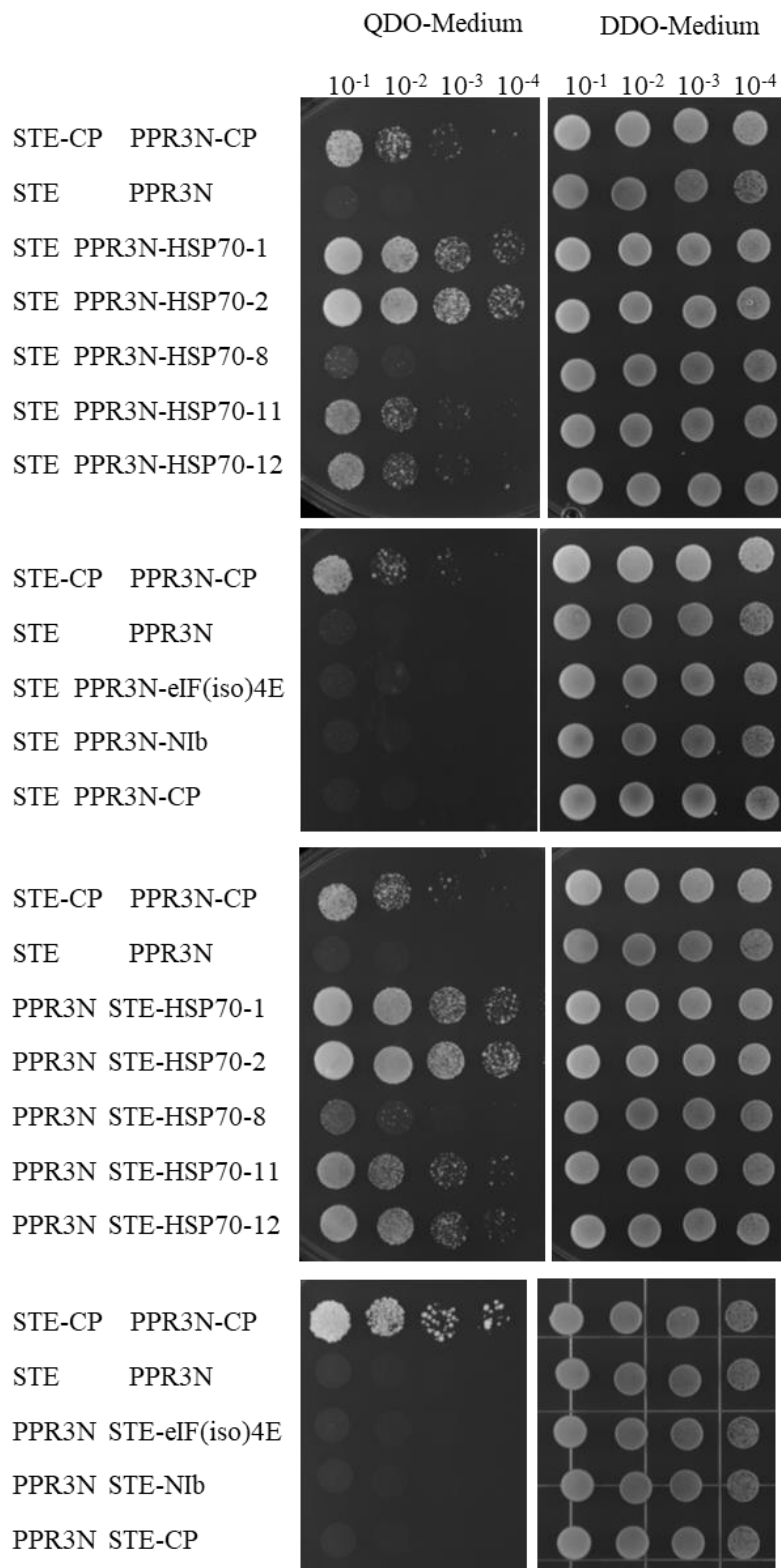
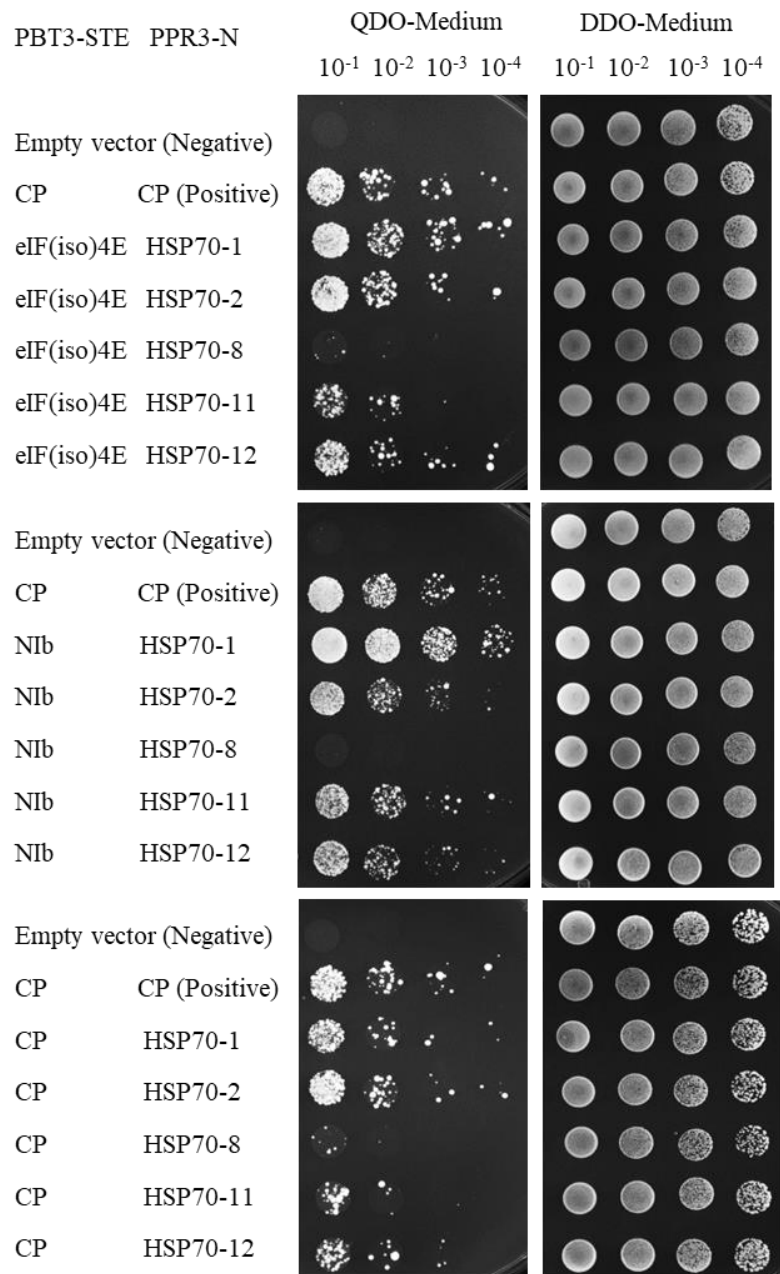**Figure S4: STE-HSP70s and PPR3N-HSP70 cause autoactivation of reporter genes in the Split-Ubiquitin Based Membrane Yeast Two-Hybrid system**

Figure S5: Positive signals could be detected between HSP70s and proteins of interest in the Split-Ubiquitin Based Membrane Yeast Two-Hybrid system
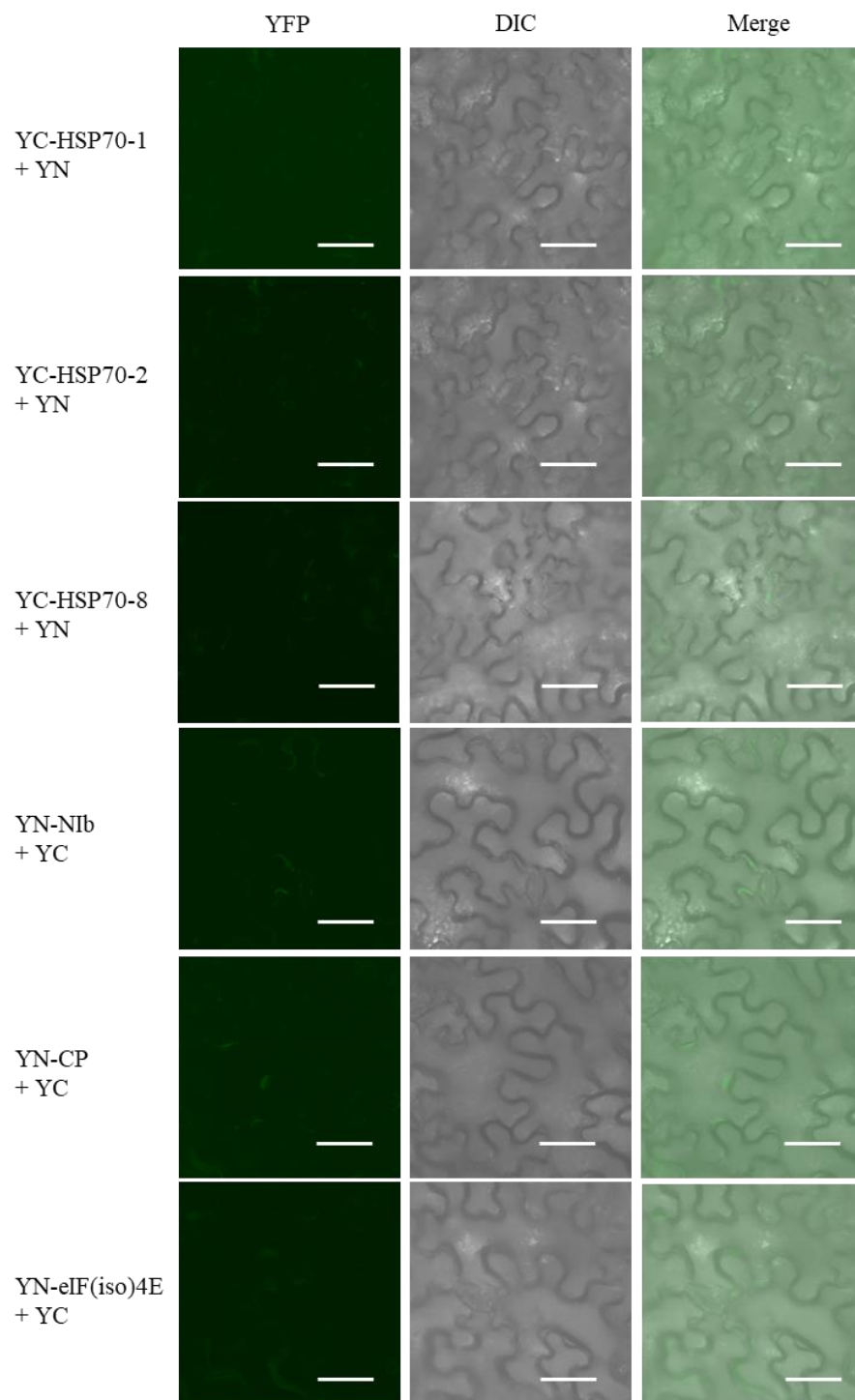
Figure S6: Negative controls for BiFC
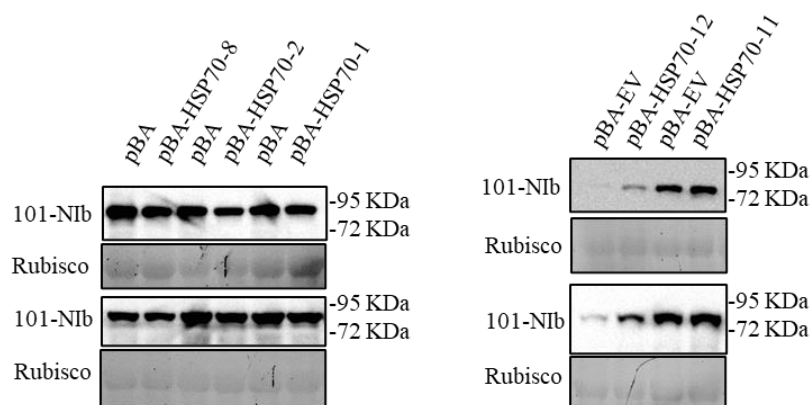
Figure S7: Repeats for HSP70s alter the protein level of transiently co-expressed NIb
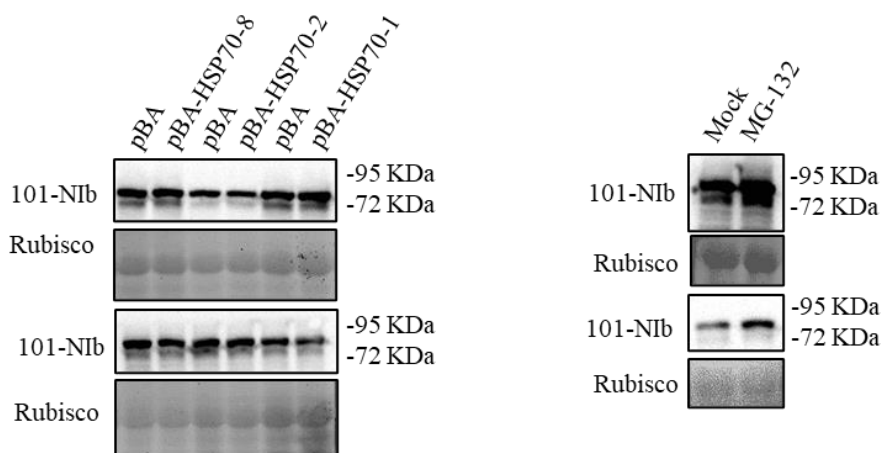
Figure S8: Repeats for MG-132 inhibiting NIb degradation and HSP70-1, HSP70-2, and HSP70-8's promoting of NIb degradation
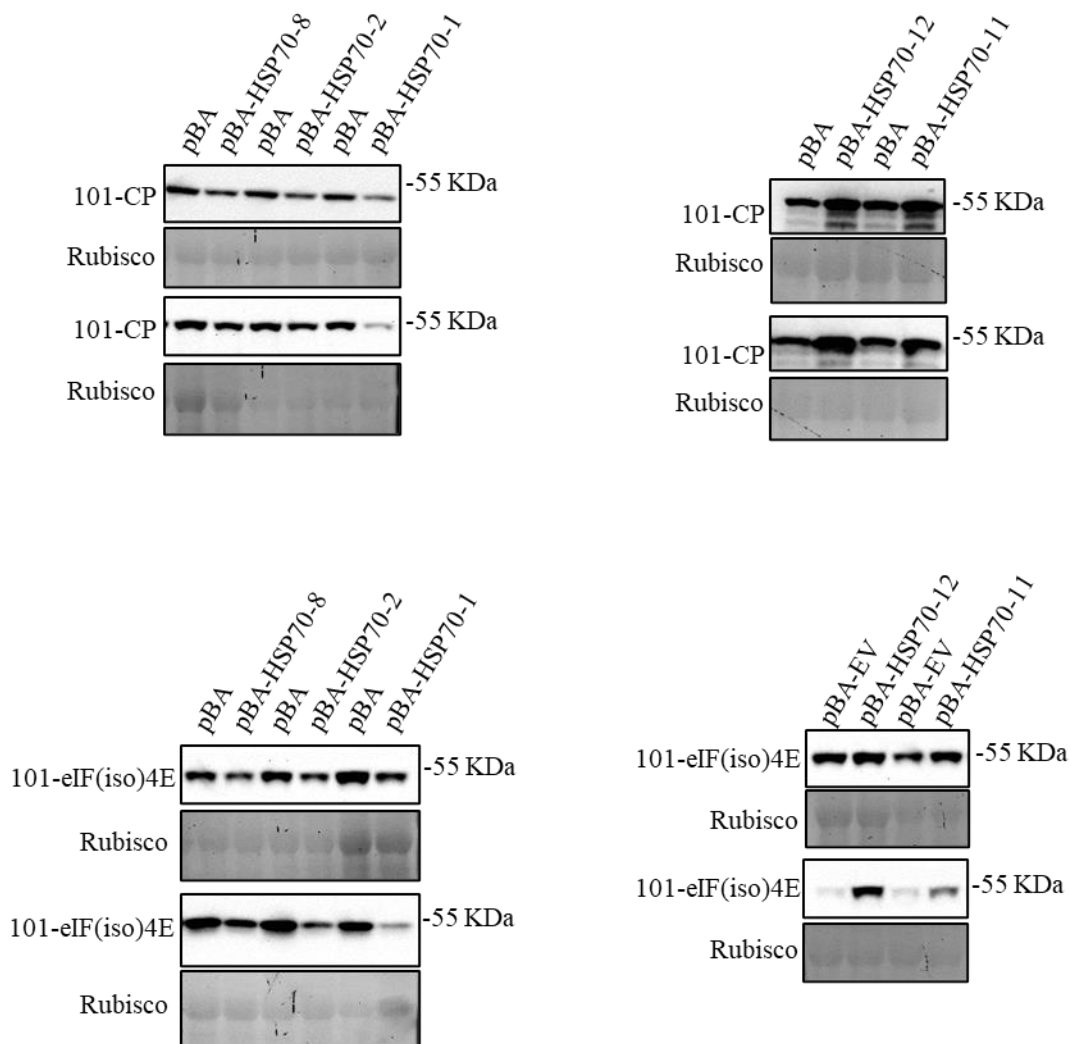
Figure S9: Repeats for HSP70s alter the protein level of transiently co-expressed CP and eIF(iso)4E
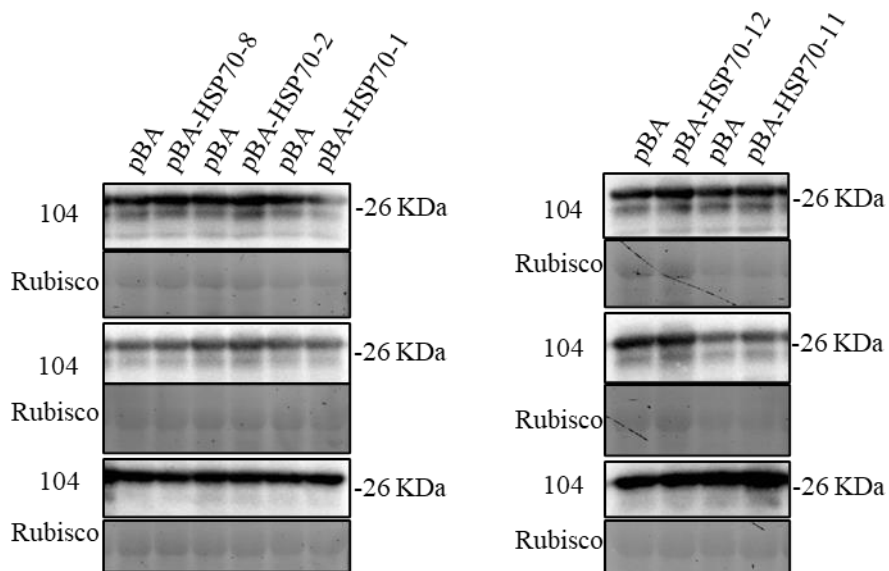
Figure S10: HSP70s do not alter the protein level of YFP tag in the 104 vector
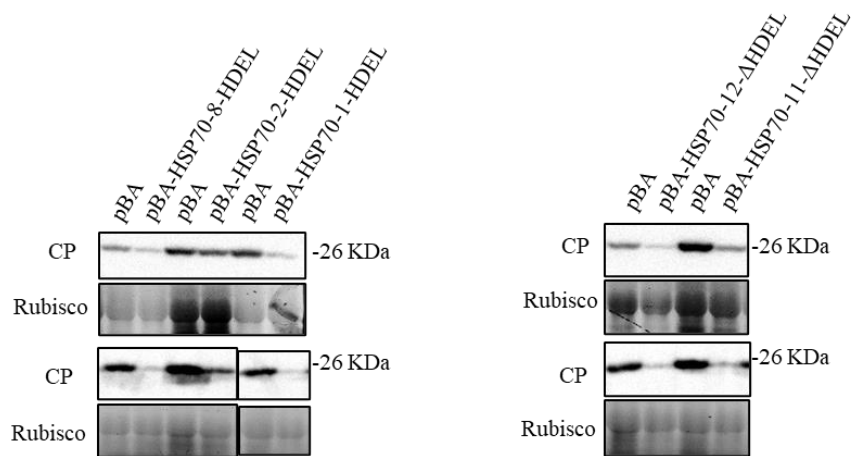

Figure S11: Repeats for TuMV local infection is affected in *N. benthamiana* transiently expressing HSP70s with altered localization signals
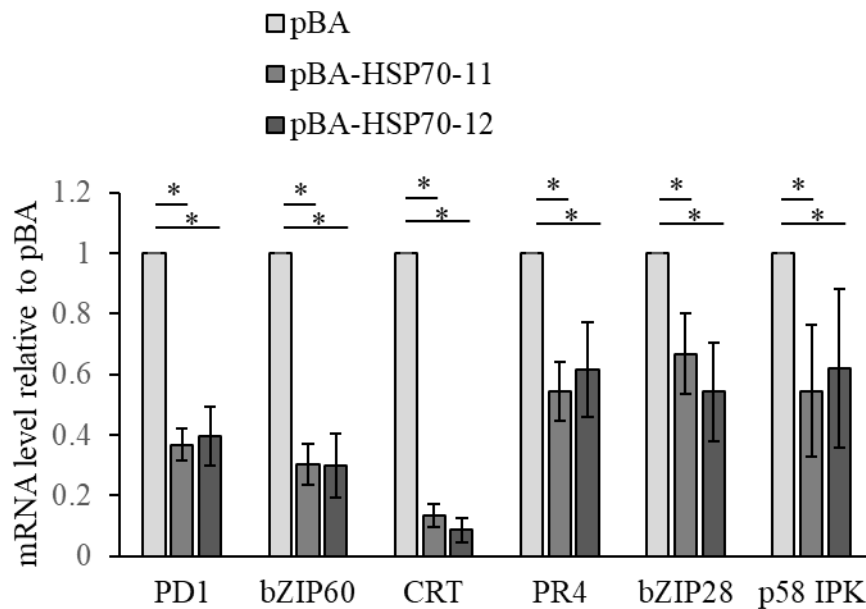
Figure S12: Expression level of UPR stress markers is reduced in *N. benthamiana* transiently expressing HSP70-11 and HSP70-12

Data were collected from five independent experiments. Error bars represent standard deviation (n=5), *P<0.05, student's t test, two-tailed, unpaired.
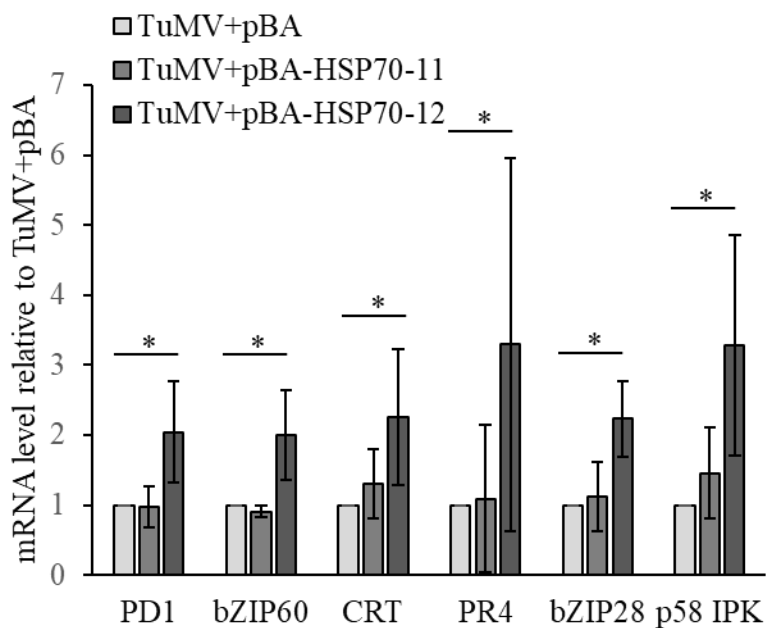
Figure S13: Expression level of UPR stress markers in TuMV-infected *N. benthamiana* is increased when transiently expressing HSP70-12 but not HSP70-11

Data were collected from five independent experiments. Error bars represent standard deviation (n=5), *P<0.05, student's t test, two-tailed, unpaired.

Curriculum Vitae

NAME   Ziwei Tang

EDUCATION

2018.09-Present   Western University (London, Ontario, Canada), Department of Biology
PhD Candidate

2011.09-2016.06   Second Military Medical University (Shanghai, China), Department of Microbiology
Master's Degree in Microbiology

2007.09-2011.06   Peking University (Beijing, China), Life Science College
Bachelor's degree in Biological Science

PUBLICATIONS   **Simultaneous Determination and Subcellular Localization of Protein–Protein Interactions in Plant Cells Using Bimolecular Fluorescence Complementation Assay,** Tang Z, Bernards MA, Wang A, Plant Virology, 2022 (pp. 75-85). Humana, New York, NY

Identification and manipulation of host factors for the control of plant viruses, Tang Z, Bernards M, Wang A, Applied Plant Virology, 2020 Jan 1 (pp. 671-695). Academic Press.

A plant RNA virus activates selective autophagy in a UPR-dependent manner to promote virus infection, Li F, Zhang C, Tang Z, Zhang L, Dai Z, Lyu S, Li Y, Hou X, Bernards M, Wang A, New Phytol, 2020, 228: 622-639

Studies on interaction between host thioredoxin-interacting protein and hepatitis C virus infection, Tang ZW, Wang SJ, Wang WB, Zhao P, Qi ZT, Chinese Journal of Infectious Disease, 2016, 34(10): 597-602

Verapamil inhibits hepatitis C virus infection via down-regulating thioredoxin-interacting protein expression, Wang SJ, Zhang W, Zhang LY, Luo ZH, Yin HZ, Tang ZW, Qi ZT, Zhao P, Academic Journal of Second Military Medical University, 2017, 38(5): 548-553

Alanine scanning mutagenesis of hepatitis C virus E2 cysteine residues: Insights into E2 biogenesis and antigenicity, Wang W, Guan M, Liu Y, Xu QQ, Peng HR, Liu XQ, Tang ZW, Zhu YZ, Wu DG, Ren H, Zhao P, Qi ZT, Virology, 2014, 448: 229-37

Serologic assay for avian-origin influenza A (H7N9) virus in adults of Shanghai, Guangzhou and Yunnan, China, WB Wang, HR Peng, QY Tao, XT Zhao, HL Tang, ZW Tang, Yan Wang, Yue Wang, P Zhao, ZT Qi, Journal of Clinical Virology, 2014, 60(3);

Pre-existing immunity with high neutralizing activity to 2009 pandemic H1N1 influenza virus in Shanghai population, Liu XQ, Liu Y, Zhang YJ, Chen ZH, Tang ZW, Xu QQ, Wang Y, Zhao P, Qi ZT, PloS one, 2013, 8(3)

Male Caenorhabditis elegans could enhance the population's resistance against heat stress, Tang ZW, Wang YB, Chinese Journal of Applied Ecology, 2012, 23(8): 2036-2040

CONFERENCES   Annual Meeting of Southwestern Ontario Regional Association-Canadian Phytopathological society (2020. 11)
Poster Presentation: Identification and characterization of Arabidopsis Heat Shock Protein 70 family proteins as potential host factors of turnip mosaic virus infection
International Advances in Plant Virology Virtual Meeting (2021. 04)
Poster Presentation: Heat shock protein 70 family proteins are involved in Turnip mosaic virus infection possibly through interactions with Eukaryotic translation initiation factor 4E isoform
The Canadian Tri-Society Meeting (2023. 06)
Oral Presentation: ER-localized Heat shock protein 70s facilitate Turnip mosaic virus infection in Arabidopsis